



NTNU – Trondheim
Norwegian University of
Science and Technology

Evaluation of algorithms and tools for 3D modeling of laser scanning data.

Joanna Alina Setkowicz

Master's Thesis

Submission date: June 2014

Supervisor: Knut Ragnar Holm, BAT

Norwegian University of Science and Technology
Department of Civil and Transport Engineering

Problem description

Following master thesis will be an in-depth study in alternatives methods and tools for post-processing 3D data acquired by 3D laser scanner. Different approaches will be examined and result will be evaluated in terms of quality, display and software package used.

Whole project includes planning, data acquisition, registering, merging scans, filtering and finally modeling point clouds. Two object are involved within the thesis. Interior of Nidaros Cathedral in Trondheim and Østre Gløshaugen building, campus NTNU.

One of the main aims of the project is to produce 3D models of both object together with textures. Textures should be applied from high-resolution images. Also issue of merging point clouds captured by two different 3D sensors will be the subject of the report.

Several tools were chosen to accomplish the goal of the thesis and to give possibilities to evaluate the work. Some of them can be used for all the necessary operation and some of them need shared cooperation.

Abstract

Following report treats about 3D modeling, merging and post-processing of laser scan data (point clouds) acquired with 3D laser sensors and high-resolution digital images. Objects that were recorded have historical value and can be counted in the branch of cultural heritage application of laser scanning. Three dimensional laser scanners have developed and brought whole new idea to the capturing, preservation and study of historical and cultural heritage. The main aim was to produce 3D models of several objects by using different available tools and algorithms and evaluate and compare the results from the point of view of the efficiency in data processing, accuracy and distinctness of the models. Also availability of each tool will be taken into consideration. Additionally, the issue of merging datasets acquired by two different 3D laser sensors will be examined.

Two objects were captured within the Master thesis, the inside of the part of the Nidaros Cathedral in Trondheim and the Østre Gløshaugen building situated in main NTNU campus- Gløshaugen. Two different 3D laser systems were used. One produced by Riegl company which includes 3D sensor with software package RiSCAN PRO and high-resolution camera, Nikon D200. Second equipment was provided by FARO company and it includes FARO Focus 3D sensor with software package FARO SCENE.

Report consists of the introduction to the topic together with the aim and the expected results. Further, there is a part of theory and basic principles of terrestrial laser scanning with description of applications and examples of already carried out projects. Main chapter consists of information on how the work was done and what kind of results were obtained. Problems, final results, comparison of different methods are included in the last chapter.

Preface

This master thesis was carried out by an exchange student Joanna Setkowicz in association with *Department of Civil and Transport Engineering (BAT)* at the *Norwegian University of Science and Technology (NTNU)*, spring 2014. The thesis includes this report and several 3D models. The CD with all report and models is also attached.

The project was specified in cooperation with professor Knut Ragnar Holm at BAT and is a continuation of working together since the Specialization Project, *3D modeling of a part of Nidaros Cathedral in Trondheim, Norway*, carried out in fall 2013. One of the main aims was to improve the same data as well as to acquire new one, presenting different object and compare the results. Evaluation of alternative available tools is the main goal of the thesis.

I would like to direct special thanks to:

- Knut Ragnar Holm, for all priceless help and time devoted for the project.
- Pasi Alto, for providing me with access to the Faro Focus 3D scanner and architecture department.
- Support Zone of InnovMetric Software Inc., for providing me with the trial version of the PolyWorks software package and for high quality advices during the work.

Joanna Setkowicz, Trondheim 23.06.2014.

Contents

Chapter 1	1
1.1 Overview	1
1.2 Introduction.....	1
1.3 Research aims	2
1.4 Structure	3
Appendix 2- Map of the Østre Gløshaugen area with GPS measurements	3
Chapter 2.....	4
2.1 Background.....	4
2.2 Overview	4
2.2.1 Terrestrial laser scanning	4
2.2.2 Advantages and disadvantages of TLS	5
2.3 Methods and basic principles.....	6
2.3.1 Range laser scanning techniques.....	6
2.3.2 Different methods for 3D digitization	9
2.4 Algorithms for mesh generation	13
2.4.1 2D Triangulation.....	14
2.4.1 3D Triangulation.....	15
2.5 From point cloud to useful information-typical workflow.....	15
2.6 Software tools	16
2.6.1 RiSCAN PRO.....	17
2.6.2. FARO SCENE.....	18
2.6.3 PolyWorks.....	18
2.6.4 Geomagic Studio	19
2.6.5 GOM Inspect	19
2.6.6. MeshLab.....	20
2.6.7 SimLab.....	20
2.7 Formats.....	20
2.7.1 ASCII	21
2.7.2 VRML	21
2.7.3 OBJ	21
2.7.4 STL	22
2.7.5 Summary	22

2.8 Main applications.....	23
2.8.1 Overview	23
2.8.2 Engineering Applications.....	23
2.8.3 Mobile mapping.....	24
2.8.4 Cultural heritage and architectural application	28
2.8.5 Forensic application.....	32
2.8.5 Summary	33
CHAPTER 3	34
3.1 Overview	34
3.2 Research and planning.....	34
3.3 Objects.....	35
3.3.1 Nidaros Cathedral in Trondheim, Norway.....	35
3.3.2 ØstreGløshaugen	37
3.4 Data acquisition	38
3.4.1 Laser scanning surveying.....	38
3.4.2 Image acquisition.....	43
3.4.3 GNSS measurements	43
3.5 Data registration.....	45
3.5.1 RiSCAN PRO registration	47
3.5.2 FARO registration	51
3.5.3 Free image registration	52
3.6 Registration data from Riegl and Faro scanner into one common coordinate system....	55
3.6.1 RiSCAN PRO.....	55
3.5.2 PolyWorks.....	59
3.6 Filtering data	66
3.6.1 RiSCAN PRO.....	67
3.6.2 FARO SCENE.....	70
3.6.3. PolyWorks.....	72
3.7 Triangulation.....	74
3.7.1 RiSCAN PRO.....	74
3.7.2 PolyWorks.....	75
3.7.3 Geomagic Studio	90
3.7.4 GOM Inspect	104

3.8 Texturing	112
3.8.1 RiSCAN PRO.....	112
3.8.2. MeshLab.....	115
3.8.3 Comment.....	116
3.9 Data flow	117
Chapter 4.....	118
4.1 Overview	118
4.2 Results	118
4.2.1 Østre Gløshaugen building.....	119
4.2.2 Nidaros Cathedral.....	121
4.3.3 Conclusions	123
Chapter 5.....	126
5.1 Discussion and further work.....	126
5.1.1 Lack of data.....	126
5.1.2 Texturing issues.....	127
5.1.3 Hardware limitations.....	127
5.2 Additional Comments	128
Appendices.....	131

List of Figures:

Fig. 2.1. Active methods for optically measuring a 3D surface	6
Fig. 2.2. Measurement principle of systems based on CW.	8
Fig. 2.5. Orthophotograph of floor mosaic (left) and with overlay of drawing (right).	12
Fig. 2.6. Floor mosaic: 2D image (left) and 3D model (right).	12
Fig. 2.7. Voronoi diagram (left) and Delaunay triangulation (right) of the same set of points.	14
Fig. 2.8. A standard laser scanning workflow.	16
Fig. 2.9. Components of 'Zebedee' handheld 3D mapping system.	25
Fig. 2.10. Point cloud of the Peel Island Lazaret generated from 'Zebedee' data.	27
Fig. 2.11. Situation of the Church of Santa Maria de Magdalena	30
Fig. 2.12. Plumb line system used to reference all three models together in the Church of Santa Maria de Magdalena	31
Fig. 2.13. Crime scene capture by a 3D sensor	32
Fig. 3.1. Nidaros Cathedral in Trondheim, Norway.	36
Fig. 3.2. Present stage of the Østre Gløshaugen building.	37
Fig. 3.3. Field work with Riegl LMS VZ420i scanner	38
Fig. 3.4. Faro Focus 3D s120 in the field.	40
Fig. 3.5. Comparison of data acquired by Riegl sensor (left) and Faro sensor (right).	42
Fig. 3.6. Three types of coordinate systems connected to scan data.	46
Fig. 3.7. Translation parameters between global coordinate system and project coordinate system within RiSCAN PRO.	48
Fig. 3.8. Advanced backsighting orientation within the RiSCAN PRO.	48
Fig. 3.9. Image registration window within RiSCAN PRO software.	53
Fig. 3.10. Free images registration with tie points. RiSCAN PRO.	54
Fig. 3.11. Coarse registration of two datasets acquired by different sensors.	55
Fig. 3.12. Coarse registration of datasets from Riegl sensor and FARO sensor.	56
Fig. 3.13. Overlapping point clouds checking after registration.	57
Fig. 3.14. Comparison of point clouds derived from Faro scanner and from Riegl system.	60
Fig. 3.15. Data alignments within the PolyWorks project.	61
Fig. 3.16. The split view mode during point pairs alignment.	62
Fig. 3.17. Misalignments between the Reference object and Data object after point-pair registration. PolyWorks	63
Fig. 3.18 Best-fit alignment within PolyWorks	64
Fig. 3.19. Differences between point pair alignment and best-fit.	65
Fig. 3.20. Initial manual cleaning of point clouds	67
Fig. 3.21. Manual cleaning of window's reflections.	67
Fig. 3.22. Octree filter within RiSCAN PRO.	68
Fig. 3.23. Octree filtering. Before process and after the process.	69
Fig. 3.24. Generation of new grid during re-sampling within RiSCAN PRO software.	69
Fig. 3.25. Re-sampling process within RiSCAN PRO software.	70
Fig. 3.26. Sampling process within RiSCAN PRO before and after process.	70
Fig. 3.27. Preprocess tool within FARO SCENE.	71
Fig. 3.28. Comparison data before and after running preprocessing tool within FARO SCENE software.	72

Fig. 3.29. Windows before and after cleaning-PolyWorks	73
Fig. 3.30. Results of plane triangulation within RiSCAN PRO.	75
Fig. 3.31. Wrap Mesh around Point Cloud parameters-PolyWorks software.	77
Fig. 3.32. Mesh created with IMSurvey.	78
Fig. 3.33. Well preserved details above the entrance of the Gløshaugen house.	78
Fig. 3.34. Reversed triangles within IMEdit module and IMSurvey module.	79
Fig. 3.35. Faro scan position 6 with problematic area.	79
Fig. 3.36. Model within IMEdit module (PolyWorks) with coarse parameters.	80
Fig. 3.37. Model within PolyWorks .	80
Fig. 3.38. Automatic hole filling algorithm within PolyWorks	81
Fig. 3.39. Parameter for automatic holes filling within PolyWorks.	82
Fig. 3.40. Single Boundary Hole mode, closing hole in the roof-PolyWorks	83
Fig. 3.41. Point cloud without bushes in front of the house-PolyWorks.	83
Fig. 3.42. Filling holes behind the bushes in front of the house-PolyWorks.	84
Fig. 3.43. Window before and after closing in PolyWorks.	85
Fig. 3.44. Parameters within smoothing process in PolyWorks.	85
Fig. 3.45. Part of surface before (left) and after (right) smoothing- PolyWorks.	87
Fig. 3.46. Parameters for importing data into IMEdit module, PolyWorks.	87
Fig. 3.47. Point cloud of Nidaros Cathedral inside IMEdit module, PolyWorks.	88
Fig. 3.48. Reversed triangles within Nidaros Cathedral model, PolyWorks	89
Fig. 3.49. Problems with the mesh in the bottom part of Nidaros Cathedral.	89
Fig. 3.50. Closing holes algorithm in Nidaros Cathedral model.	90
Fig. 3.51. Nidaros Cathedral model after filling holes and smoothing, PolyWorks.	91
Fig. 3.52. Østre Gløshaugen house imported to Geomagic Studio.	92
Fig. 3.54. Model of Østre Gløshaugen house after applying Mesh Doctor function.	92
Fig. 3.55. Mesh Doctor operation types-Geomagic Studio	93
Fig. 3.56. Interactive holes filling dialog-Geomagic Studio.	93
Fig. 3.57. Østre Gløshaugen house before and after closing holes.	94
Fig. 3.58. ReWrap function within Geomagic Studio.	94
Fig. 3.59. Decimation algorithm within Geomagic Studio.	95
Fig. 3.60. Polygonal model after decimation. Part of the roof- Geomagic Studio.	95
Fig. 3.61. Relax polygons function within Geomagic Studio.	96
Fig. 3.62. 3D model of Østre Gløshaugen house without textures- Geomagic Studio.	97
Fig. 3.63. Left :model created in PolyWorks, right: point cloud from RiScan PRO.	98
Fig. 3.64. Nidaros Cathedral while mesh repairing-Geomagic Studio.	99
Fig. 3.65. Nidaros Cathedral model improved in Geomagic Studio.	100
Fig. 3.66. Noise reduction carried out on point cloud data from Nidaros Cathedral	101
Fig. 3.67. Wrap function in Geomagic Studio.	101
Fig. 3.68. Generate Texture Maps function within Geomagic Studio.	102
Fig. 3.69. Final versions of Nidaros Cathedral model - Geomagic Studio.	103
Fig. 3.70. Nidaros Cathedral opened in SimLab software.	104
Fig. 3.71. Point cloud displayed in GOM Inspect.	104
Fig. 3.72. Polygonize Point Cloud operation within GOM Inspect.	105
Fig. 3.73. Holes within the roof of the house. GOM Inspect.	106
Fig. 3.74. Closing holes automatically. GOM Inspect.	106
Fig. 3.75. West side of the building before and after automatic closing holes.	107
Fig. 3.76. Closing holes interactively. GOM Inspect	107
Fig. 3.77. Chimney reconstruction and closing the surrounding. GOM Inspect	108
Fig. 3.78. Filling holes behind bushes in front of the Østre Gløshaugen building.	108
Fig. 3.79. Window before and after filling with the plane surfaces. GOM Inspect	109

Fig. 3.80. Smoothing parameters. GOM Inspect	109
Fig. 3.81. Part of the house before smoothing and after the operation. GOM Inspect.	110
Fig. 3.82. Model of the house generated in GOM Inspect software.	112
Fig. 3.83. Textured house in RiSCAN PRO software.	113
Fig. 3.84. Error after importing and texturing 3D model of the house.	113
Fig. 3.85. Textured house displayed in Geomagic Studio.	114
Fig. 3.86. Errors in texturing the roof of the house, displayed in Geomagic.	114
Fig. 3.87. Front of the house with textures. Gemagic.	115
Fig. 3.88. Texturing options within MeshLab software.	115
Fig. 3.89. Raster registration within the MeshLab software.	116
Fig. 3.90. Work flow for Østre Gløshaugen house.	117
Fig. 3.91. Work flow for Nidaros Cathedral.	117
Fig. 4.1. Østre Gløshaugen building from the south side.	119
Fig. 4.2. Østre Gløshaugen building from the north-east side.	120
Fig. 4.3. Østre Gløshaugen building from the north-west side.	120
Fig. 4.4. Final, textured model of Nidaros Cathedral.	122
Fig. 4.5. Final, textured model of Nidaros Cathedral, zoomed part.	122

List of tables:

Table 1. Laser scanning techniques used in cultural heritage management activities.	29
Table 2. Results of GNSS measurements	45
Table 3. Global coordinates of control points.	45
Table 4. Statistic results of RiSCAN registration.	50
Table 5. Coordinates of scan position before and after registration in RiSCAN PRO.	50
Table 6. Statistic results of FARO registration.	52
Table 7. Results obtained during free images registration.	54
Table 8. Standard deviations obtained with coarse registration of datasets from Riegler and Faro scanner.	57

Chapter 1

1.1 Overview

In this paper, the adaptation of different methods and tools in digital photogrammetry and terrestrial laser scanning is examined for cultural heritage documentation in relation to data capturing, data processing and results. The thesis intends to show a wide review of the evaluation of historic and cultural sites documentation methods and algorithms available nowadays. Descriptions of the theoretical background, newest developments and techniques in documentation and display procedures are included. Main criteria are effectiveness, availability, accuracy and presentation of final products. Moreover, the issue of merging two datasets from two different 3D laser sensors will be examined. Both, digital photogrammetry and terrestrial laser scanning will be used and assessed from the point of view of automation possibilities and technical aspects.

1.2 Introduction

The application of digital photogrammetry and three-dimensional laser scanning techniques has become very important within the documentation of cultural heritage sites. While aiming at a constant monitoring and documentation of the related spatial information at different times, production of 3D models of architectural and historical sites is highly important task. Mentioned 3D models intends to provide high precise, geometric accuracy and detailed data. [1] Efficiency of the image-based techniques has been developed considerably for the past few decades. However, development of terrestrial laser scanning methods with all its possible applications made a huge step forward the quick and convenient way of 3D documentation and modeling. It has become an additional standard tool for creation of high quality 3D models of wide variety of places and structures, including cultural and heritage sites. Laser scanning techniques are beyond doubt the fastest and most powerful tool, although the combination of both laser scanners and digital photogrammetry is nowadays the most popular. [6]

There are several reasons for using both techniques together. Laser scanners provide with data that can be transformed to highly accurate reconstruction of the surface of particular

object. It allows to keep and present the geometry of the object very precisely. Digital photogrammetry introduces the possibility to keep realistic colors of the objects and improve widely the final products. It is very important when concerning the cultural and historical sites to obtain accurate documentation, especially when there is a possibility that the object can be destroyed.

1.3 Research aims

Objects that are used within the thesis are both historically valuable. First place is an old, beautiful medieval Cathedral in Trondheim- Nidaros Cathedral. The object is not the whole Cathedral itself by the inside of the Cathedral, the western wall with huge stained glass. Second object is one of the oldest building in the Norwegian University of Science and Technology campus- the Østre Gløshaugen . The paper shows entire preparation process, data acquisition and later data processing and improving the final products. Data processing and improving the results will be carried out in few different available tools for 3D modeling. Set of chosen tools includes highly expensive software packages as well as open-free sources. The main reason to use them was to have wide variety of criteria to compare. Additionally, nowadays to obtain the best possible final product it is almost impossible to use only one tool. It is wise to combine several available methods. This will be also examined in the thesis.

Another objective of the thesis is to check different ways to register datasets from two different 3D laser sensors. The aim is to analyze and asses the accuracy and easiness of the registration procedure. Sensors do not use the same tie points, they organize point clouds differently and have completely different formats. During data acquisition one part of the object-the building situated on the NTNU campus was captured by RIEGL 3D sensor-LMS-Z420i and other part of the object by FARO Focus 3D equipment. The entire Nidaros Cathedral data was acquired by Riegl 3D laser scanner- LMS-Z420i.

Also important point within the 3D modeling is to apply textures (colors) on the generated surface. It makes the model realistic and easier in reception. Different tools for proceeding with texturing will be also investigated.

Furthermore, as can be noticed nowadays, computer applications for handling laser scanning data and producing models of any object has developed over the last years successfully. It improves the entire methodology for working with 3D datasets but on the other hand it is very complicated to decide on the tool that is the best for each step of

processing. This problem is also one of the aims of the thesis and different workflows were investigated.

1.4 Structure

Report of the thesis consists of five main chapters and eight appendices. Structure of chapters is following:

Chapter 1- Introduction, overview of the scope of the project and research aims.

Chapter 2- Background information, methods, principles and techniques. Review of available tools, formats and algorithms.

Chapter 3- Main part of the thesis. Description of processes carried out within the project. Different functions, operations and implementation of the data.

Chapter 4- Sum up of results obtained within the processes described in Chapter 3.

Chapter 5- Discussion and further work together with additional comments.

Report includes also eight appendices:

Appendix 1- Map of the Østre Gløshaugen area with planned scan stations.

Appendix 2- Map of the Østre Gløshaugen area with GPS measurements

Appendix 3- Final map of Østre Gløshaugen area with scan stations and control points.

Appendix 4- Specifications of Riegl 3D system.

Appendix 5- Specification of FARO 3D system

Appendix 6- Specification of GPS controller CS15

Appendix 7- Specification of GPS receiver GS15

Appendix 8- Hardware specification

Chapter 2

2.1 Background

Chapter 2 consists of three main parts. Introduction to the terrestrial laser scanning, methods and basic solutions and the most significant applications. Within each part there are some extensions. First briefly state-of-art of terrestrial laser scanning is mentioned. Also here few advantages and disadvantages of laser scanners are presented. Next part introduces technologies and principles of laser scanners work. This paragraph includes also short description of other methods used for 3D digitization with emphasis on digital photogrammetry. Additionally, detailed information about different applications is provided together with examples of projects carried out based on terrestrial laser scanning and photogrammetry. Finally, tools and algorithms applied to point clouds, are described together with a general work flow for typical surveying project using 3D sensors. Each part is summarized to give an overall idea of the issue.

2.2 Overview

Nowadays, 3D laser scanners are being consider as a standard source that deliver an input data in many application areas ranging from cultural heritage documentation, industry and manufacturing, surveying to medicine. 3D sensors are capable to work in majority of real world environments under wide variety of conditions. They provide large datasets with millions of points for each object. Usually all these applications require generating high-quality geometric models. Therefore the modeling issue of unorganized point clouds, derived from terrestrial laser scanning, is receiving more and more attention. All these changes and developments opened up numerous of new studies and solutions for existing problems. [18]

2.2.1 Terrestrial laser scanning

Terrestrial laser scanning (TLS) is a technique designed for a contactless, non-invasive measurements that allows the acquisition of dense and precise both geometric and radiometric data of the investigated area . Majority of scanners work on basic principle of measuring the distance from the sensor to the surface of an object. Laser beam, usually work

on infra red light, is being sent in different directions in the area of an object. However, there is also other principle implemented, that will be describe in next part of the chapter.

Laser scanners are able to automatically calculate the 3D coordinates of complicated geometrical shapes , characteristic features of an object which makes terrestrial laser scanning one of the most efficient method among such a wide variety of applications. It allows to make a complex and accurate 3D model of an object from a 3D point cloud in relatively short time. Unfortunately, some systems are not equipped in possibility of image acquisition or if it is available the quality of color images is insufficient. To obtain model of an object with true color representation, more precisely photographs must be taken. [8] That is why usually, 3D systems are equipped with high-resolution digital camera.

Besides terrestrial laser scanning there should be also pointed out airborne laser scanning which is designed to cover large areas with slightly worse accuracy. As there should be noticed there are also several different methods for these measurements: infrared thermography, image-based observation, digital photogrammetry and combinations of more than one of these techniques.[10]

2.2.2 Advantages and disadvantages of TLS

Terrestrial laser scanning method has been employed at number of cultural heritage sites because of its precision and efficiency. 3D models that can be derived from laser scanning measurements are usually very accurate and realistic. There are however some drawbacks of using 3D terrestrial sensors regarding different types of objects and areas.

Whenever there is a need nowadays to capture and document historic monument or object there the TLS finds its application. It enables precise measurement of important natural and architectural features. [7] Although, when the large cultural heritage area needs to be captured there occurs a problem of inefficiency and time-consuming work. Surface measured by 3D scanners is the surface only visible from its current scan position. To acquire data for complex site , the instrument has to be placed at multiple positions. [25]

2.3 Methods and basic principles

3D sensors record three-dimensional coordinates of numbers of points on an object surface. The method to obtain the measurements is to project a laser beam onto the object surface with a use of one or two mirrors which change the deflection angle of the beam in small increments. Additionally, to acquire full 3D measurements, entire instrument or the object may be rotated. Basic measurements are distance and angles which determine the reflecting point position. [3]

Entire field of 3D measurements can be divided into several categories in respect to different systems implemented. Techniques based on speed and coherence of light, so called ranging lasers which use either the 'time-of-flight' principle or phase-shift method and techniques based on triangulation principles, where CCD cameras are in use, are distinguished. [20]

Both techniques are illustrated in Figure 2.1. [20]

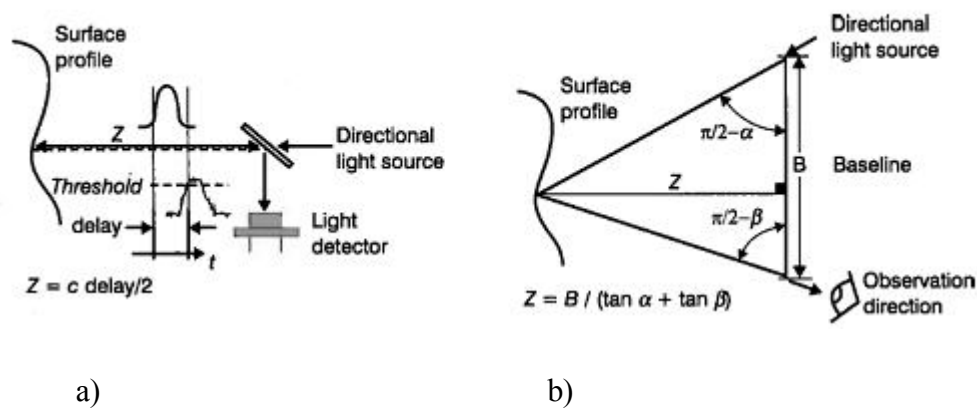


Figure 2.1. Active methods for optically measuring a 3D surface: (a) light transit time, (b) triangulation. (Source: [20])

2.3.1 Range laser scanning techniques

Within the range laser scanners there are two principles implemented. The distance between the instrument and the object surface can be computed either by the time-of-flight principle (TOF) or parallel the sent and received wave form of modulated signal.

2.3.1.1 Time-of-flight technique

TOF (time-of-flight) technique use a laser source to scan a surface. Principle of the method computes distance based on time of light (Δt) measurement of the laser pulse between sending and receiving signal. Pulsed laser beam is being sent to the scanned object. The receiver is returned by a part of the light reflected by the surface. This construction gives a possibility to measure time delay formed by light traveling from a source to a reflective object (target) and back to a detector. Assuming speed of light as a speed of light in a vacuum it is an easy way to calculate the distance. [23]

Equation 1 presents basic formula for calculation.

$$\rho = c \cdot \frac{t}{2} \quad (1)$$

ρ - range

c -speed of light in a vacuum

t -round trip

The principle implemented in TOF scanners is currently the most popular and common used method. TOF system allows to measure at the distance of several hundred of meters with satisfying accuracy of few millimeters to centimeters depending on the range. [23]

Instruments with 'time-of-flight' principle are able to measure longer distances and cover a larger volume of the area than scanners that use triangulation method. Unfortunately, they are less accurate if we consider close range measurements.

2.3.1.2 Phase comparison method

Phase comparison method is realized by amplitude modulation (AM) and frequency modulation (FM) (shown in Figure 2.2). [20]. Phase-shift method uses a continuous wave to measure a distance between a 3D sensor and object. Continuous, modulated signal is sent out and compared with the returned, reflected signal. The phase difference between sending and receiving wave is used to calculate accurate distance. Two wavelengths are needed to resolve ambiguity. This method is considered to be the most precise.

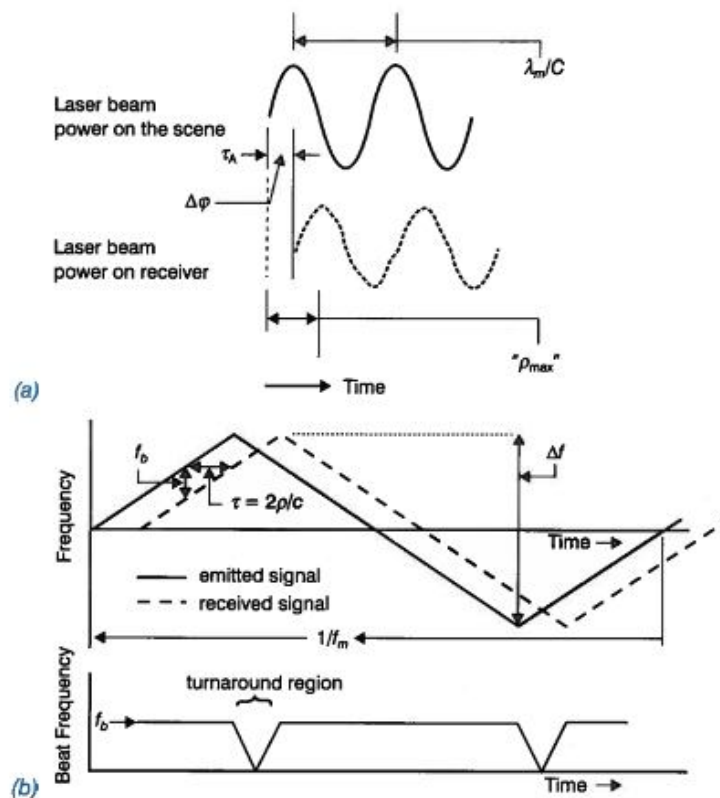


Figure 2.2. Measurement principle of systems based on CW (continuous wave): (a) AM and (b) FM. (Source: [20])

Phase-shift method is another common method for distances up to 100 m. Within this range, the method can provide accuracy at a few millimeters. Additionally, instruments based on phase measurements are capable to capture up to 1 000 000 points per second what is around 20 times more than TOF instruments. [23]

2.3.1.3 Triangulation laser scanning technique

Triangulation systems are divided into passive and active methods and are based on optical triangulation method. Passive is based on stereo image processing and active use light sheet and strip projection techniques.

In triangulation method (shown in Figure 2.2), the cosine law is used for constructing a triangle with an illumination direction that goes towards a reflective surface and an observation direction at a known distance -baseline from the illumination source.

The instrument sends a laser signal on the surface and a CCD camera mounted within the device detects the laser beam at the end of the baseline. 3D coordinates are derived from resulting triangle.

Triangulation laser system allows measurements up to few meters with accuracy at few millimeters. Triangulation based devices are, therefore, suitable for precise and close range measurements such as sculpture within the cultural heritage area. [23] Capability of capturing points per second is the smallest one within all methods, from 200 to 10 000 points per second.

2.3.2 Different methods for 3D digitization

2.3.1.1 Overview

Precise digital recording of cultural heritage sites is a multidimensional process. During restoration and renovation operation it is relevant to obtain an accurate documentation of the status of investigated area. 3D scanning and modeling of sites and features of cultural heritage have increased highly in recent years. However, there are still in use different methods of 3D digitization of monuments. Techniques used for modeling small object, like sculptures, might be slightly different than ones used for monuments. In this paper, methods for monuments digitization will be presented as the thesis concerns modeling of larger objects.

For the past years close range photogrammetry has been efficiently in use for cultural heritage documentation. Last development in information technologies introduced a replacement for regular photogrammetry methods in form of digital close range photogrammetry. This new method allows for automatic orientation and measurement process

resulting with 3D vector data, ortho-images and surface models. [23] Within the digital photogrammetry there are several opportunities for capturing data which enables to use different types of images acquired by CCD cameras (Charge Coupled Devices). This approach has a numbers of advantages in photogrammetric applications. Good geometric features, high automation and quality control are just few of them. [23] It is consider to be relatively simple and has rather low cost. Additionally, it is helpful with objects that direct access or contact is prohibited.

Methods within digital photogrammetry differ according to the needs and characteristics of the object. Therefore, digital image rectification, stereo digital photogrammetry, monoscopic multi-image evaluation and digital ortho-images are distinguished. [23]

2.3.1.2 Digital image rectification

The method has strong application if the cultural heritage monument is considered as a plane. It uses tilted images regarding to the plane of the object surface. With the help of four control points images can be rectified and scaled. For a complex buildings this method is usually not suitable. [23]

2.3.1.3 Monoscopic multi-image evaluation

This method is applied to handle several overlapping images. The main principle used within the monoscopic method is multi-image bundle- block adjustment. Camera calibration, it means lens distortions and interior orientation parameters, is calculated within the bundle-block adjustment process. The results of the adjustment procedure are 3D coordinates of investigated object. When the object is characterized by poor texture and problems with identifying homologous points on images monoscopic, method might be insufficient.

The example of using monoscopic multi-image evaluation method is described in the article of NaciYastikli, *Documentation of cultural heritage using digital photogrammetry and laser scanning* [23]. Beyoglu Municipality in Istanbul, Turkey was in charge of a restoration and rehabilitation project- Beyoglu. First steps of work concerned the 34 building facades in the Tarlabasi area, residential district with historical value buildings. The task was carried out

in 2005. Since facades of buildings were not considered as a planes the monoscopic method was chosen.

2.3.1.4 Stereo digital photogrammetry

If the previous method is insufficient the stereo photogrammetry is able to provide 3D digitization and generation of digital surface model. This process can be carried out semi-automatic or automatic and is possible due to application of LCD eyewear (liquid crystal display) mounted on top of the monitor within the digital photogrammetric system. Image correlation is used to generate stereo model and model orientation. Both procedures can be done semi-automatically or automatically. Perspective techniques, automatic pattern recognition and illumination rules is used within the stereophotogrammetry. Positive point of this method is the speed of acquisition. [11]

The example of using the stereo digital photogrammetry is also described in the article [23]. The performance was carried out on the data set from the Fatih Mosque project in Fatih district of Istanbul. Due to 3D nature of the Fatih Mosque facade the stereo photogrammetry was the most suitable.

2.3.1.5 Digital ortho-image

The result of digital ortho-image method is analogue to the previous method's result-line drawing. With the assistance of digital surface model the effects of lens distortions, tilt and relief displacement are eliminated. Not only, digital ortho-image method has the same precision as digital line drawing but also presents photographic information. [23]

The example of application of digital ortho-image method is presented in article [3]. Authors carried out measurement of two churches within Byzantine Ruins on Gemiler Island. It is located at the Lycian coast, southwestern Turkey. Within the project different methods of 3D capturing were used but orthophotograph was produced for a Floor Mosaic in one of the Churches. Figure 2.5 shows the result of the procedure.



Figure 2.5. Orthophotograph of floor mosaic (left) and with overlay of drawing (right).
(Source:[8])

To produce the ortho-image of the mosaic 25 images, from a inclined angle, were taken. RTK-GPS was used to measure four reference points. The overlapping precision was equal 1 cm.

Within the same task, the possibility of 3D model generation, was examined. For this work another area was chosen. Figure 2.6 presents the result of this attempt.



Figure 2.6. Floor mosaic: 2D image (left) and 3D model (right). (Source: [8]).

Because of the concavity of leaves and bird on the left that information is missing. The software PI-3000 enabled to model the details while authors claim that 3D model based on point cloud was unable to model it. Resolution of the model is equal 1 mm. [8]

2.3.1.6 Summary

As we can notice beside terrestrial laser scanning, nowadays the most popular device for cultural heritage purposes, we can find several different methods for 3D modeling. Each of them has an application in different types of objects. None of these methods can be applied to every situation. The most important issue during planning procedures is to select the most suitable method or to combine few of them. [8] Currently, large application of laser scanning combine with digital photogrammetry, can be noticed. Laser scanning techniques ensure high geometric quality while digital photogrammetry improved texturing and coloring the 3D models. Without the high resolution images, 3D models derived from laser scanners, would not present the real situation of the object regards the RGB values.

2.4 Algorithms for mesh generation

Following section is dedicated to most popular algorithms and methodology for mesh creation within the reverse engineering software packages. It is the essential part of all modeling programs. A triangulation (meshing) transforms the acquired set of points into a constant polygonal model. This operation usually produces vertices, edges and faces that meet at shared edges. Two types of methods can be distinguished, first the finite element methods usually discretize the measured field by dividing it into small elements, commonly triangles or quadrilaterals, when it considers two dimensions and tetrahedra in three dimensions. Another type of methods is called optimal triangulation and it measures angles, edge lengths, height or the area of the elements. The vertices can be either exactly the input points or additional, inserted points. Triangulation can be accomplished in 2D or 3D, depends on the input data. [12]

2.4.1 2D Triangulation

Within 2D Triangulation the most popular methods are Delaunay triangulation (DT) and Voronoi diagram (also called the Thiessen or Dirichlet tessellation). As the input data of 2D triangulation a polygonal region of the plane is used and the result of the operation are triangles that intersect only at shared edges. Additionally, vertices are created. [12]

Figure 2.7 presents both methods that were proceeded on the same set of points.

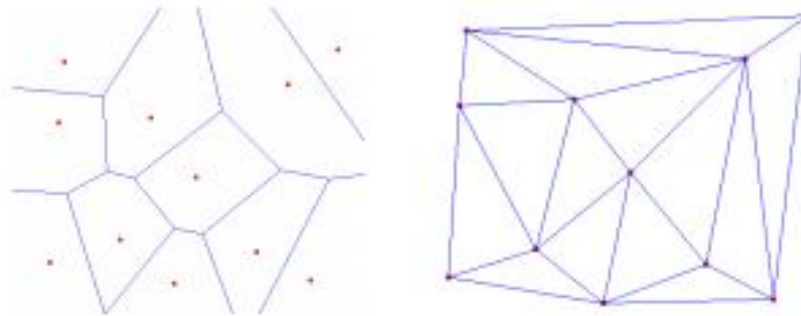


Figure2.7. Voronoi diagram (left) and Delaunay triangulation (right) of the same set of points.
(Source: [12])

The Delaunay triangulation works on the basis that a circle through the three points of any triangle does not include any other point of the data set. It generates compact triangles with the largest minimum angle. [5]

Delaunay Triangulation also works in higher dimensions than 2D, however, triangles are being replaced by tetrahedras and spheres. Together with Voronoi diagram it is commonly used with geometric calculations. It characterizes with simplicity and efficiency. Regard Voronoi diagram, the method works as each region of the surface consists of the part of the plane that is nearest to that node.

Both techniques usually cooperate together. Delaunay Triangulation of a particular set of point is the dual of the Voronoi diagram. [12]

2.4.1.1 2.5 D Triangulation

As the input data normally in this triangulation is a set of points P in a plane along together with a real, unique elevation function $f(x,y)$ at each point of the set. During the 2.5D triangulation a linear function F is generated which interpolates P and is defined on the area

bounded by the convex hull of P. For each point, function F is the weighted average of the height value. Usually, the interpolation function is calculated by Delaunay triangulation. Generated surface is called usually elevation grid or TIN model (Triangulated Irregular Network). [12]

2.4.1.2 3d models surfaces

The input data in this case is normally a set of points P in three dimensions and it is no more limited on a plane, hence the elevation function $f(x,y)$ is no more unique. The input, in other words, is called unorganized point cloud. [12]

2.4.1 3D Triangulation

Other words for 3D triangulation are tetrahedralization or tetrahedrization. It is a division of the input dataset into series of tetrahedras that meet at shared edges. Shared edges are vertices, edges or triangles. The entrie operation results in more complicated calculation and processing than 2D triangulation. Input set for the 3D triangulation can be plain polyhedron (sphere), non-plain polyhedron (torus) or point cloud. [12]

2.5 From point cloud to useful information-typical workflow

Basically there can be distinguished four steps while converting measured data into common and constant polygonal surface.

1. Pre-processing, which includes all manual cleaning, noise reduction and sampling points in order to reduce the computation time.
2. Registration and determination of the global topology, at this stage all adjacent scans should be register into one common coordinate system. Also if available, global coordinate system should be introduced.
3. Triangulation, creating a polygonal surface of the object, with certain parameters and available tools meshes are generated. More about triangulation type is written in previous paragraph 2.4.

4. Post-processing, all operations that lead to improving and repairing models. Lot of alternative functions can be used, as smoothing, closing holes and many more. Also, on this stage, if images available, texturing is performed.

Figure 2.8 shows basic workflow, beginning with measurements and finishing on conclusions. The figure 2.8 was derived from [2].

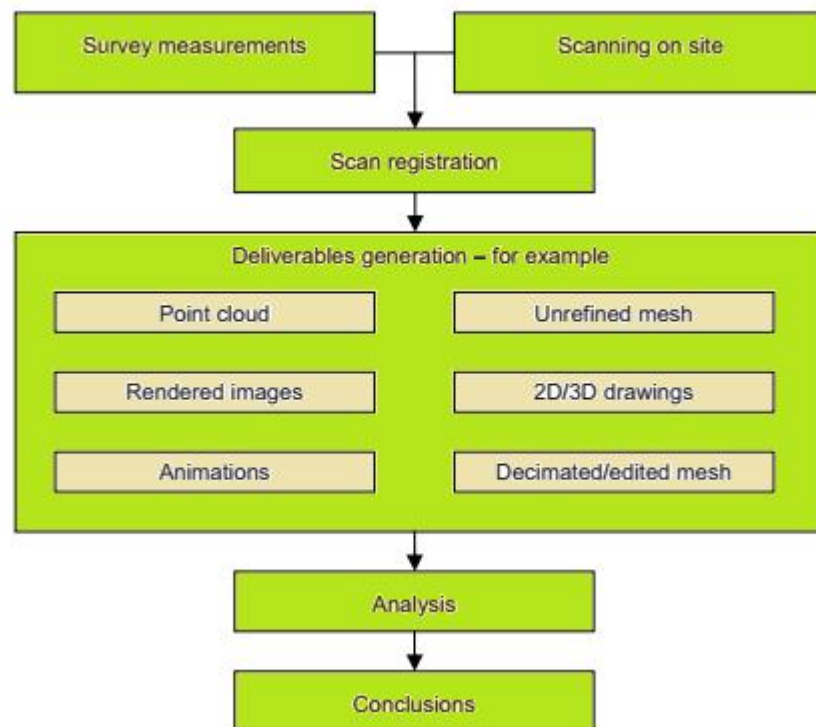


Figure2.8. A standard laser scanning workflow. (Source:[2]).

2.6 Software tools

The market of 3D laser scanners for terrestrial application has grown rapidly for the past few years. It resulted in developing numerous new tools and solutions for handling the data and improving the final output. Tools that can be used with laser scanning data usually also have an application in other disciplines, like architecture, industrial design, computer graphics and much more.

Nowadays, to obtain high-qualified 3D model of an object and to process data efficiently there is almost obligatory to use different packages. It is impossible to proceed with all operation within on software package. Of course, there are tools that provide the final output

but the question is if the output is the most advanced and the most accurate as can be. It is very difficult to decide on few packages and what is more to decide which one should be used in each step of workflow. That issue is one of the main aims to examine within the thesis. In this part all used software packages will be shortly described. Different assumptions were taken into consideration while choosing tools. Software packages will be compare from the point of view of accessibility, efficiency, price, intelligibility and of course the final outputs and products. On the market, there is a group of very expensive and highly advanced tools for processing the data as well as the group of open-sources free software available to work with 3D data.

2.6.1 RiSCAN PRO

RiSCAN PRO is the software used while working with any Riegl's LMS-Z series scanner. It is essential for pre-processing the data acquired by the scanner. A large number of tasks can be carried out including scanner configuration, data acquisition, visualization, manipulation and data archiving. RiSCAN PRO is project orientated software. The whole data are saved within one single directory structure where all scans, images, registration information and outputs are kept.

The whole project is saved as a .rsp file and the main file format is 3DD which contains the raw data captured by a Z- or LPM series instrument. 3DD file is also an output format for the instrument.

Software of course allows to work on different formats as well. To import any of them, operator needs to use a 'Polydata' folder. File formats available to import into RiSCAN PRO are TXT, 3PF, POL, PLY, STL, OBJ, DXF, SDW, LAS. List of formats that can be exported from RiSCAN PRO is almost the same, only VRML format is added.

RiSCAN PRO can operate on three different levels of license. The first one, Viewer License enables only basic visualization and viewing functions, the second one, Acquisition License allows to proceed with data acquisition, global registration, visualization and processing of the point cloud, the last one, Processing License consists of all point cloud processing functions and also advanced meshing, texturing and evaluation options. [15]

Basically, working in the software includes 5 parts, data acquisition, data visualization, data registration, data post-processing and data exchange.

2.6.2. FARO SCENE

FARO SCENE software is a 3D point cloud post-processing and managing tool. It is designed by FARO company, one of the biggest 3D measurement technology provider. It cooperates with different and extensive 3D scan data acquired by laser scanner. The company also produces the equipment for measurements, FARO Focus 3D, which has been used also in the thesis.

Wide range of functions and tools are available within the software. From viewing, administration, merging, filtering to meshing and evaluation. It can easily manage huge datasets by having automatic object recognition function. Also automatic scan registration and positioning are available. [4]

The basic format for point cloud is .fls and is obtained by FARO Focus 3D. Other files can be imported in VRML, TXT and e57. As for the export, the data can be saved in various point cloud formats and CAD formats.

The software is not open-free source for data processing and can be used as a trial version only for 30 days. For the future work there are three licensing options. First, Licensing with a product key, the key can be obtained from the SCENE package, in a mail from FARO Customer Service. Second licensing option is Licensing with a Port Lock and it can be moved between multiple computers. The third option is a Network Licensing which allows multiple licenses over a network. [5]

2.6.3 PolyWorks

PolyWorks software is one of the best and highly advanced 3D processing tool on the market. It is provided by InnovMetric Software Inc. Version that has been used in the project is Polyworks 2014. The software is not available in any trial version but because of the courtesy of the company the 30 days license key has been sent. License is in two parts, the dongle needs to be sent by post and the license key is being sent by mail. Both solutions give the possibility to use wide range of options. The software consists of few basic modules, IMInspect, IMAlign, IMEdit, IMSurvey, IMTexture, IMMerge. Each of the module is designed to process and prepare data. Some of them can proceed with the same operations so they can be substituted. The license used within the thesis allowed to use IMAlign, IMEdit, IMMerge and IMSurvey what was sufficient to carry out the work.

IMAlign, as name indicates, deals with registering and merging datasets. IMSurvey tool is dedicated for measuring and verification purposes. Registration, filtering and meshing operation can also be achieved. Editing, repairing and delivering polygonal models are included within IMEdit module. Besides creating polygonal models, IMEdit enables to create NURBS patches and parametric sketches.

Among all wide range of options for the purpose of this master thesis few are very significant. Possibility of multiple scan alignment then polygonal model creation, polygonal model editing tools like hole closing, edge and corner reconstruction and smoothing. Features and measurement extraction is also very important but not particularly used within the work. The software also allows to visualize data and produce short videos.

The list of file formats, both for point clouds and for polygonal models, available during importing and exporting data is very long and the software works with almost all possible formats. One of the best thing with this is possibility to import raw scanned data in their native formats, .3DD and .fls files are accepted.

2.6.4 Geomagic Studio

3DSystems Geomagic is a company that provides multiple solutions for managing 3D data and objects. Besides managing and processing, Geomagic also deals with design. Among wide range of tools Geomagic Studio can be found as a complete package for processing and transforming 3D data into highly precise surface, CAD and polygon models. In general, post-processing and reverse engineering options are available. Additionally, besides accurate 3D processing tools, Geomagic Studio introduces incredible automated functions.

Geomagic Studio 2014 is the version that has been used. Trial installation is available for 14 days, after this time, the license key is required.

Geomagic offers wide list of formats that can be supported with all the most common ones as .ply, .stl, .wrl and .obj.

2.6.5 GOM Inspect

GOM Inspect is one out of two free software packages used within the thesis, for inspection and processing three dimensional data. As typical modeling software it offers multiple mesh processing tools, as polygonizing point clouds, smoothing, thinning, hole

filling. Moreover, alignments process can be carried out with few different options. Construction and measurement planning as well as inspection and reporting are also available within the tool.

G3D-ATOS, STL, ASCII, POL, PSL are the formats that are supported within the GOM Inspect for importing point clouds.

2.6.6. MeshLab

MeshLab is an open source, free, portable system for processing and editing unstructured 3D triangular meshes. It is designed by the ISTI-CNR research center according to requirements of the General Public License. MeshLab can be used both as fully complete tool or as a library supporting other software. System provides numbers of tools for editing, inspecting, cleaning, and rendering.

Software can work with numbers of formats like: OFF, PLY, STL, 3DS, VRML, OBJ, USD, X3D and COLLADA. It can be mentioned here that format U3D is the format that needs to be used when creating a 3D PDF with Adobe Acrobat software. MeshLab could be also used for converting final file into this format. In the end another software for building a 3D PDF was implemented.

2.6.7 SimLab

SimLab Soft includes packages for presenting 3D data. It is one of the best tools for creating a 3D scenes. Composing and rendering 3D data is one of the main goals of the software. SimLab enables sharing 3D models with wide range of recipients.

2.7 Formats

On the market there are numerous ways to store data. Especially, when working on the project and multiple software packages are used it is important to operate with different formats. In the paragraph 2.6 several tools were described and all of them are used within the thesis. In order to exchange data between each software essential formatting was required.

Following chapter will present briefly alternative types of formats used while working on the project.

2.7.1 ASCII

ASCII is The American Standard Code for Information Inerchange. The code represents any text in the computers and other equipment that use text. It was originally based on the English alphabet. In encodes numbers, letters and basic punctuation symbols into the 7-bit binary integers. [21]

ASCII data files are simple text files that can be edited by many programs. The files are adapted to move easily between multiple software packages. Because of its simplicity ASCII files can lose some information while coding. However, they can be imported to so many programs that are highly popular. [21]

Within the thesis the format was used to transfer point clouds, mainly raw data from scanners, between initial tools-RiSCAN PRO and FARO SCENE to modeling tools.

2.7.2 VRML

VRML is the Virtual Reality Modeling Language. It is one of the most popular 3D file format and navigation language. The current standard is VRML 2. It is a standard model (ISO standard) for presenting 3D models. Using a browser plug-in, for example Cosmo Player, user can navigating through a different 3D scenes. It is also possible to create a key-positions defined in few viewpoints and later generate automatic flights through the model. [12]

Within the thesis format was used to export the 3D model of the house from Geomagic Studio and import it into RiSCAN PRO in order to texture object. It did not work very well so was replaced by other format.

2.7.3 OBJ

OBJ is a geometry format developed by Wavefront Technologies. It finds its application in 3D graphics area. It is a plain data format for representation 3D geometry, it includes position of each vertex, the UV position of the texture coordinate vertex, vertex normals and faces that define polygon. The coordinates have no units, but can contain scale information. [22]

The OBJ format was mainly used within the thesis to move models between several tools. Especially, when exporting from Geomagic Studio and importing into RiSCAN PRO and then into SimLAB in order to create a 3D PDF.

2.7.4 STL

STL stands for STereoLithography and is also known as Standard Tessellation Language. It is a triangular representation of the 3D object. The surface is broken down logically into small triangles-facets. Each of the triangle is described by a perpendicular direction and three points-corners of the triangle. [26]

The format was used to transferred polygon models created in PolyWorks software into Geomagic Studio and others.

2.7.5 Summary

Formats presented in this chapter are just a small group of available formats. New tools are appearing on the market together with new formats. All of them have their advantages as well as disadvantages in terms of storing, application, efficiency and compatibility with other software.

The first stage of the project was mostly done on the raw, original formats of the scanner- FLS and 3DD. However they can be used only within one software. The exception here is PolyWorks, which is able to operate on raw data from Riegl and Faro scanner. This is a huge advantage of the software.

Next parts, when the models were already created were done on either OBJ or STL formats. One model was tested in VRLM format but the software could read it. OBJ is also the format that all the final models are stored. It was also easier to import final datasets into SimLab software to create a 3D PDF files.

Together with formats, different tools were described, the following group has been chosen because of availability and alternative approaches to the topic in each of them.

Algorithms that are commonly use for triangulation were also included. This part is very important for basic understanding the main process within the thesis.

2.8 Main applications

2.8.1 Overview

In last few years terrestrial laser scanning has become a regular piece of surveying methods, used in wide variety of fields like architecture, geomatics, mobile mapping, manufacturing, engineering and medicine. In this chapter the example of terrestrial laser scanners applications will be presented. Applications of airborne laser scanners will be mentioned briefly within the overview part.

Airborne laser scanning gained significant meaning in number of applications. It is a very valuable tool in case of forestry applications, Geographical Information Systems (GIS) and all complex and large areas that need to be investigated. Nevertheless, the most popular product of airborne laser scanning is a digital terrain model (DTM) which helps to understand landscape of many complex areas, including historical ones. Through DTM the elevation data are available which might be very suitable for mainstream GIS. Application in forestry consists of quite range and complex 3D modeling task, such as forest inventory, forest management, carbon sink analysis, biodiversity characterization, ecosystem analysis and habitat analysis. [20]

2.8.2 Engineering Applications

Engineering applications include both airborne and terrestrial laser scanning for monitoring and control of newly built and already existing infrastructures. However, greater importance is assigned to a TLS due to higher accuracy. It has become an alternative to traditional surveying techniques. Laser scanning has a wide range of application in areas with poor access, for example industrial plants or under hazardous conditions. Expansion of laser scanning within the engineering works allowed researches and companies for construction of different as-built models of engineering projects and for monitoring their conditions and safety.[20] The modeling procedures, though still requires comprehensive user interaction which still is a time-consuming task.

2.8.3 Mobile mapping

Basically there are two modes of terrestrial laser scanning techniques: the static mode (typical laser scanners mounted on the tripod) and kinematic mode (mobile mapping system). In the latter one scanner position and orientation is variable during scan time what brings us many analogies to airborne laser scanning. [20] Observation of objects such as building facades placed on the large area, rail-road tracks and road scenes takes less time if the kinematic mode is used.

Because of continuous movement of the laser scanner each scan point relates to a different coordinate system. The same principle as in airborne laser scanning, mobile mapping data has to be georeferenced to one, unique, spatial coordinates system (for example WGS84). Hence, respective position and orientation is observed by introducing GNSS system (global navigation satellite system) for positioning and IMU system (inertial measurement unit) for orientation.[20]

Usually, entire imaging sensor (laser scanning with GNSS and IMU systems, digital camera and time referencing unit) is mounted on a moving platform and this platform is usually placed on a motor vehicle, trolley or train. However, there are some examples for introducing a handheld mobile 3D laser mapping system. Studies on handheld 3D mapping system are described in an article of R. Zlot, M. Bosse, K. Greenop, Z. Jarzab, E. Juckes, J. Roberts, 'Efficiently capturing large, complex cultural heritage sites with a handheld mobile 3D laser mapping system.' [25]

2.8.3.1 Handheld mobile 3D laser mapping system- 'Zebedee' project in Australia

Authors of the paper explored the use of a recently developed handheld mobile mapping system called '*Zebedee*' in cultural heritage applications. Mentioned system is capable to successfully map an area in 3D by continuously acquiring data as an operator is holding the device while walking through the site. The system was developed at the Peel Island Lazaret in Queensland, Australia. The site consists of numbers of buildings in different sizes, spread through the area of around 400×250 m. [25]

The site was measured in half of the day with the '*Zebedee*' system and a 3D point cloud model consists of 520 million points was acquired. The system accurately captured both the context and details of the buildings. Processing of raw data took less time than the acquisition

was proceeded automatically without human work. The '*Zebedee*' system was also enhanced by adding a video camera due to possibility of generating a true-color models. [25]

Figure 2.9 presents components of '*Zebedee*' handheld 3D system. Components include handheld sensing device, acquisition laptop and battery. [25]

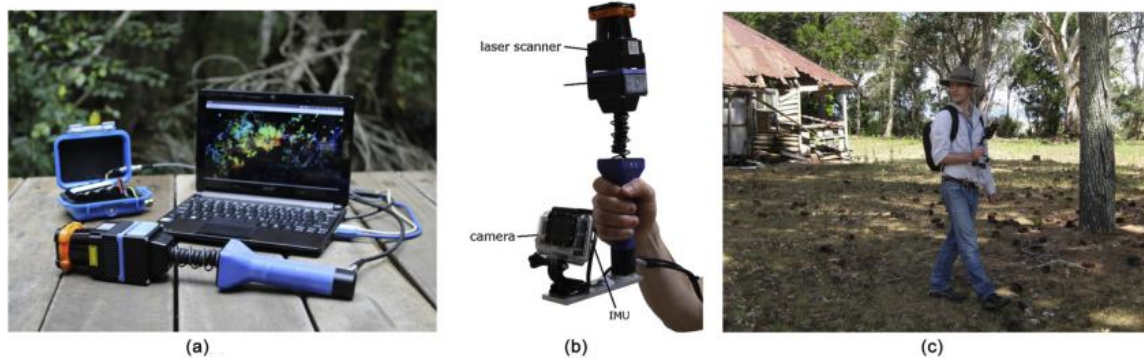


Figure 2.9. a: components of '*Zebedee*' handheld 3D mapping system, b: a modified '*Zebedee*' system containing a GoPro camera mounted in front of the handle, c: '*Zebedee*' system in use on Peel Island. (Source: [25]).

The primary sensor of the '*Zebedee*' system is a 2D laser scanner with ability of capturing 43,200 points per second. The system is based on time-of-flight principle of an infrared laser pulse. Extension of '*Zebedee*' system from two-dimensional field of view into a three-dimensional field of view was done by attaching a flexible spring that connects the scanner to the device's handle. [25].

The spring allows the scanner to pivot relatively freely (sweeping up to 170° in amplitude and tuned to a desired frequency of approximately 0.5 Hz) as a result of the operator's natural walking or arm motion. [25]

The inertial measurement unit which estimates the scanner's orientation is mounted on scanner's spring. To transform raw measurements into coherent 3D point cloud there must be scanner trajectory available. Computations are carried out based on the sensor measurement-laser and IMU. Additionally, the system consists of small laptop for acquiring data with very resistant lithium-ion battery. [25]

Workflow

Place, Peel Island, chosen for 'Zebedee' experiments is located few kilometers off the coast of Brisbane, Australia. The place is highly important for both Aboriginal and colonial cultural heritage. The entire area consists of dozens of small huts designed for different groups of people to inhabit and as well other types of buildings. Complex physical attributes of the site (buildings are in different states of repair, ones fully restored others completely destroyed) demands highly advanced documentation. Traditional methods for capturing this type of area have proved impracticality and inefficiency in using.

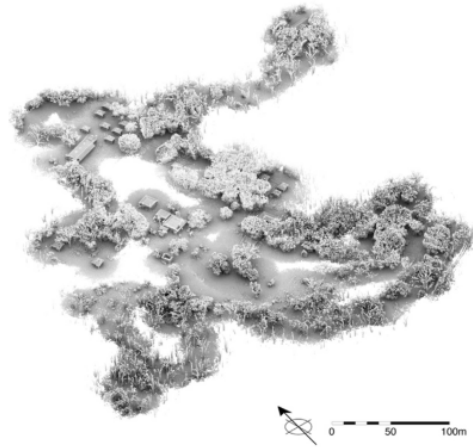
For approximately four hours, 13 overlapping datasets covered various section of the Peel Island site, was acquired. During entire capturing time, operators tried to maintain paths remote from the nearest structures within about 10 meters. Good distribution of surface normals visible from the scanner was also very important. It was recommended to introduce loops in the operator's paths to guarantee sufficient overlap amount. Mostly, initial processing of raw data was carried out in the field- trajectory estimation and point cloud model. Next step was to align and merge individual models into one 3D model including 520 million points.[25]

Results

Processing all datasets required around 56-67 % of the time of collecting the data, which brings the possibility of processing data in real-time during capturing. [25] Just over 20 minutes took combining and registering in one coordinate system all of data sets.

Figure 2.10 illustrates the model of the site produced by the 'Zebedee' system, which allows for a detailed investigation of individual buildings, both their internal and structural features. The median point spacing for whole Peel Island site is about 1 cm. The walls , floors and other structures were well captured as well as internal fittings and furniture. When access difficulties occurred, operators were capable to reach in through windows and doors. [25]

a



b



Figure 2.10. a: Point cloud of the Peel Island Lazaret generated from '*Zebedee*' data, b: aerial view of rendered *Zebedee* point cloud, the point cloud has been subsampled to 9% of the original data. (Source: [25])

As there can be noticed the invention of '*Zebedee*' system has an opportunity to change and influence large-scale site documentation in cultural heritage applications. The system provides faster scanning, quick and automatic data processing and possibility to access unobtainable areas. The basic precision of the measurements is in the order of 2-3 cm. Solutions for better accuracy are being investigated. Integrating '*Zebedee*' system with traditional methods of capturing could also improve precision and range limitations. [25].

Modeling sites like Peel Island Lazaret is necessary in case of conservation monitoring and documentation, continuation of the research and virtual tourism and education. Handheld 3D mapping system ensures a large step forward more accessible techniques for 3D data collection. [25].

2.8.4 Cultural heritage and architectural application

Centuries after centuries humanity have gathered enormous number of impressive monuments with its immeasurable value. This obviously forced to discover and develop new techniques for documentation and capturing historically important places. 3D laser scanning methodology combines often with photogrammetry is the newest and the quickest solution for the documentation. Generally, main objective in introducing documentation of valuable monuments at all, is a necessity to prevent and restore objects in case of possible damages. Crucial in preventing significant defect is a chance to control historic objects, analyzing their faults and eventual future consequences.

Cultural heritage is, therefore, a wide range of testimony of past human activity. Objects characterize in great variety of their nature, size and complexity, from small artifacts and museum items to cultural landscapes, from historic buildings and ancient monuments to city centers and archeological sites [20].

Laser scanners work on one of three ranging principles, as mentioned in chapter 2-paragraph 2.3, triangulation, time of flight and phase comparison. Usually, the accuracy and resolution of measurements depends on the size of an object. The larger the object the lower accuracy can be achieved.[2] As should be notice, cultural heritage applications demand high accuracy within the acquisition methods. There are numbers of small details that should be captured. Table 1 presents all available methods for recording and document cultural heritage objects together with typical accuracy. The table was adapted from the Technical Report of English Heritage 2011, [2]. All bellow techniques were described or mentioned in Chapter 2-paragraph 2.3

Table 1. Laser scanning techniques used in cultural heritage management activities. (Source: [2])

Scanning system	Use	Typical accuracy/operating range
Triangulation-based scanners	Rotation stage	<ul style="list-style-type: none"> · scanning small objects · To produce data suitable for a replica of the object to be made 50 microns/ 0,1m-1m
	Arm mounted	<ul style="list-style-type: none"> · small objects and small surfaces · performed on the site if necessary · to produce replica 50 microns/ 0,1m-1m
	Mirror/prism	<ul style="list-style-type: none"> · small object surface areas · to produce replica sub-mm/0,1m-25m
Terrestrial time of flight	<ul style="list-style-type: none"> · to survey buildings facades and interiors with results as line drawings and surface models 	3-6 mm at ranges up to several hundreds meters
Terrestrial phase comparison	<ul style="list-style-type: none"> · to survey buildings facades and interiors with results as line drawings and surface models- specially when rapid data acquisition and high point density are required 	5 mm at ranges up to 50-100 m
Airborne laser scanning	<ul style="list-style-type: none"> · to map and prospect landscape 	0,05 m + (depending on the parameters of the survey)/ 100-3500m
Mobile mapping	<ul style="list-style-type: none"> · to measure highways and railways · city models · monitoring coastal erosion · large cultural sites 	10-15 mm/ 100-200m

Laser scanning is unlikely to be performed in insulation and that is why usually with cultural heritage applications the photogrammetry finds its application. Images are collected on site to ensure high level of presentation. Photographs are used to attribute colors to the data as they occur in real life. The process is called coloring the point cloud.

The variety of applications includes pure visualization, heritage recording and documentation for further restoration or revitalization process. [20]

Few basic tasks potentially suitable for the application of laser scanning were mentioned in [2]. Laser scanning though has an influence in design process and archive

record, it might help when a feature, structure or site is in danger of destroying and changing forever. 3D capturing has also influence in investigation of the behavior of an object in response to weather, pollution or vandalism. It makes possible to create a replica of an object by providing an accurate digital geometric model. Generating a 3D models, animations and illustrations will help to improve understanding contemporary visitor centers, museums and monuments. [2]

2.8.4.1 Modeling the thickness of vaults in the church of Santa Maria de Magdalena (Valencia, Spain) with laser scanning techniques.

One of very interesting and recent project using terrestrial laser scanning techniques within cultural heritage application was conducted in Valencia, Spain. Entire work of J. Herraes, P.Navarro, J.L.Denia, M.T.Martin and J. Rodriguez is describe in an article *Modeling the thickness of vaults in the church of Santa Maria de Magdalena (Valencia, Spain) with laser scanning techniques*. [6] As the title suggests the state-of-art of the project was to calculate the thickness of vaults in the Church. By combining the interior and exterior 3D representation it was easy to establish the difference between vaults inside the Church and the roof. Although, the problem was with the interior of both geometries, which is entirely unknown. The paper presents methods used to model interior sections of the vault and determine the thickness of it. The objective was to obtain a complete model of the Church, especially including invisible part under the roof for the purpose of structural consolidation project. Figure 2.11 presents the overall situation of the object together with inside of the Church, inside of the vaults under the roof and roof. [6]



Figure 2.11. Situation of the Church of Santa Maria de Magdalena, left: interior of the church, middle: exterior of the church, right: interior of the vaults (Source: [6])

The main issue resulting from lack of visibility between parts of the object was to register all scans together. There were no common points to merge point clouds. System implemented to handle the problem consists of few plumb lines with spheres, scanned from inside of the church as well as from inside of the vaults. In order to mount plumb lines, few, already existing holes were used. Figure 2.12. shows how the system was fixed with the help of tripods and 4kg load.



Figure 2.12. Plumb line system used to reference all three models together, left: tripod with a plumb line inside of the vault, middle: plumb line from inside of the church with the load, right: plumb line from inside of the church with spheres (Source: [6])

General field work includes performing 25 scans inside of the Church, 16 scans for exterior part of the object and 6 scans of the interior corridor of the invisible part. Additionally, there were three more scans for the purpose of registration the interior of whole Church with the exterior. After generating three main 3D models, scanning of the plumb lines was carried out. Authors used three lines with two spheres on each. The distance between spheres were determined and the plumb lines were raised up so one sphere was inside of the church and one was inside of the vault. Registration required calculation the centers of the spheres in both coordinate systems, what was done by applying the Cayley matrix.

Solution implemented in this case ensured lack of errors in the coordinates and eliminated questions regarding orientation error when joining two models.

Any similar project when no common points are visible requires to implement conditions that allow to establish one absolute system. Methodology presented in the article can be develop and used in certain situations when no common objects exist.

2.8.5 Forensic application

3D laser scanning devices enable to acquire millions of data points at a crime scene with high precision and saving time. As mentioned before the result of capturing the scene is a 3D point cloud that allows for virtual analyzing and examination of the area of investigation. 3D models, produced nowadays by numerous of different producers, take an advantage in a wide range of investigative fields, that includes crime, fires and road accidents.

Usually, crime scenes need to be documented in a very challenging timing. Complex of the scene makes it even more difficult. In comparison to the old methods used within forensic documentation, 3D laser techniques work perfectly, more efficient, faster and more accurate.

Documentation of the scene required to be fully complete, accurate and done at the minimum invasiveness and time. Conventional methods such as wheels measuring, tape measures and digital camera both with video camera do not meet all the requirements of documenting crime scenes.

Figure 2.13. presents the example of 3D modeling the crime scene. The picture is excerpted from the article [16] .



Figure2.13. Crime scene capture by a 3D sensor (Source: [16])

Basically, the main advantage of using 3D sensors to obtain information from the crime scene is the time that is used for gathering data. Introducing laser scanners on the scene, forensic specialist save lot of time. Furthermore, all necessary measurement can be proceed with millimeter accuracy.

2.8.5 Summary

As proved above, terrestrial laser scanning finds multiple application in wide variety of fields. All of these disciplines are connected together by the final result that should be obtained. All the time, new and innovative projects are being carried out. Combining different techniques is highly important and more and more popular.

CHAPTER 3

3.1 Overview

This chapter intends to present both implementation of the project, showing each step of work as well as processing of acquired data in order to accomplish goals stated in chapter1.

One of the purposes of this chapter is to present and understand how the project was conducted. The work flow of the thesis will be shown here. This includes description of each process within the work, preparations, planning, descriptions of objects and functions of used tools. The results will be presented both by writing explanation as also by images from software.

As one of the main objective of the thesis is to compare different tools in terms of efficiency, accuracy, intuitiveness, accessibility and general visual effects, all information concerning testing each software should be included in this paragraph.

Presented project is meant to be an attempt to show different possible approaches to overcome some obstructions connected to reverse engineering as well as to present current tools available on market. The results might not be the best solution for the defined problem and might not work for any other similar projects.

3.2 Research and planning

Today the 3D laser scanning techniques represents the most advanced methods accessible for measuring and documenting objects, landscapes and structures. In order to realize any project based on application of 3D techniques careful preparations are highly needed.

First of all, all information about objects of interest is necessary. The test case for this paper are two different data sets. One , the western wall inside the Nidaros Cathedral in Trondheim, Norway and second one, well-preserved, one of the oldest building within the technical campus (Gløshaugen) of the Norwegian University of Science and Technology - Østre Gløshaugen , meaning the Eastern Gløshaugen. Short description of each object is placed in the paragraphs 3.3 in following chapter.

One of the first factor to think about is the accuracy. It is important to think what accuracy can be provided by the particular system available and the accuracy that should be obtained within the object of interest. Another issues is to plan possible scan stations, which will cover all the surface of the object and in the same time will ensure the overlapping areas between neighboring scans. During this step of preparations it is useful to do an investigation on site. Not only investigate the object for overlapping areas but also for capturing all details which should be preserve. As a result of on-site planning , the map with possible scan's stations was created (Appendix 1).

Another point to think about before starting the measurements is how to merge all scans together. Are we going to use tie points, checkerboards, spheres, do we need a global coordinate system. This procedure is called registration and can be done in different ways depending on 3D scanner system. The basic principle standing behind the registration is to use reference objects that are common for at least two scan positions. Solutions used during the data acquisition are described in the paragraph 3.4.

3.3 Objects

3.3.1 Nidaros Cathedral in Trondheim, Norway

Nidaros Cathedral was the object of study within the Specialization Project course conducted at NTNU, fall 2013. People responsible for restoration and maintance the Nidaros Cathedral have cooperated with NTNU in several projects to explore methods for 3D documentation of parts of the building. In 2013 the western end of the nave was visible and accessible because the large Steinmeyer organ was taken away for restoration. The work was commissioned by the NDR Restoration (Nidaros Domkirkes Restaureringsarbeider). That was a unique opportunity for documenting the inside of this part of the building, and in June 2013, measurements and data collection was carried out with both photogrammetry and laser scanning. The 3D system used during measurement was RIEGL LMS-Z420i which consists of a high performance long-range 3D scanner, processing software RiSCAN PRO and calibrated high resolution digital camera-Nikon D200. The goal of the project was to create a 3D model with the acquired data, textured from photos. It should be useful product for geometrical documentation as well as for display. Within the project only the Riegl software was used. The same data was used again in this paper in order to improve the results and compare different possible tools. As a whole work flow of preparation, registration and

filtering of data was described in the Specialization Project, here only the final results will be attached. In this thesis, the work with the second object of investigation will be emphasized.

Nidaros Cathedral is the largest and northernmost medieval cathedral in Scandinavia, built over the tomb of St. Olav. The oldest parts are from the 12th century. It is the traditional location for the consecration of the King of Norway. The history of this magnificent building began in 1035, and the Cathedral was completed around 1300. Being damaged by several fires in the 15th and 16th century, large parts of the Cathedral lay in ruins for several hundred years.

In 1869 extensive restorations began, and a century later the Cathedral was fully restored to its original size. [9] A re-built copy of the Cathedral is an example of neo-Gothic architecture. On the front wall of the monument there are 57 sculptures of apostles and saints. Below -Figure 3.1 shows a picture of the Cathedral from outside and the picture of the western wall inside of the object.



Figure 3.1. Nidaros Cathedral in Trondheim, Norway. Left image: The West Front of the Cathedral (Source: [9]), right image: west wall of the inside of the Cathedral (Source: [17]).

3.3.2 ØstreGløshaugen

Second object of investigation was chosen to satisfy few conditions set up in the beginning. It should be a medium-sized, historical building, easily accessible from each side. Trondheim is full of old monuments and churches that could use the 3D documentation. However, for the purpose of this master thesis, one of the oldest NTNU's building was chosen. It is valuable in terms of historical, the access to each side is assured and additionally it is not too far away to carry the equipment.

Østre Gløshaugen has been a part of Campus NTNU Gløshaugen, Trondheim since 1957. The building was built in 1872 as a summer house for merchant Halvor Jenssen. Henrich Ernst Schirmer was a probable architect. It has been restored and is used as local for Gløshaugen academic club. The building is included in the land protection plan.

The building has lot of small details around the roof, there is also a complicated pattern in the front wall, above the entrance. Each side of the building is covered by numerous tabs.

Figure 3.2. presents the current stage of the building.



Figure 3.2. Present stage of the Østre Gløshaugen building (Author: Joanna Setkowicz)

3.4 Data acquisition

Equipment used while carrying out all necessary measurements consists of two different 3D scanner systems- Riegl LMS-Z420i and Faro Focus 3D Scanner. Additionally, Riegl system is equipped with digital camera- Nikon D200. In order to acquire a global system within the object, the GNSS Leica Viva system was used.

3.4.1 Laser scanning surveying

3.4.1.1 Riegl 3D system

As a first 3D system, the Riegl LMS-Z420i was used. The same one as within Nidaros Cathedral project. The system is durable and fully mobile sensor designed for rapid data acquisition of three-dimensional images. [14] Specification was downloaded from the producer's web page and is attached in the Appendix 4. As mentioned before, the system consists of high performance long-range 3D scanner, processing software RiSCAN PRO and calibrated high-resolution digital camera-Nikon D 200. [14].Field work with the Riegl system is presented in the Figure 3.3.

The measurements were conducted on 1st of March, 2014. The temperature on the working day was very low- around 2-3 °C with strong wind for whole day. The scanner required additional cover in order to work properly. Controlling the scanner is done through the portable computer equipped with RiSCAN PRO software. The camera is mounted on top of the scanner.



Figure 3.3. Field work with Riegl LMS VZ420i scanner (Author: Joanna Setkowicz)

The desired final resolution was established at around 0,5 cm for 10 m. The resolution depends on the distance between the sensor and the object. This distance was not bigger than 20 m which gives resolution between 0,5 cm - 1,0 cm depending on the distance.

Usually registration of adjacent single scans within the Riegl system is carried out using tie points. Tie points are represented by retro-reflective targets- flat 5 cm diameter reflectors placed around the area. RiSCAN PRO is able to extract reflectors from overview or panorama scans and automatically detect them. When sufficient number of tie points is fixed, scan data can be transformed into project coordinate system. [15] During the measurement there were 15 tie points, including four reflectors with global coordinates. Three of them were fixed few years ago by another student conducting laser scanning measurements nearby and one was introduced for the purpose of this thesis. The new one was placed on the tripod and measured by GNSS system. During the registration procedure the goal was to use at least 5 common tie points for each pair of adjacent scans. Mathematically sufficient is to acquire only 3 reference objects, however surveying work always aiming in having more observations than necessary ones.

Additionally, to obtain global coordinate system of the object, three out of four scan stations were measured by GNSS equipment. The antenna was mounted on the top of the sensor.

In total 4 scan positions were taken, each from one of the corner of the building, but due to the heavy conditions and not that easily portable equipment, whole time needed for finishing field work was about 6-7 hours. Finally, four point clouds were acquired with numbers of points accordingly :

SP01- 15 221 411 points

SP02- 13 665 332 points

SP03- 17 124 114 points

SP04-10 654 566 points

In total, entire building was captured with around 55 millions points.

3.4.1.2 Faro Focus 3D

The idea of using another 3D sensor came as a possibility to acquire more precise and bigger amount of data in shorter time. Faro Focus 3D scanner belongs to the architecture department at NTNU and was kindly provided to the geomatics department for few weeks. In this way the additional objective appeared, merging two different data sets from two 3D sensors became a part of the thesis.

The model Faro Focus 3D s 120 was used during acquisition, specification, downloaded from the producer's page is attached in Appendix 5. Following the description of equipment, it is a high-speed 3D laser sensor perfect for detailed measurement and documentation. The scanner is controlled by touch operated screen. The whole equipment can be carried in only three suitcases what makes the Faro Focus system very easy portable. [4] The simplicity of the whole Faro system is shown in the Figure 3.4.



Figure 3.4. Faro Focus 3D s120 in the field. (Author: Joanna Setkowicz)

Field work was carried out on 30th of March, 2014. The weather conditions were satisfying, only strong wind sometimes made the work harder. As can be seen Faro Focus sensor is not quite good resistant for wind.

The resolution was established in the way to get similar results with Riegl's equipment. For the distance of 10 m the resolution was set for 6,136 mm. In Faro Focus 3D system there is also a setting called Quality that can be fixed before scanning. The quality has an influence on quality of the scan and the scanning time with constant resolution. More higher level of Quality more noises are being reduced. Levels of quality are divided from 3 times-8 times. Within the project , 4 times quality was chosen which allowed to keep the resolution at the 6 mm level and in the same time acquire data in a short time. At each scan position, detailed scan took around 9 minutes.

Faro scan positions were planned as a supplement to scan data acquired before with Riegl sensor. That is why more attention was turned to the front wall of the building, where more details have to be captured. The map of Faro scan positions is enclosed in the Appendix3.

To register all scans to one coordinate system, Faro Focus system mostly uses spheres. They can be attached to the wall or fixed on the ground. There is also a possibility to use checkerboards. This time only spheres were used. On the contrary to RiSCAN PRO, Faro Scene-software package for processing Faro Focus data, does not use panorama scans to extract spheres. They have to be placed in the area of detailed scans if that ones are going to be processed later. The same as before the aim was to place spheres in the way that at least 5 of them will be visible for two scans.

In total there were 7 new positions with the final time for the entire field work was about 4 hours. Finally, 7 point clouds were captured with total number of points:

SP01- 16 055 665 (57 MB)

SP02-25 627 408 (83 MB)

SP03-29 848 646 (88 MB)

SP04-27 433 223 (103 MB)

SP05- 25 433 211 (80 MB)

SP06- 25 009 344 (85 MB)

SP07- 19 229 990 (65 MB)

Total number of points for entire building was equal around 166 millions . As can be compared with Riegl, it is almost twice as many points as in Riegl case. Together both datasets create huge point clouds to process. Necessary filters need to be done.

3.4.1.3 Comparison of both datasets

In following paragraph few examples of differences between Riegl dataset and FARO dataset will be shown. As can be seen in the figure data are slightly different. In concerns mostly noises and accuracy in details.

Figure 3.5. presents the same area acquired by Riegl sensor and by Faro sensor.

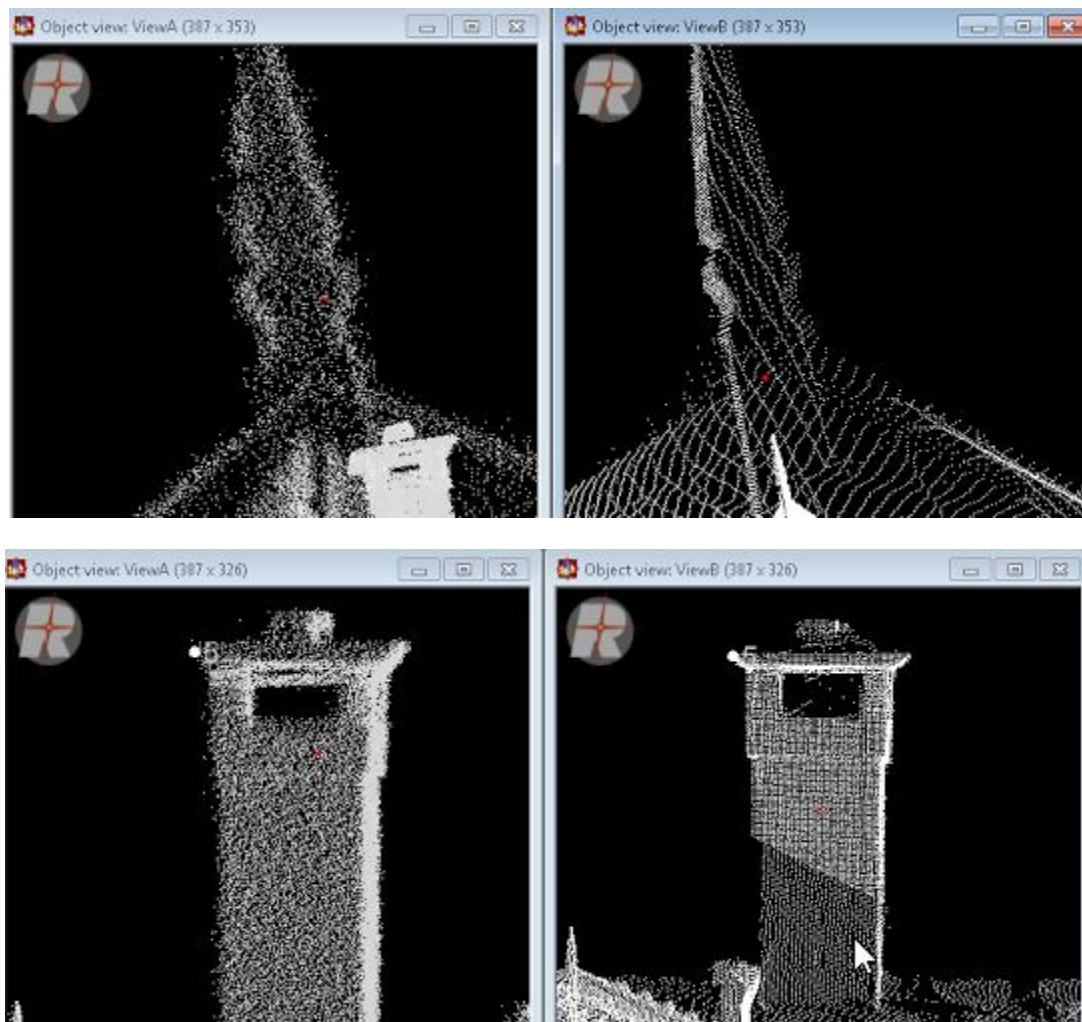


Figure 3.5. Comparison of data acquired by Riegl sensor (left) and Faro sensor (right).

As can be seen in both examples, Faro data are more precise and don not include too much noise around the object. As will be also presented later, mesh generated only with

FARO data is way more arranged without too much noise. However, compilation of both datasets is the best solution.

3.4.2 Image acquisition

In order to acquire images , which later can be used for texturing the 3D model, Nikon D200 was used. The digital camera with focal length of 20 mm. Camera calibration and camera mounting was imported from the original Riegl file, both from 2013.

As the Faro Focus does not support any external digital camera mounted on top the only solution was to take free images and later register them to point clouds. However, there is a possibility to acquire RGB values by internal camera in Faro Focus, but the quality of the colors is very poor.

Free images were decided to take not only because of Faro Focus equipment. During last Riegl scan position , the sun was almost down and it resulted with completely different brightness on part of the building.

In the end, in order to proceed with texture and coloring scans, free images were used. They were taken another, sunny day. In total, 17 images were acquired. Settings used during acquisition: aperture: f/5.6 and exposure time: 1/60 sec, ISO-100 .

3.4.3 GNSS measurements

As mentioned before, the global coordinate system should be introduced. To do so, GNSS system was used. One of the newest sets of receiver and controller from Leica Geosystem, Leica Viva GS 15 and CS15 were available. Specifications for both, controller and receiver are attached in Appendix 7 and 8.

In Appendix 2, a map showing the scheme of stations were GNSS was used as well as points which have had already global coordinates, can be found.

All measurements were accomplished by RTK technology with few centimeters accuracy. GPS measurements were carried out during first day of field work with Riegl VZ 420i sensor.

GPS measurements encompassed three scan positions- 1, 2 and 4. Position 3 was not suitable due to location near to a huge building. Part of the horizon was completely covered.

Each station was measured three times. The receiver was attached on top of the scanner. Special equipment to mount the receiver was attached to Riegl 3D system.

To acquire correct height of scan position, the difference between laser beam and the level zero for GPS measurements, should be taken into account. This difference in case of used equipment is 366 mm. Each Z-coordinate, was corrected accordingly.

Furthermore, few points, with already known global coordinates, which were also included into calculations, required transformation of the height systems that was used. Few years ago, when they were measured, system NN1954 was valid, nowadays system NN2000 is introduced. Transformation of heights was conducted in land surveying software- GisLine.

Table 2.presents results of GPS measurements. Calculations of corrected height are attached in the last column. Coordinates N', E', H' are estimated as a mean value of three measurements. Value ΔH whereas represents the final height of each point. It includes the difference between the zero level of GPS and the laser beam coming out and in point. Control point CP01 was an additional control point which was not a scan position. The reflector was fixed on the tripod where later the GPC receiver measured the coordinates. That is why ΔH of SP01, SP02 and SP04 was calculated according to the equation 2 and ΔH of CP01 used equation 3.

$$\Delta H = H' - 0,366 [m] \quad (2)$$

Value 0,366 m, in equation 2, stands for the difference between the point where the laser beam goes out and in and the zero level of GPS receiver.

$$\Delta H = H' + 0,122 [m] \quad (3)$$

Value 0,122 m, in equation 3, applies only to point CP01 and is the difference between the middle of reflector and the zero level of GPS receiver on this point.

Table 2. Results of GNSS measurements

	$N(X) [m]$	$E(Y) [m]$	$H [m]$	$CQ [m]$	$N'(X) [m]$	$E'(Y) [m]$	$H' [m]$	ΔH
<i>SP01</i>	7033128,264	570082,366	48,625	0,011	7033128,264	570082,366	48,621	48,255
	7033128,264	570082,366	48,623	0,010				
	7033128,263	570082,366	48,616	0,012				
<i>CP01</i>	7033140,447	570075,455	47,796	0,011	7033140,445	570075,450	47,794	47,916
	7033140,446	570075,450	47,795	0,011				
	7033140,443	570075,446	47,791	0,015				
<i>SP02</i>	7033123,174	570047,767	48,108	0,011	7033123,174	570047,767	48,112	47,746
	7033123,174	570047,768	48,116	0,011				
	7033123,173	570047,766	48,113	0,010				
<i>SP04</i>	7033097,840	570082,884	48,171	0,029	7033097,839	570082,883	48,168	47,802
	7033097,841	570082,882	48,164	0,030				
	7033097,837	570082,882	48,157	0,030				

List of coordinates of all control points is enclosed in table 3.

Table 3. Global coordinates of control points.

<i>ID</i>	$N(X) [m]$	$E(Y) [m]$	H_{NN1954}	H_{NN2000}
<i>108</i>	7033078,318	570069,701	48,610	48,748
<i>109</i>	7033062,852	570063,427	48,731	48,869
<i>110</i>	7033089,748	570047,033	49,102	49,240
<i>CP01</i>	7033140,445	570075,450		47,916
<i>SP01</i>	7033128,264	570082,366		48,255
<i>SP02</i>	7033123,174	570047,767		47,746
<i>SP04</i>	7033097,839	570082,883		47,802

3.5 Data registration

As the data was obtained by two different 3D sensors not only the project coordinate system of each datasets was the task of the registration but also finding the common coordinate system for Faro and Riegl datasets together was a challenge. Additionally, both sets need to be connected to global coordinate system.

Basic principle of registration scan data is to place and then scan reference objects, for instance reflectors or spheres, in the way that at least 3 of them are visible in adjacent scans. There is also a possibility to use natural targets as corners or some edges that can be unambiguously recognized.

In general, three types of coordinate systems can be connected to all types of 3D measurements. Figure 3.6. presents division for these basic coordinate systems that occur within the laser scanning.

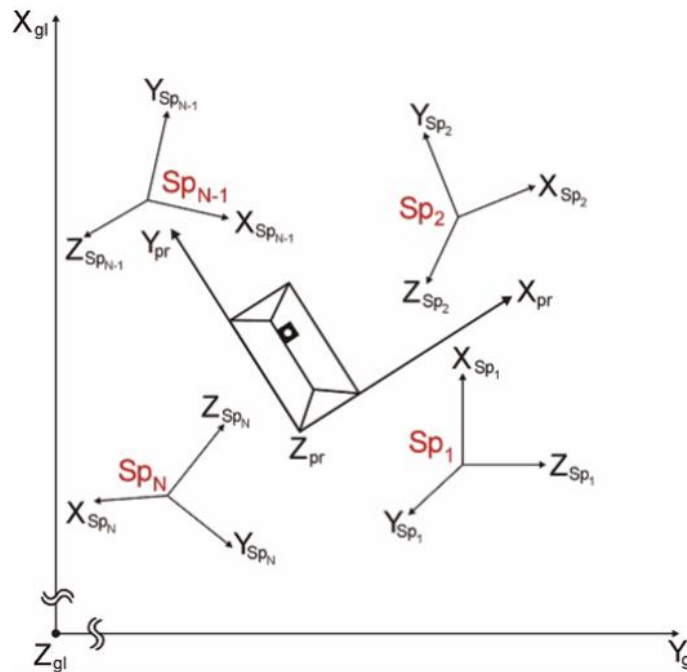


Figure 3.6. Three types of coordinate systems connected to scan data. (Source: [15])

Scanner's Own Coordinate System (SOCS) – coordinates system of the raw data delivered by the scanner. All data acquired by 3D laser scanner contain geometry information (Cartesian x,y,z or polar r, φ, Θ coordinates). That makes the output of 3D laser scanning an organized point cloud.

Project Coordinates System (PRCS)-is defined by a user and brings all scanner coordinate systems into the one common for the whole object. In majority of software packages the coordinates of this system need to be shorter than specified value. It is required due to accuracy that can be lost if the coordinates are too big.

Global Coordinate System (GLCS) - is the coordinate system that includes project coordinate system, usually it contains large numbers and is normally introduced by total station measurements or GPS measurements.

Above terminology is derived from Riegl materials but can apply to any types of 3D measurements. It is presented here for better understanding the process of registration.

In general, initial data registration was performed in software packages that belong to each scanner company. For the Riegl's data, RiSCAN PRO was used and for FARO's data, FARO SCENE was used. Later two different ways of joining all point clouds were applied. First attempt was carried out within RiSCAN PRO software, where also global coordinate system was introduced and second solution was performed in PolyWorks package.

3.5.1 RiSCAN PRO registration

The most typical way to register data within the RiSCAN PRO is using tie points. It allows to register in one time data into project coordinate system as well into global coordinate system. The point here is to have sufficient number of tie points with known global coordinates.

Data within the case of Nidaros Cathedral was collected in the way to proceed with typical tie points registration. Whole workflow is described in Specialization Project, fall 2013. [17]

The case with the object of investigation within this master thesis (Østre Gløshaugen) was more complicated. Global coordinate system was decided to be introduced by only GPS measurements of scan positions supplemented by four control points around the area. Three of them were reflectors placed on buildings surrounding the object and one -CP01 was the control point mounted on tripod only for the Riegl measurements. The aim was to have at least 5 tie points for each pair of overlapping scans.

In order to calculate transformation between all coordinates system RiSCAN PRO uses two matrixes: SOP matrix, describes transformation between SOCS (Scanner's Own Coordinate System) and PRCS (Project Coordinate System) and POP matrix describes transformation between PRCS (Project Coordinate System) and GLCS (Global Coordinate System).

3.5.1.1 Import of control points

First the control points with global coordinate system were imported then the transformation to project coordinate system was performed. It is important to remember that coordinate X should be switched with coordinate Y. Translation parameters are shown in figure 3.7. In this was the project coordinates system is being described.

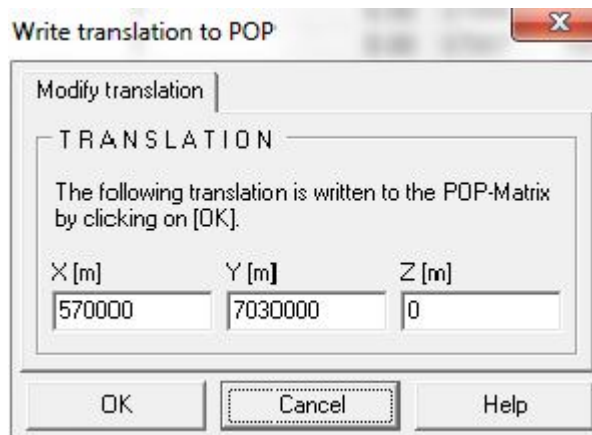


Figure 3.7. Translation parameters between global coordinate system and project coordinate system within RiSCAN PRO.

Having these types of data the best solution for registration was to combine both registration via tie points together with back sighting registration.

3.5.1.2 Back sighting orientation

The back sighting registration can be conducted based on well-known coordinates of scan position and coordinates of at least one certain point in the area. There is an option of basic back sighting registration (one additional point) and advanced back sighting orientation (two additional targets). Figure 3.8 shows the operation of advanced back sighting registration.

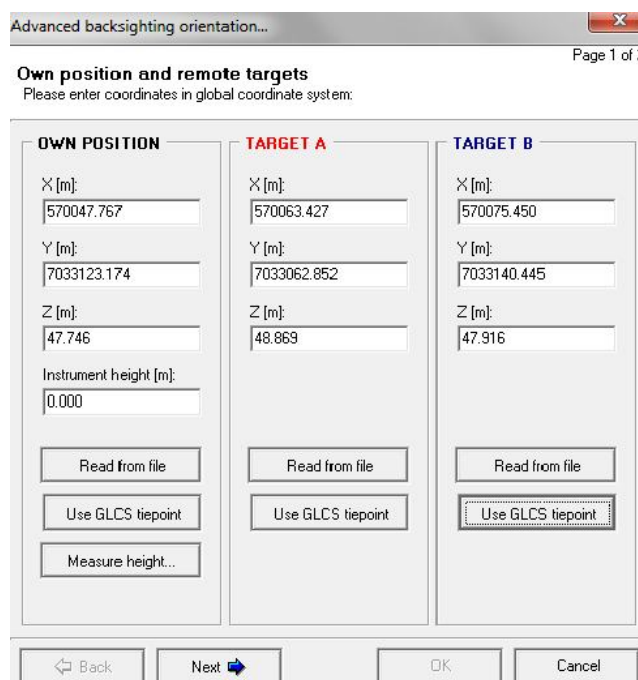


Figure 3.8. Advanced backsighting orientation within the RiSCAN PRO.

The workflow in this part was to register by advanced orientation position number 2. The position has good view for two other targets- point 109 and CP01 and seems to be the most stable. The result gives an average standard deviation at the level of 0,015 m.

Next, positions 1 and 4 were registered by simple backsighting orientation where only one additional point is used. In case of position 1, again point CP01 was used and position 4 was orientated on point 110.

Both ways of orientation requires introducing coordinates of additional points both in global and scanner coordinate system.

3.5.1.3 Registration via tie points

In order to finally accomplish full registration, all reference objects were used. This operation allowed merging all scans into one common coordinate system. As position 2 was decided to be a fixed position, registration was preceded on scan position 1, 3 and 4. Option *'Find corresponding points..'* within each scan position, provided the list of corresponding points between two position which were being registered. Additionally, statistic results were presented. On this point, there is a possibility to find the best arrangement of tie points. When, the lowest standard deviation together with maximum possible corresponding points are obtained, the registration can be considered to perform correctly. Table. 4 presents final results of registration .

Table 4. Statistic results of RiSCAN registration.

Scan Position	Number of corresponding points	Standard deviation [m]	Average radial deviation [m]	Average θ deviation [m]	Average φ deviation [m]
SP01	8	0,0039	-0,0008	0,0001	-0,0009
SP02	8	0,0056	0,0010	-0,0014	-0,0037
SP03	9	0,0059	-0,0009	-0,0007	-0,0024
SP04	7	0,0053	-0,0001	-0,0003	-0,0021

Evaluation of the registration process was also performed by comparison scan position's coordinates after the procedure with these acquired by GPS measurements. Table 5 shows results of the comparison.

Table 5. Coordinates of scan position before and after registration in RiSCAN PRO.

<i>ScanPosition</i>	X_{PRCS}^{GPS} [m]	Y_{PRCS}^{GPS} [m]	H_{PRCS}^{GPS} [m]	X_{PRCS} [m]	Y_{PRCS} [m]	H_{PRCS} [m]	ΔX [m]	ΔY [m]	ΔH [m]
<i>SP01</i>	82,366	3128,264	48,255	82,366	3128,265	48,279	0,000	0,001	0,024
<i>SP02</i>	47,767	3123,174	47,746	47,767	3123,174	47,746	0,000	0,000	0,000
<i>SP03</i>				48,932	3095,035	47,426			
<i>SP04</i>	82,883	3097,839	47,802	82,878	3097,806	47,764	-0,005	-0,033	-0,038

Above tables prove that despite of small number of control points, accuracy of registration was conducted with really decent results. Standard deviations do not exceed 6 mm what, according to Riegl Training materials [13], is consider as a very good result. Additionally, table 5 demonstrates that coordinates of scan positions before and after registration have similar values and correspond to coordinates acquired by GPS system.

3.5.1.4 Summary

One of the conclusions while analyzing results is that the methodology applied during measurements cannot be counted as the easy one. It obviously saved a lot of time in the field since GNSS data were acquired much faster than traditional total station technique. Moreover, GPS data does not require post processing. Coordinates are available immediately. The drawback of this solution was necessity to combine several methods to register all data to one project coordinate system and to the entire global system. Results would probably improve when using more tie points with known coordinate system. In comparison to the Nidaros Cathedral project where traditional method was used with total station measurements, accuracy is slightly worse. However, presented results are sufficient to continue with next step of post-processing.

3.5.2 FARO registration

Second dataset was acquired with completely different 3D system what required different approach to registration process. In order to merge raw data from Faro Focus 3D scanner, Faro Scene software package needs to be used. Also different reference objects are necessary. Within this project only spheres and natural targets were used. The arrangement of scanner positions is shown in Appendix 3.

Registration operation within Faro Scene was slightly easier since only project coordinate system was desired. Data for global coordinate system were not available. Global coordinates were introduced in the next step of the project while merging Faro scans with Riegl data.

Entire process of orientation is done automatically. To extract spheres, checkerboards and natural targets ‘Pre-processing’ tool is used. Next, all points that were not detected should be marked manually by adding markers in Quick View. When all necessary points are detected tool ‘Place Scans Auto’ tool can be used. First the initial registration is performed then option ‘Fine registration’ is added.

Scan Manager contains all statistic information about the final registration. Table 6.presents them together with number of points used as a reference objects.

Table 6. Statistic results of FARO registration.

<i>Scan Position</i>	<i>Number of spheres</i>	<i>Number of natural targets</i>	<i>Tensions</i>	<i>Weighted statistic</i>	
				<i>Average tension</i>	<i>Deviation</i>
<i>SP01</i>	4	3	0,0033	0,0035	0,0049
<i>SP02</i>	6	2	0,0038		
<i>SP03</i>	4	2	0,0053		
<i>SP04</i>	4	1	0,0019		
<i>SP05</i>	6	0	0,0017		
<i>SP06</i>	4	1	0,0016		
<i>SP07</i>	2	4	0,0059		

Faro Scene uses different terminology for presenting results. Tensions can be explained as a value that describes divergence in the general coordinate system between the orientation and position of the pair of corresponding reference targets in two adjacent scans.

3.5.3 Free image registration

In order to obtain uniform textured model, set of free images were taken. Images taken during first day of scanning with Riegl system were taken in different light conditions and were useless for texturing. During image acquisition the same camera was used with already known calibration. In total, 17 images were taken.

Free images are images acquired while camera was not mounted on top of the scanner. Hence, those images are not automatically registered. To register these images, into the Project coordinate system, RiSCAN PRO was used. It offers two options of proceeding with image registration. First one includes tie points, second one angle definition. In the project, the option with tie points was decided to perform.

This tool allows to register project images that have been acquired from any position in the scan area. The COP matrix, describing the registration, is computed by pointing relations between points within point clouds and points in an image. To proceed with the registration, all scan positions need to be registered, also right camera calibration must be assigned.

To perform image registration, the view and the image need to be defined. Then, the mode of picking the point pairs is about to be decided. The last part is to analyze results- standard deviation, mean deviation. Figure 3.9. presents basic window during Image registration.

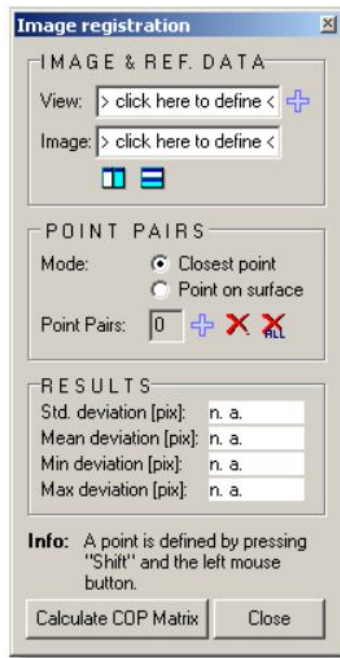
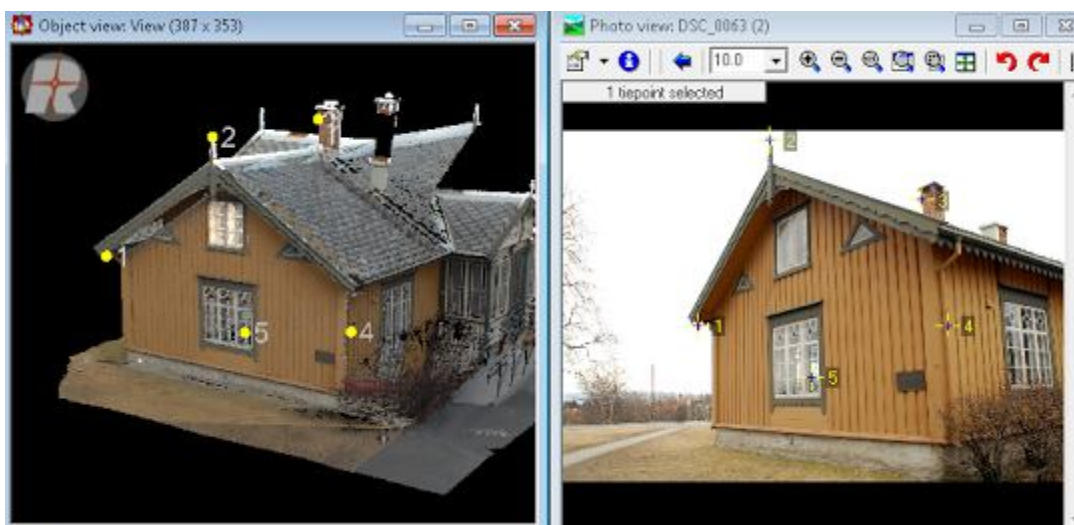


Figure 3.9. Image registration window within RiSCAN PRO software.

In order to calculate COP matrix, at least four points need to be defined. First, the point within point cloud is determined, then the same point in the image needs to be pointed. When, all necessary points are chosen, COP matrix calculation can be proceeded. Figure 3.10. shows the example of choosing tie points. Table 7. includes all standard deviations for all images. The results after changing few tie points were acceptable and the image registration was considered to be done.



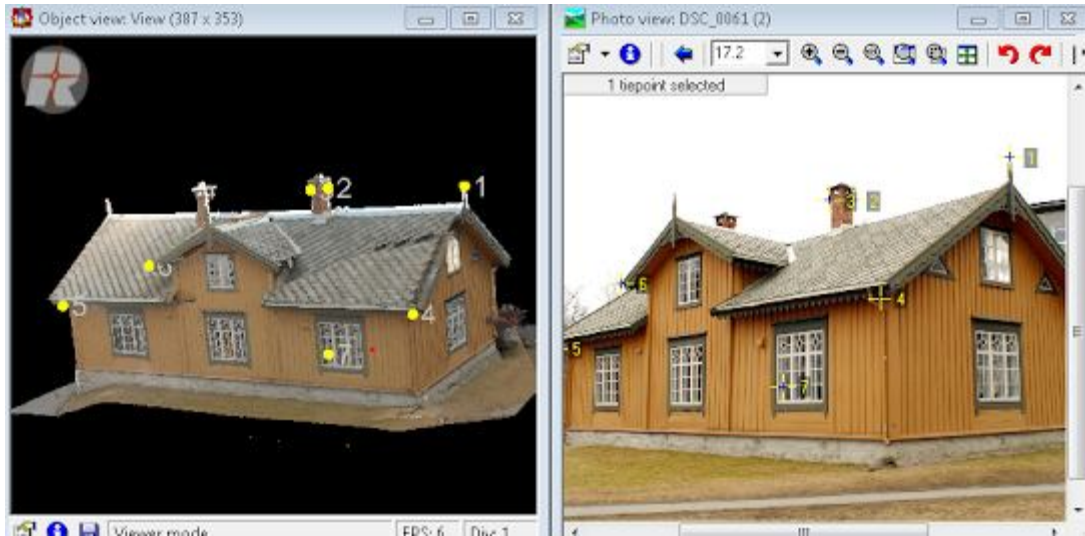


Figure 3.10. Free images registration with tie points. RiSCAN PRO.

Results will be presented by standard deviation and mean deviation for each image. Values are included in the table 7.

Table 7. Results obtained during free images registration.

ID	Standard deviation [pix]	Mean deviation [pix]
1	0,31524	1,05441
2	0,56588	1,21145
3	0,87445	1,32555
4	0,23665	0,58874
5	0,41156	0,99856
6	0,54774	0,89665
7	1,20144	1,88544
8	0,89655	1,65223
9	0,89574	1,65233
10	0,84512	1,65887
11	1,33544	1,95585
12	1,24155	1,85444
13	0,75412	1,21142
14	0,89556	1,23662
15	1,21144	1,65542
16	0,33254	0,53662
17	0,95566	1,36555

The only issue while doing the free image registration within RiSCAN PRO is that all models created in other software needs to be textured within the RiSCAN PRO.

3.6 Registration data from Riegl and Faro scanner into one common coordinate system

3.6.1 RiSCAN PRO

3.6.1.1 Manual registration

Registration of Riegl data itself was considered to be the main dataset which FARO data will be registered to. Decision was made because of better geometry and higher number of tie points while scanning by Riegl sensor. Additionally, initial registration within the RiSCAN PRO has been already examined during working on the Specialization Project [17] and was assessed as a good algorithm. The procedure is described in the previous paragraph.

Registering data from FARO sensor started with creating new scan position within the RiSCAN PRO software and importing all ASCII files containing FARO scans inside this scan position. Only option was to import polydata objects.

In order to register data together Manual Registration procedure was used. Specifically, Coarse Registration via tie point was chosen.

Window with all available parameters and options, shown in figure 3.11., looks the same as in case of registering free images.

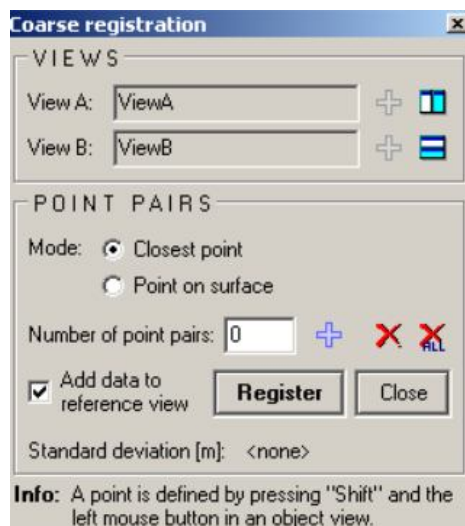


Figure 3.11. Coarse registration of two datasets acquired by different sensors, RiCAN PRO.

Basically, function requires to pick up at least four points presenting the same spot in two data sets and then proceed with calculation. After pressing Register button, proper SOP matrix is being generated.

Figure 3.12. presents examples of choosing tie points within the data.

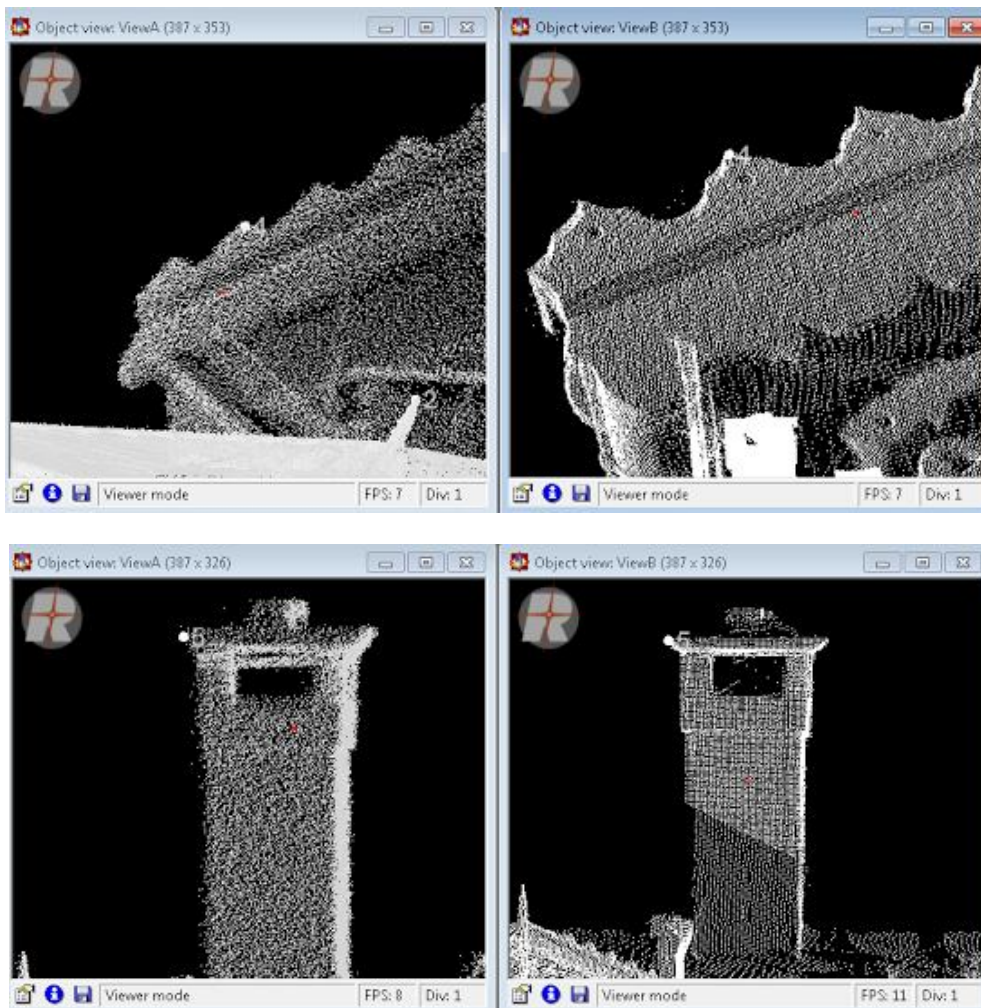


Figure 3.12. Coarse registration of datasets from Riegl sensor (left) and FARO sensor (right).

All 7 scan positions were register in following way and for each standard deviation was obtained. Table 8. present the final results.

Table 8. Standard deviations obtained with coarse registration of datasets from Riegl and Faro scanner.

ID	Standard deviation [m]
1	0,012
2	0,005
3	0,019
4	0,009
5	0,008
6	0,022
7	0,017

Final result of registration was checked in several areas of the whole object. Figure 3.13 presents one of the place where overlapping of point clouds was examined.

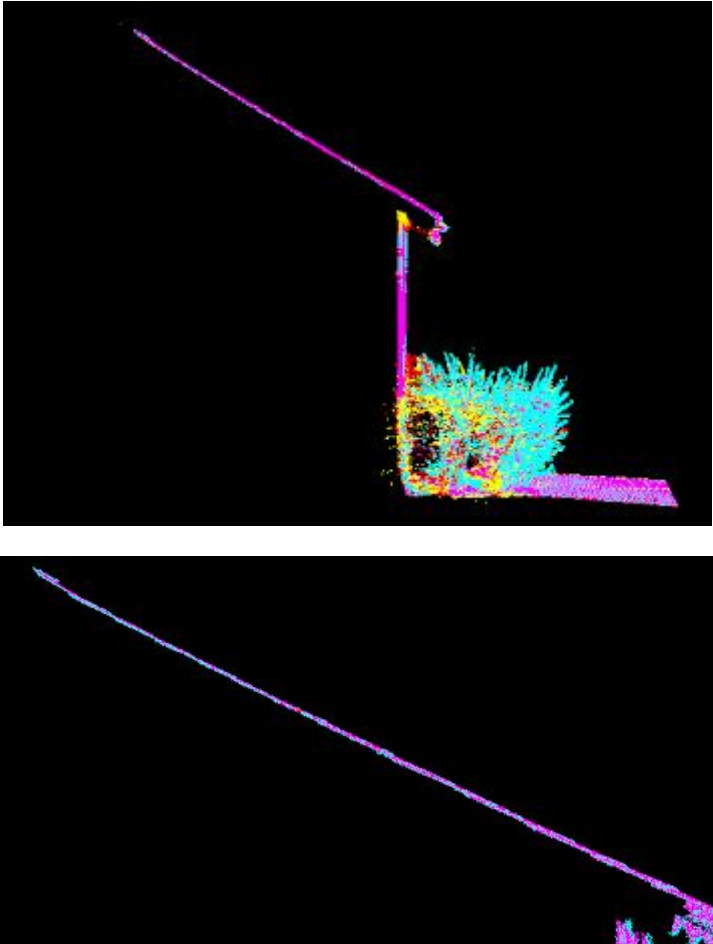


Figure 3.13. Overlapping point clouds checking after registration.

3.6.1.2 Multi Station Adjustment of both data

When all data was registered together the final step of alignment could be done. As the standard procedure of registration is based on tie points and although it gives good result in fitting tie points together it might give some alignment errors in other parts of data. As mentioned before it might be caused by unfavorable set-up of reflectors in one of the scan position or measurements errors.

To decrease these errors, RiSCAN PRO offers a plugin function-‘Multi Station Adjustment’. This algorithm tries to improve the registration of the scan positions by changing the orientation and position of each scan. It is done in several iterations and can use both tie points, tie objects and polydata objects. [17]

As for the beginning we used only tie points. RiSCAN PRO gives possibility to choose which object we want to use. There are also few parameters to fix.

1. Mode of NEAREST POINT SEARCH, it can either search *one nearest point (fast)* or *all nearest points*. It is recommended to use the second option. It tells us how RiSCAN PRO should search for corresponding points within point clouds.
2. ADJUSTMENT: *Min. change of error 1* and *min. change of error 2*. The process stops when the change error is less than first min. change error. If the improvement of the alignment between two following iterations is less than given value the algorithm is slopping and searching for new corresponding planes. Until improvement between two following iterations is less than second min. change error, the iterative alignment is running. Here we fixed values of errors to 0,100 m and 0,005 m respectively.
3. *Outlier threshold* , outliers -all point-pairs showing a distance greater than this parameter multiplied by *standard deviation error*, are removed. Outlier threshold was fixed to value 2.
4. *Calculation mode*, it defines how the error is calculated. It can be chosen between least square mode and robust fitting. The least square fitting was chosen.
5. *Update display*, we can choose between never, seldom and often. It is recommended to choose seldom. [17]

Unfortunately, there were not so many tie points and MSA procedure did not introduce any special changes into the data. By proceeding with the operation coordinates of Riegl scan

positions were also checked. They were compared to ones that were measured by GPS. Coordinates differed not more than few millimeters.

3.5.2 PolyWorks

As mentioned at the beginning of this chapter, registration of data derived from two different scanners was carried out also in PolyWorks. The work was done to check and compare the algorithms used in both programmes.

3.5.2.1 Import data

After consulting with support system of InnovMetric Software Inc., IMSurvey module was used to import and then to register data. As the software supports wide variety of file formats, the first idea was to use all original data, so for Faro's scans, format .fls and for Riegl's data .3DD files. Unfortunately, files .3DD have generated an error while importing, hence ASCII files were used for Riegl's point clouds. Format .fls was imported with success. The only drawback of using these files was very slow loading process.

Nevertheless, the time was worth waiting since as can be seen in the Figure 3.14, Faro data is more accurate and with less noise than the data from Riegl. It is of course the matter of the scanner but also when compared to the same data imported within ASCII files, the .fls gives way better results. The native formats of scanned data hold more complex and complete information, for example besides XYZ, scanner orientation and possibly RGB values which can result in better and more effective processing.

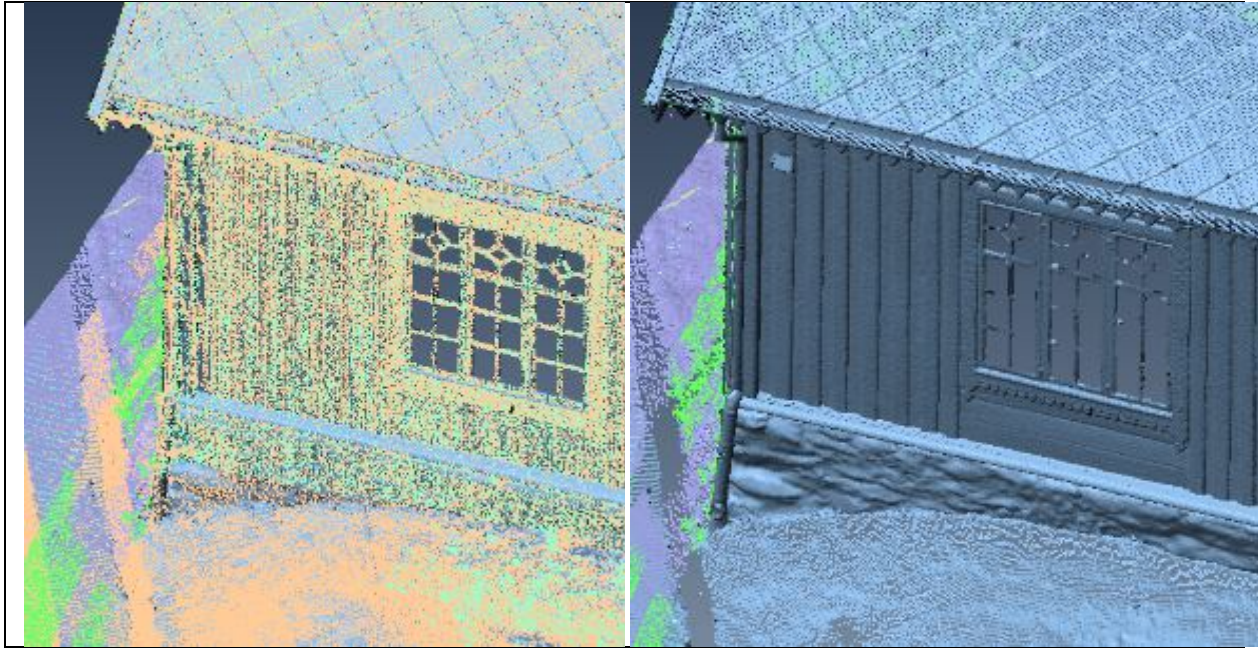


Figure 3.14. Comparison of point clouds derived from Faro scanner and from Riegl system.

Left: Riegl point clouds, right picture: only faro data. Display in PolyWorks software.

As can be noticed in the figure 3.14, using native formats while using PolyWorks software is the best idea and in case of future work that solution will be implemented.

3.5.2.1 Registration

Basically, as in majority of packages that allow for alignment of point clouds there are two steps of performing this. First, initial registration must be carried out in order to bring elements near to each other, then more accurate and precise process can be done. Data objects, how point clouds are entitled within the PolyWorks software, can be manually aligned to one or several Reference objects by pointing point pairs within each data. The *Align* menu offers also different others alignment object methods for better fit. They also will be described shortly. An alignment performed on Data object occurs as a data alignment under the Data alignments branch in Tree View. [7] The alignment that is active is shown in bold. For better understanding Data Alignments group Figure 3.15. presents this section within the project.

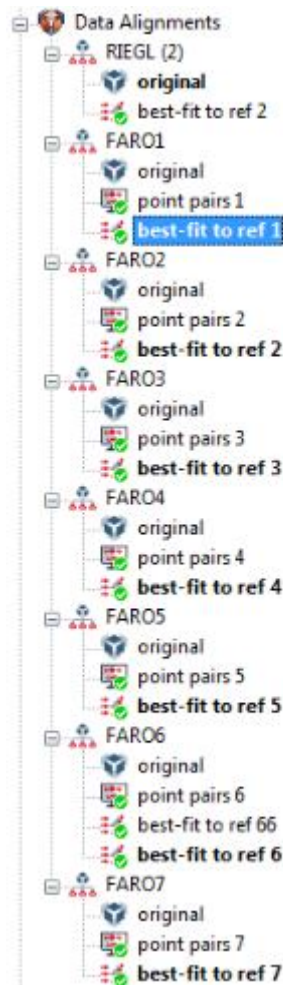


Figure 3.15. Data alignments within the PolyWorks project.

Following the IMSurvey manual guide [7] the data alignments branch can be described as a group of data alignments that refer to one or multiple Data objects in data alignment groups. Each of data object that shares the data alignment is a part of the same alignment group. In case of the following project each Faro scanner station got its own data alignment group.

In general, data alignment includes the position of point clouds after registration process and also the parameters used and the type of alignment carried out. Each of alignment performed is automatically added to the list of Data alignment group, then it can be changed, compare and investigated.

Overview of object alignment methods

As mentioned before there are few techniques to bring a data of points to the Reference surface. The software requires creating a Reference object while registration. As for this project the main datasets were acquired by Riegl system, that data were considered to

be a referenced one. A Reference object can be understood as a surface-based model to which others Data object are compared. There might be two categories of Reference objects: CAD objects and polygonal objects. During the registration polygonal reference objects, created from the Riegl point clouds, were used.

1. Point-pairs alignment

The process can be performed as a matching either one point pair or three point pairs between Data object and Reference object to ensure an approximate alignment. Figure 3.16 shows the procedure of point pairs alignment that can be accessed from the split view mode. For each Faro scanner position the new alignment was performed. [7]

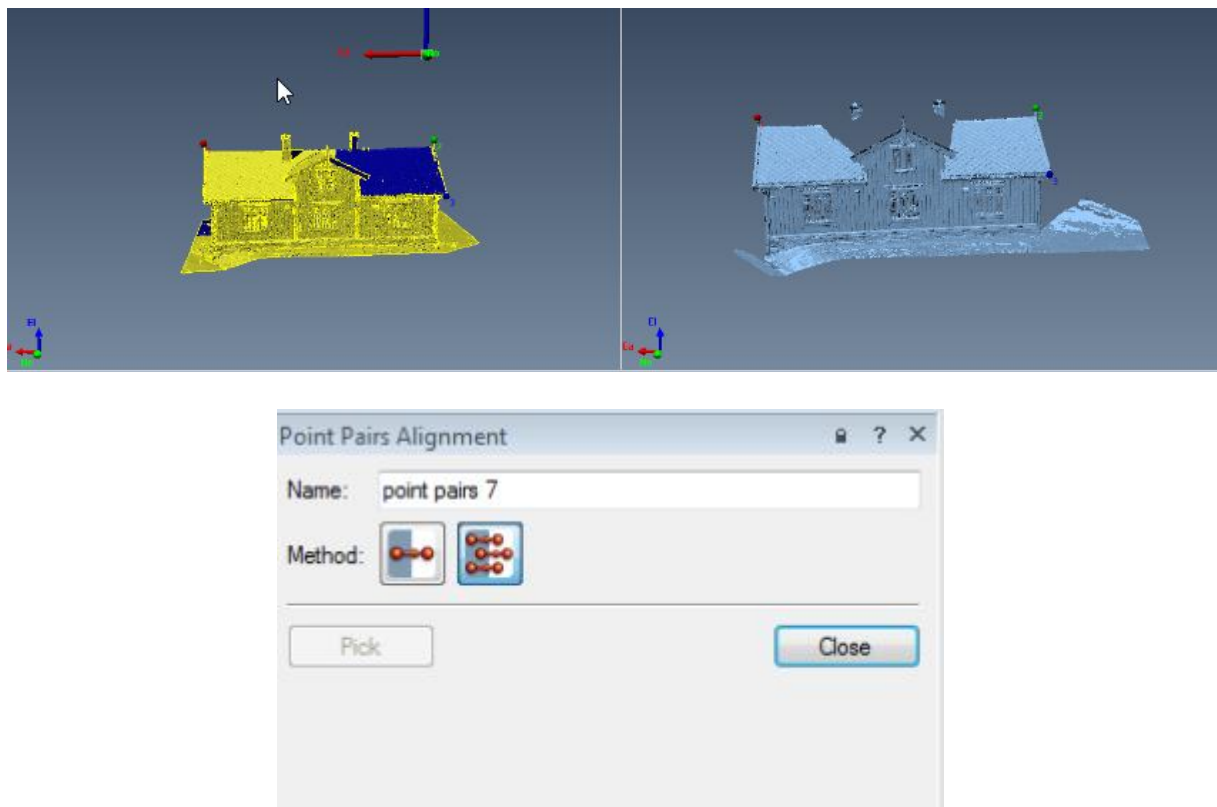


Figure 3.16. The split view mode during point pairs alignment. Left window includes the Reference object, right window shows the object to be registered.

The algorithm works nice but as there is possibility to use only three point pairs the misalignments can be noticed. Figure 3.17. shows an example after the point pair registration.

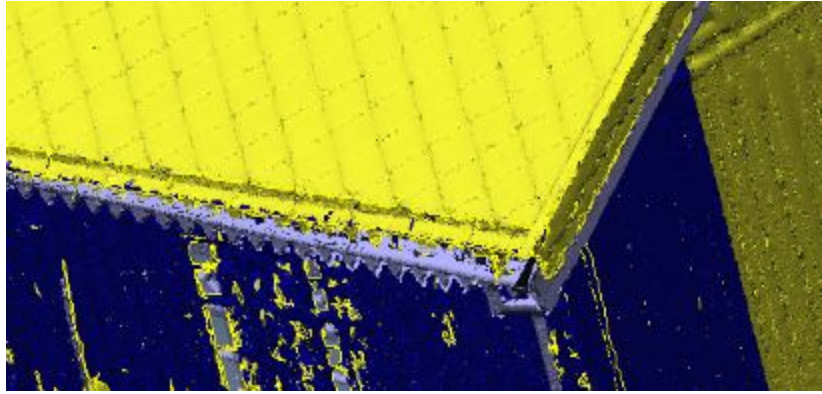


Figure 3.17. Misalignments between the Reference object and Data object after point-pair registration. Bright blue data: Data object to be registered and yellow-dark blue data: Reference data.

To improve the registration best-fit procedure was implemented.

2. Best-fit point-to-surface alignment

The process of best-fit alignment of selected Data object to the surface of available Reference object. The iterative methods that best-fits sets of data. The algorithm automatically detects high-divergence areas and then compute more accurate alignments. [7] After proceeding with point pairs registration, the best-fit was performed.

Figure 3.18. presents the Dialog Zone of the best-fit procedure with all necessary parameters and also already with performed alignment. The statistics part shows the results.

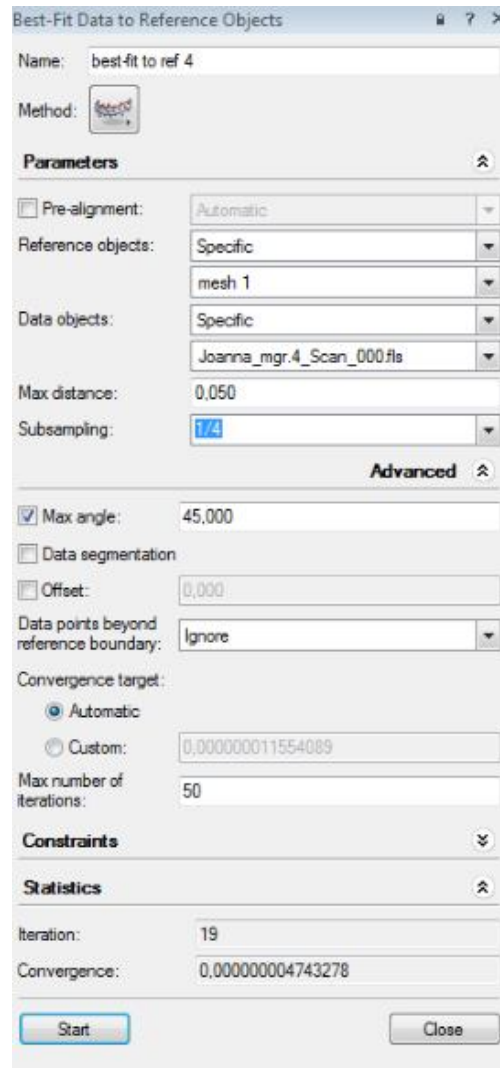


Figure. 3.18 Best-fit alignment within PolyWorks

Results show that for this datasets algorithm performed good alignment after 19 iterations with obtaining the convergence target.

Figure 3.19. shows the difference before and after performing the best-fit alignment

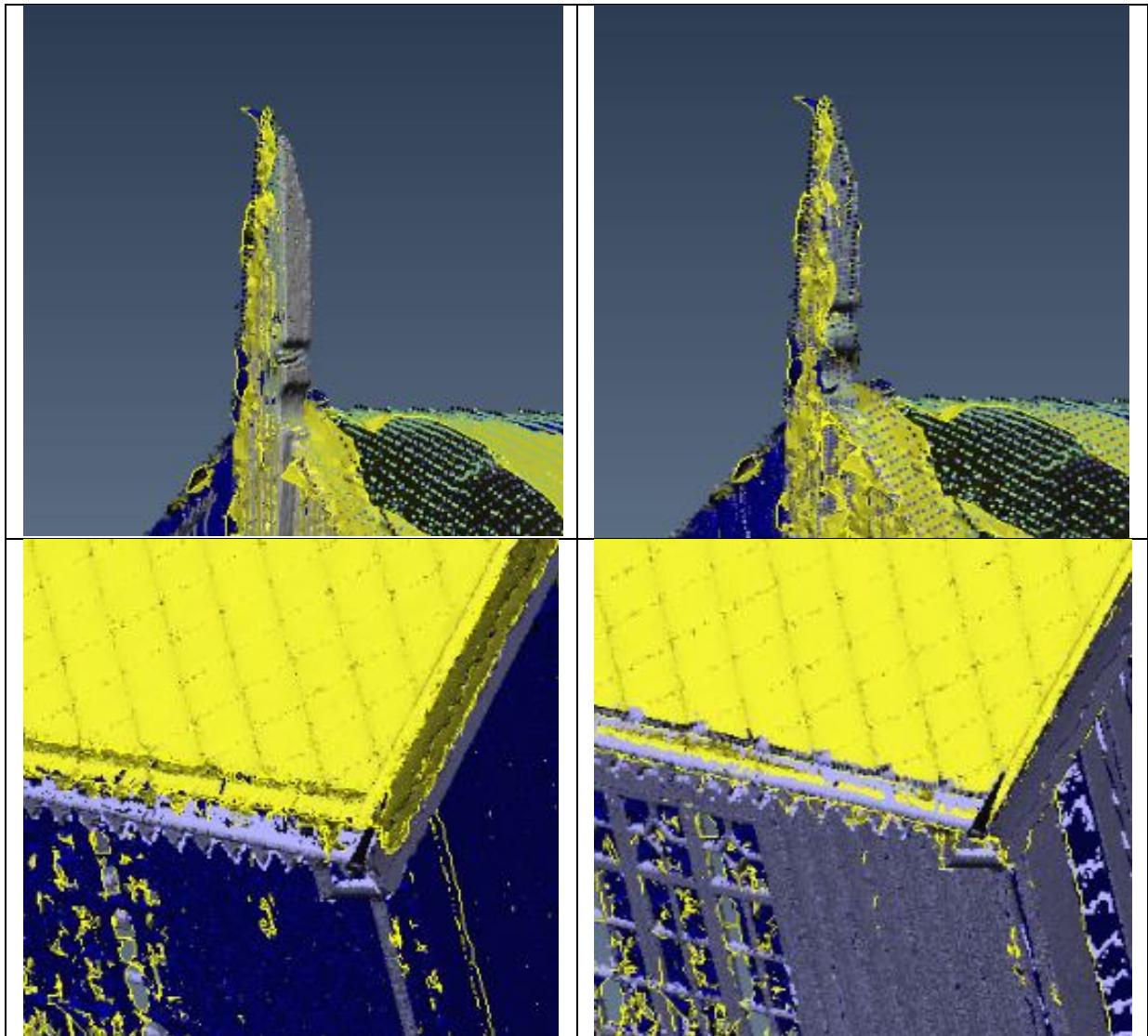


Figure 3.19. shows the examples of differences between point pair alignment and best-fit. Left images shows data before best-fit procedure, right images presents data after best-fit alignment.

For each Faro scan position best-fit registration was performed with the similar results. Convergence value was kept on the same level only the number of iterations was varied.

3. Best-fit Cross sections

Aligns a Data coss-section to a Reference cross-section. The point is to minimizing the deviations between the two. [7]

4. Manual alignment

Procedure allows to specify manually precise translations and rotations. This procedure was not used within the thesis.

5. Center points alignment, Plane, Axis, Center Point alignment, Perpendicular Planes alignment

All three methods apply to primitives. They match primitives extracted on Data objects to primitives derived from Reference objects. [7]. None of these alignments were used.

3.5.2.3 Comment

Registration performed within the PolyWorks software was carried out at very high-level. Algorithm works very accurate and handled data professionally. Results of this alignment process, after comparing several areas within the object, can be considered as slightly better. PolyWorks offers also many others possibilities to register similar datasets. In future work another one probably could bring even better results.

3.6 Filtering data

As all data acquired by scanner includes all kind of noises and unnecessary scanned areas the first thing to improve working within every software is to clean manually all noises. Then all other filters can be introduced. Sampling procedure is one of the most common in each software but also Octree filter, automatic cleaning filter and lot of others can be used.

Figure 3.20. shows areas before and after manual cleaning

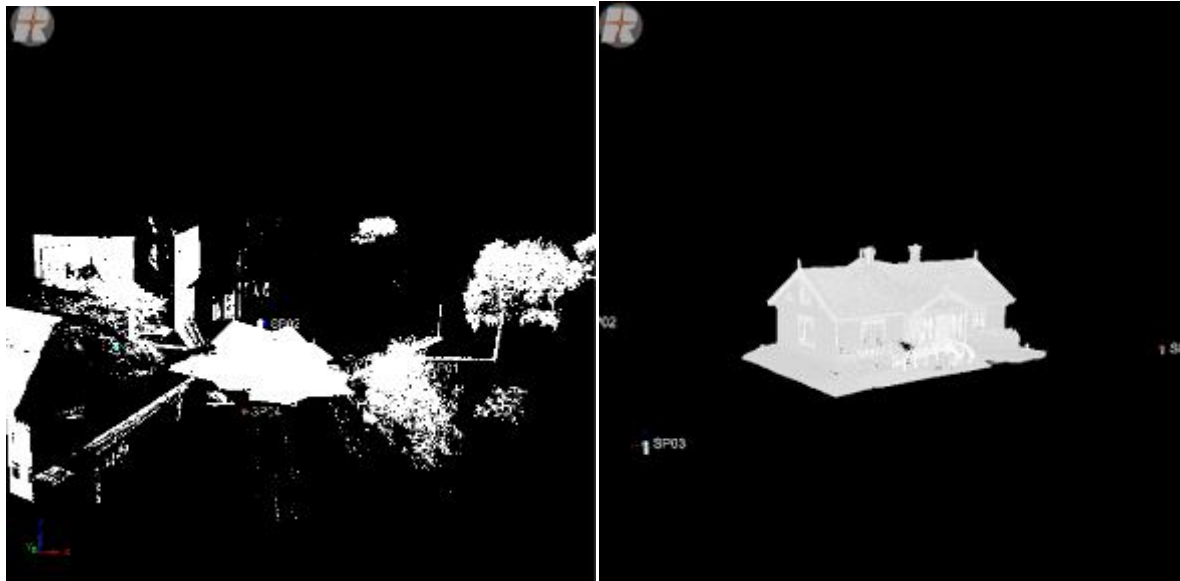


Figure 3.20. Initial manual cleaning, left raw data from the scanner, right after cleaning.

Figure 3.21. also presents cleaning reflections from windows inside the house. Each window produced these kind of reflections which required manual cleaning.



Figure 3.21. Manual cleaning of window's reflections.

3.6.1 RiSCAN PRO

After manual cleaning of all Polydata objects, more advanced filters could be applied. In RiSCAN PRO all copies of raw point clouds are named Polydata, and since the beginning, the work is proceeded on polydata objects.

Octree filter

The main structure within the algorithm is a cube, which is divided into 8 equally sized cubes which are again divided and again and so on. The division is stopped as soon as a given minimum cube size is reached. After carrying out the octree filtering, one cube contains one point, and the point is the center of gravity of the averaged points, representing a larger number of points. Figure 3.22. shows options that should be fixed before starting the filtering.

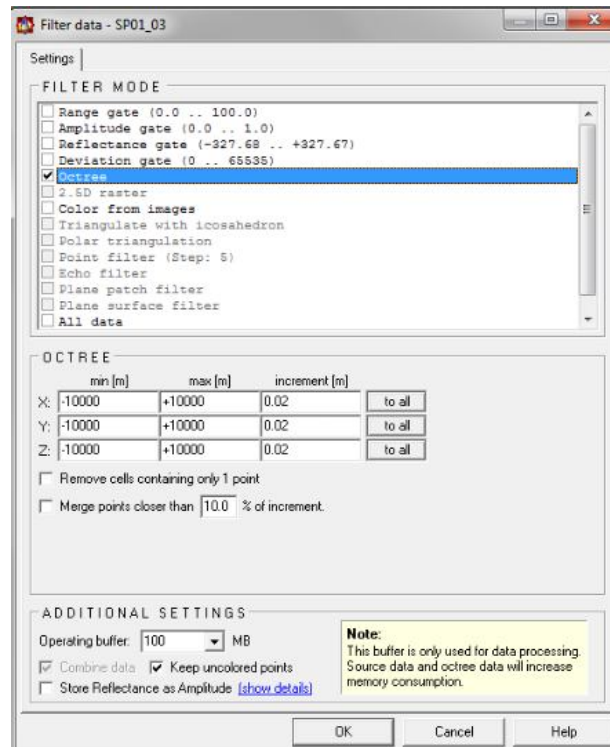


Figure 3.22. Octree filter within RiSCAN PRO.

To filter out isolated points we can use option *'Remove cells containing only 1 point'*. There is also an option *'Merge points closer than given increment'*, this can provide more homogeneous point cloud. In the project we haven't used any of these options. The increment was set to 0,02 m.

Figure 3.23. presents the comparison of data before and after octree filtering.

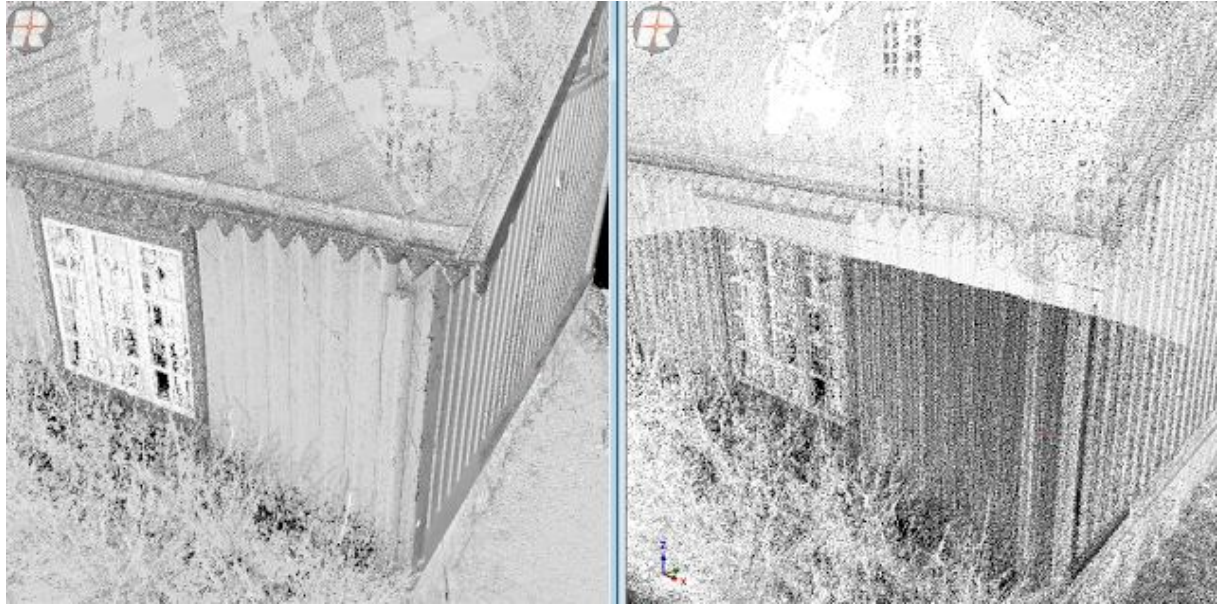


Figure 3.23. Octree filtering. Before process (left), after the process (right).

Re-sampling

Another implemented filtering option was Re-sampling. The figure 3.24. below shows the result of re-sampling as a 3D data with a strictly regular grid. While performing with re-sampling procedure new grid is generated. The extend of the grid is determined by one of the original scans. The resolution of the grid needs to be defined by a user. [15]

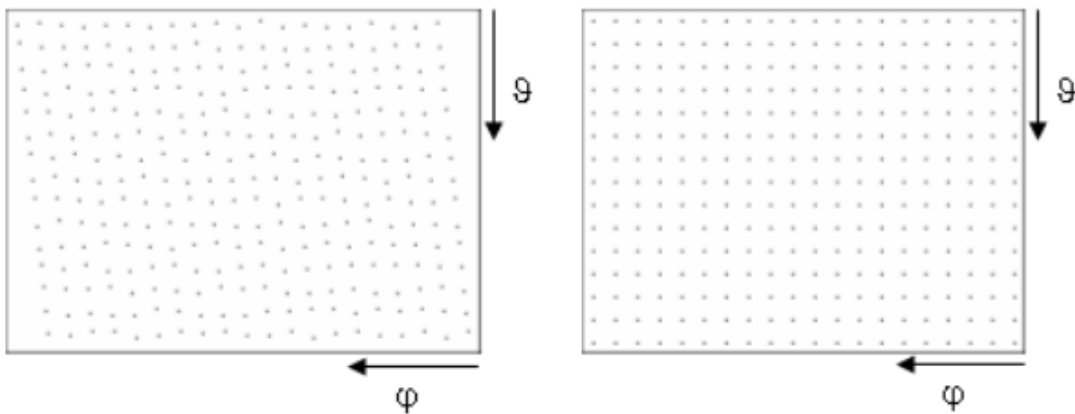


Figure 3.24. Generation of new grid during re-sampling within RiSCAN PRO software.

(Source: [15])

Figure 3.25. shows the process of re-sampling while all range and amplitude falling within one cell is averaged.

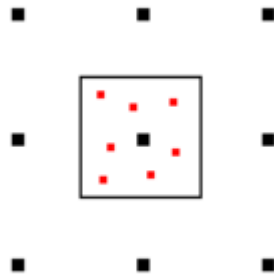


Figure 3.25. Re-sampling process within RiSCAN PRO software. (Source: [15])

Results of sumpling process is shown in figure 3.26.

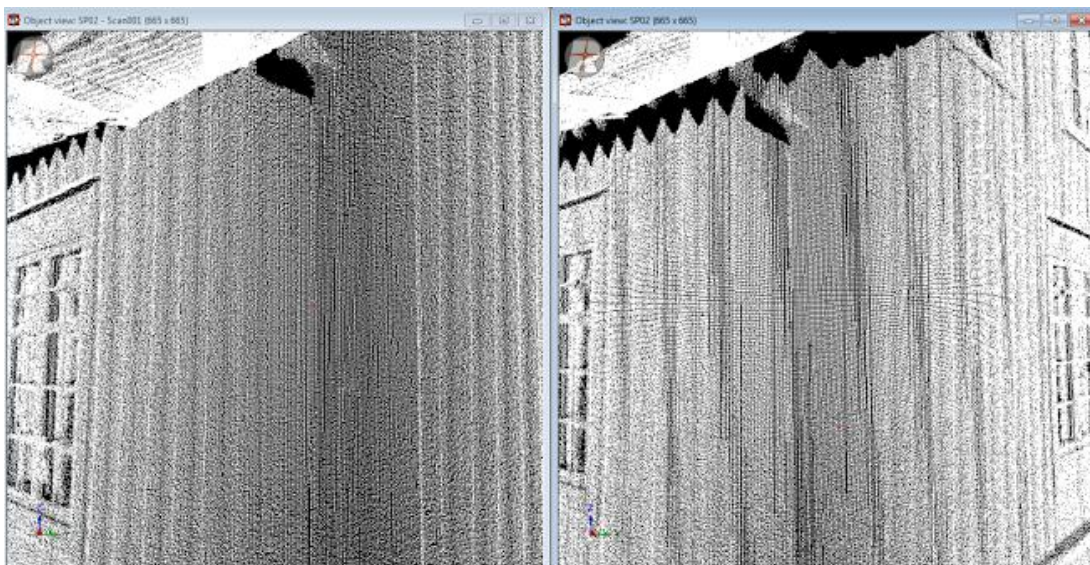


Figure 3.26. Sumpling process within RiSCAN PRO, before (left) and after process (right).

3.6.2 FARO SCENE

Within Faro SCENE there are few available filers:

1. Stray

When the scanner hits two objects or no object at all (for example sky) the filter can remove scan points resulting from these noises. The stray filter is very efficient for correcting faulty measurements. It also works well applied near edges.

2. Distance based

Removing scan points that occur in a certain distance from the scanner.

3. Dark Scan Points

The selection procedure is based on the reflective value of the dark points

4. Smooth

Minimize noise on surfaces. It substitutes the value of the point, that was measured, with the mean value from its surrounding area.

However, the most popular and common filter tool within Faro SCENE is *Preprocess Scans*. It allows to apply a series of filters both to the entire scan or numbers of scans at once in a batch processing mode. This excludes the need of introducing filters, detecting and identifying objects. Figure 3.27. shows the parameters that need to be set before starting the processing.

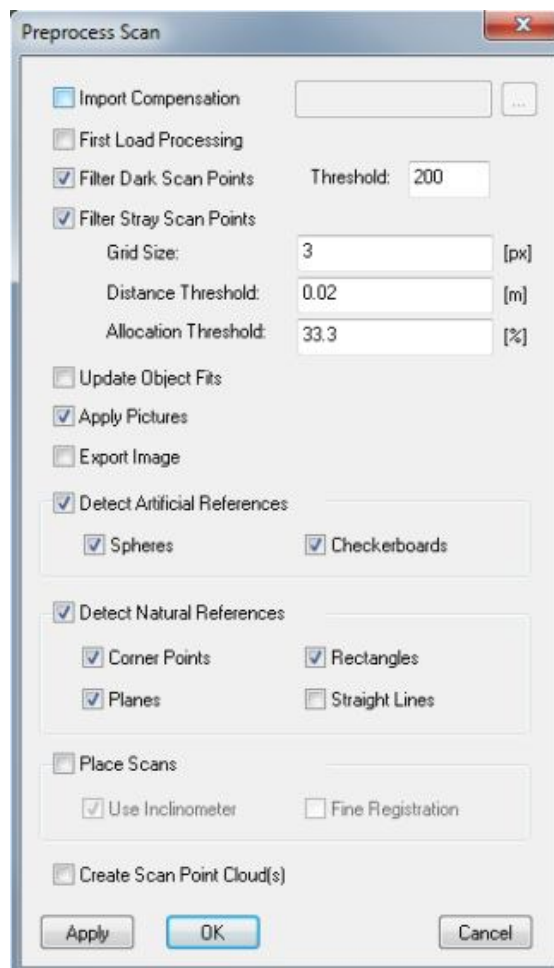


Figure 3.27. Preprocess tool within FARO SCENE.

Figure 3.28. presents the difference between data before Preprocessing and after. The reduction of noise can be easily seen . The left pictures shows data before operation and the right one presents data after running preprocessing tool.

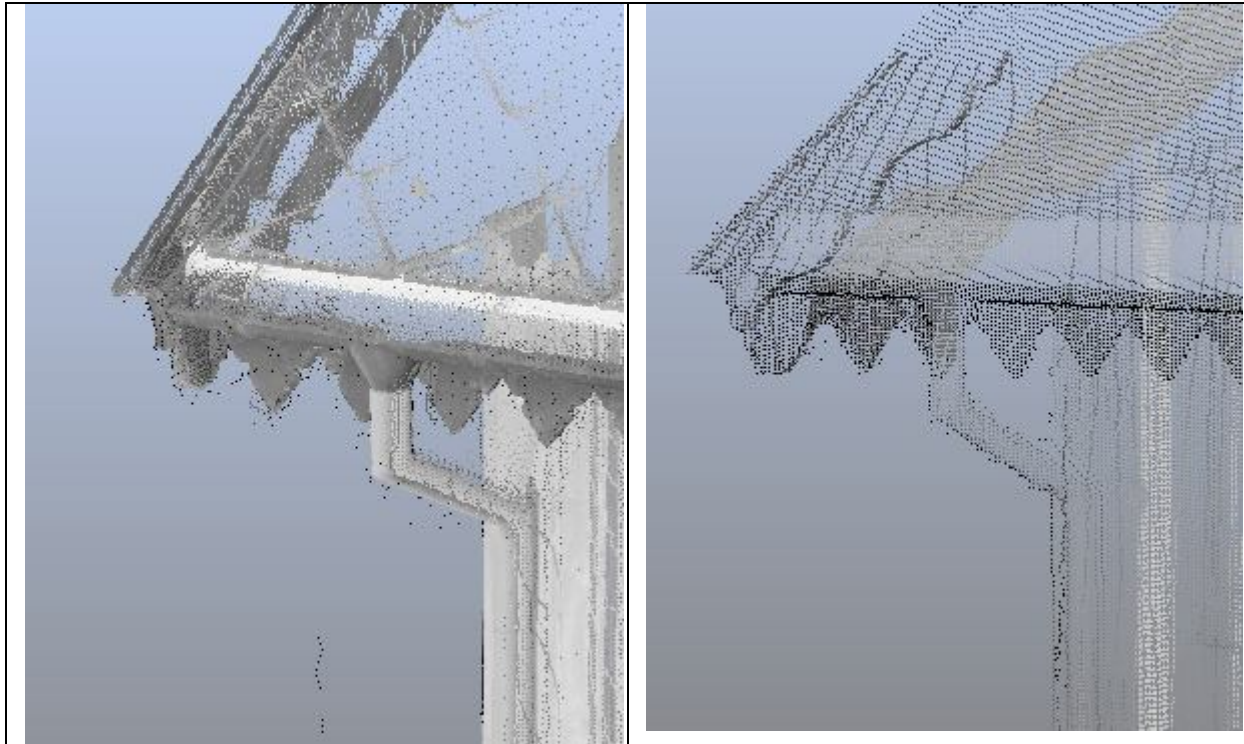


Figure 3.28. . Comparison data before and after running preprocessing tool within FARO SCENE software.

3.6.3. PolyWorks

All data that have been used within PolyWorks were initially processed either in RiSCAN PRO or Faro Scene. Few filters have been applied in order to speed up the process of loading files and later the work within the software.

Although, point clouds have been also processed in term of cleaning from useless points and areas (like reflections through windows), there were still some points to clean off. Figure 3.29. shows windows before and after cleaning carried out in PolyWorks.

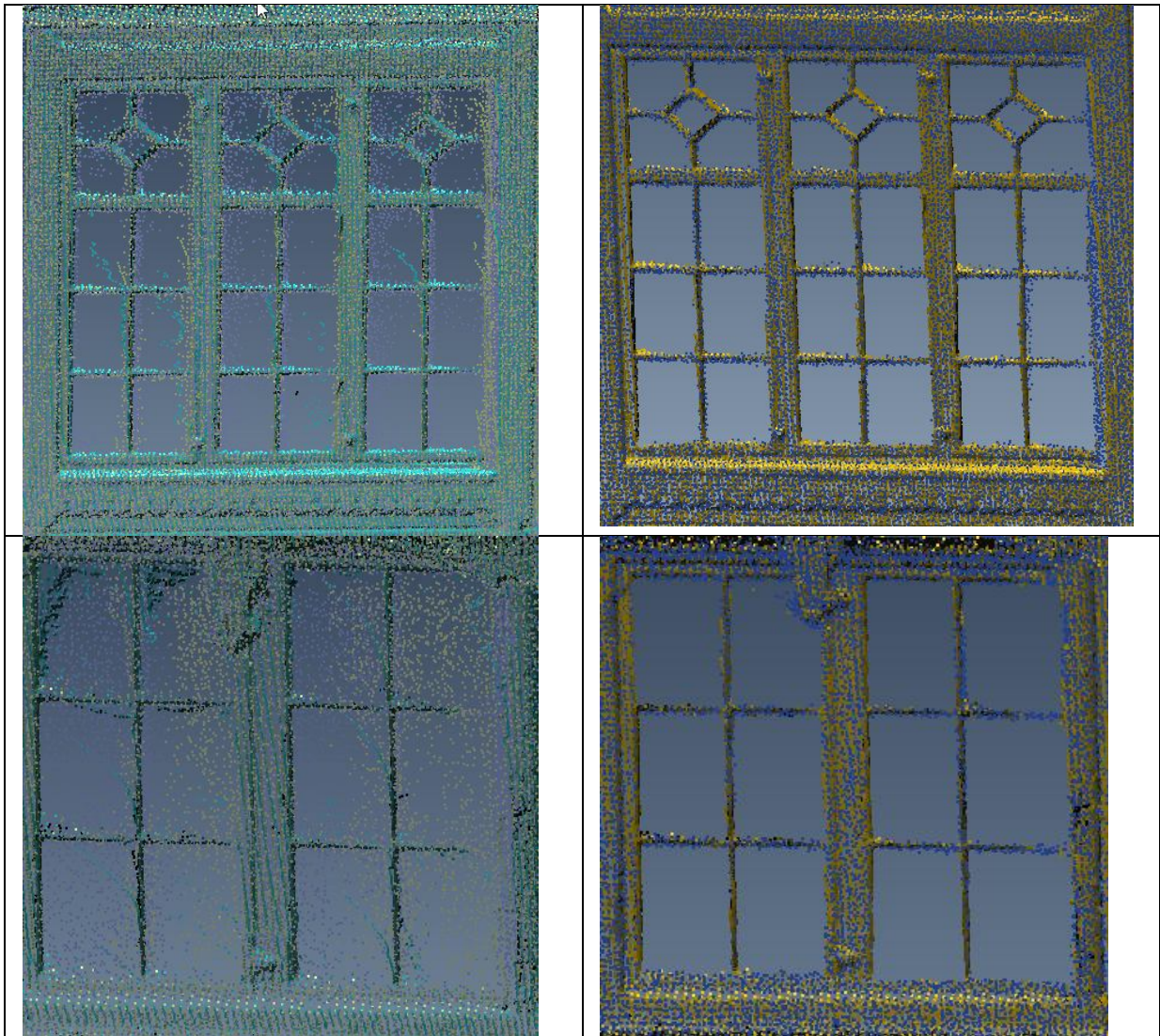


Figure 3.29. Windows before and after cleaning-PolyWorks

This kind of cleaning was done in order to close windows properly with flat surfaces. Results will be shown in next chapter-triangulation.

The main PolyWorks tool for filtering data when the point cloud is too dense is called Subsample. The tool offers random, uniform and curvature-based sampling methods. The point cloud needs to be visible and selected to perform the procedure. Chosen method was the Uniform method and the tolerance value 0,005m or 0,01 m, depending on how much the point cloud were supposed to be reduced.

3.7 Triangulation

3.7.1 RiSCAN PRO

To create a surface from point cloud, triangulation procedure needs to be performed. The surface consists of triangles connecting the data points. Triangulated data is also called 'mesh'. It provides a familiar representation of scanned object. Triangulated data can be also colored from images, it is called texturing.

RiSCAN PRO provides two options for triangulation: '*Triangulation of a scan*' and '*Triangulation of arbitrary point clouds*'. Since all work is done on polydata object the second option was chosen. This option uses 2D- Delaunay algorithm. There are two modes within this algorithm: '*Plane triangulation*' and '*Polar triangulation*'. To proceed with each of points only from one polydata object can be used. The result is stored in the same object. The selection tool was implemented to choose the points to be triangulated.

Plane triangulation is computed from 2D coordinates of the points mapped to the computer screen, computer screen defines the plane. To obtain 3D-Triangulation the orientation during each triangulation needs to be changed. Triangulation is done from current point of view.

There is a possibility to set following parameters:

- Max. triangle edge length – value defines the maximum length of the triangle's edges. A larger value results in better gaps closing in the mesh. We tried different values since the surface wasn't satisfactory.
- Max. triangle tilt angle- it's the angle between the line of the sight and the surface normal. No triangles are created if a triangle angle is bigger than the value. In general , angle equal approximately 80 degrees was used.
- Min. triangle angle- triangles won't be created if at least one of the triangle's angles is smaller than given value. This value can be used to remove needle triangles. To closed as many holes as we could the angle was really small. Around 10 degrees. [15]

Polar triangulation is based almost on the same rules except that selected points to triangulate are projected onto a disk not onto plane. This triangulation is independent of the current point of view. To perform this algorithm the scan position where the data was taken needs to be fixed. Since, polydata objects were used and they contains of different scans from different scan positions, the plane triangulation was chosen to examine. Results can be seen in figure 3.30., as we can see lot of needles triangles were created and the whole surface is very noisy. The reason for that is that RiSCAN PRO triangulation depends on point of view. [15]

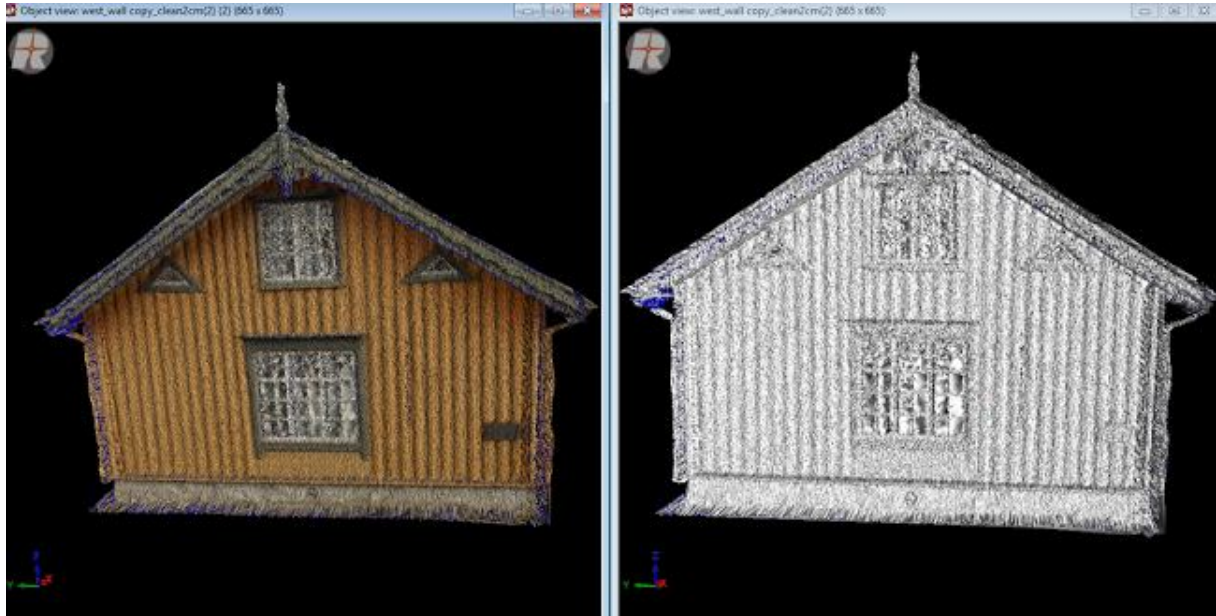


Figure 3.30. Results of plane triangulation within RiSCAN PRO.

Results for triangulation of each wall of the building were really poor with many needles triangles and noises around. Decision was made to use RiSCAN PRO software only for pre-processing data, registration, cleaning and then texturing without generating surface.

3.7.2 PolyWorks

As the main objective of the thesis was to create a 3D mesh of data acquired on scene and compare different algorithms and tools available to accomplished this, after registration, the triangulation process began.

3.7.2.1 Types of triangulation algorithms

Basically, within the software there are three types of data triangulation: Triangulate Data Points, Triangulate Terrain Data Points and Wrap Mesh around Point Cloud. First two

are not suitable for this particular data, and was discouraged by the InnovMetric support system.

Triangulating Data Points algorithm creates a polygonal mesh from chosen Data points and a plane. Break lines in the form of polylines can be also used. It is possible to select plane from XY, YZ and ZX or any existing plane. Points are projected onto the plane and next triangulated with a 2D Delaunay triangulation method, which is described by the way of triangulation within RiSCAN PRO.

Triangulating terrain Data Points method builds a DTM surface for each available point cloud Data Object. Within the algorithm only sampling grid size can be chosen that specifies a grid that is used to subdivide each point cloud.

Wrap Mesh around Point Cloud is probably the best method implemented for creating a mesh. wrapping a polygonal mesh around selected point clouds allows the triangulation to be best-fitted to a collection of points by subdividing triangles and changing their vertices in 3D space. The module offers additional options: rejection of outliers, noise reduction and curvature-based subsampling.

Figure 3.31. shows one of the attempts to create a mesh with chosen parameters.

Reject outliers allows to eliminate outlier points and can be parameterized by maximum point-to-point distance and maximum cluster size.

Noise reduction is fixed by a tolerance value. This value describes the maximum distance on which each point can be moved in comparison to its original position. With increasing the value the mesh will result with smoother surface.

Curvature-based subsampling is parameterized by percentage value that relates to the target of current number of points to achieve. Points are eliminated until the number of points is equal to the target number of points.

Maximum edge length specifies a maximum triangle edge length. It means that points that are further away than the fixed distance cannot be combined by triangles. The value of the maximum edge length should be around 5-10 times of point spacing value.

In the figure 3.31., one set of parameters are shown. Since it has given different results, few groups of parameters were examined. The initial value of maximum edge length

0,05 m and tolerance at 0,005 that was suggested by support system gave detailed but incomplete model.

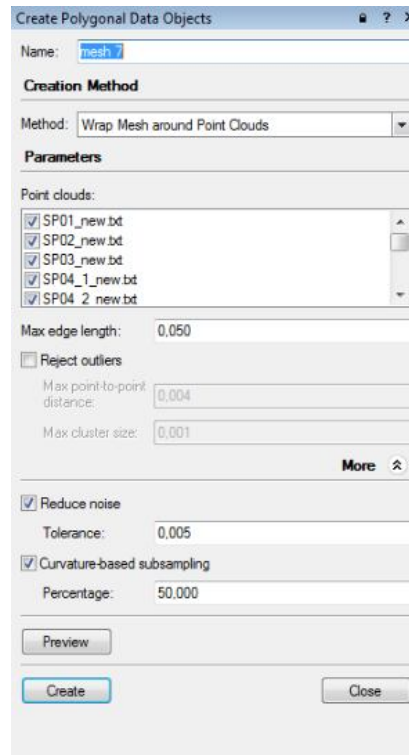


Figure 3.31. Wrap Mesh around Point Cloud parameters-PolyWorks software.

3.7.2.2 Østre Gløshaugen

3.7.2.2.1 Wrap Mesh around Point Cloud

The result of implementation above parameters is shown in figure 3.32.. As can be noticed, there are lot of holes, especially on the roof surface. Additionally, some areas consist of reversed triangles.

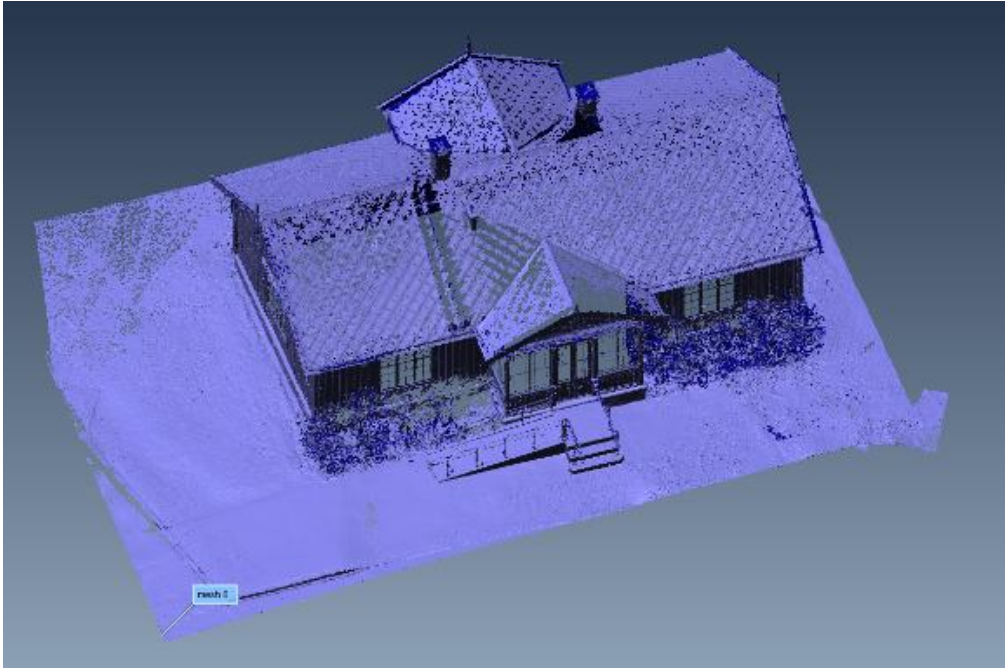


Figure 3.32. Mesh created with IMSurvey with the edge length 0,05m and tolerance 0,005m.

On the other hand, details are well preserved. The example, shown in the figure 3.33, might be the sculpture which is above the entrance and can be distinguished very accurately.

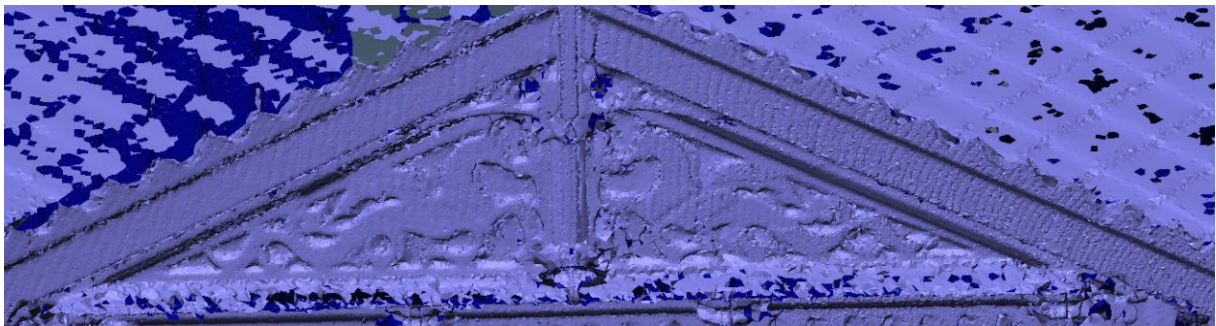


Figure 3.33. Well preserved details above the entrance.

Above model consists of 13 457 194 triangles and can be easily handle in IMSurvey module. However, when it has been exported into IMEdit module, where all processing on mesh can be done, it required reduction of triangles due to very slow work.

There were several attempts to proceed with triangulation, different parameters were applied but with increasing the maximum values of all parameters less details were kept in the model. Also the problem of reversed triangles arose. In the beginning, model presented in figure 3.34. was obtained.

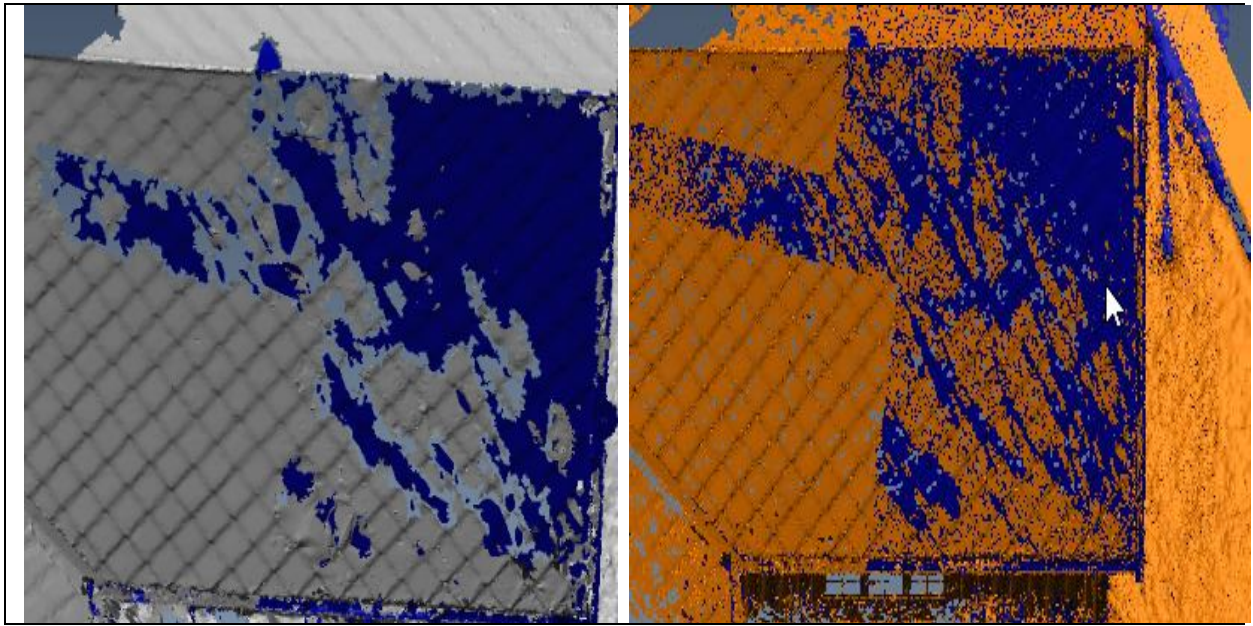


Figure 3.34. Reversed triangles within IMEdit module (left) and IMSurvey module (right).

The shape and the position of the problematic area was connected to the one of the point cloud acquired by FARO scanner. Position 6 (map of the position in appendix 3) seems to have an influence on triangles created on the roof. Part of the point cloud is shown in figure 3.35.

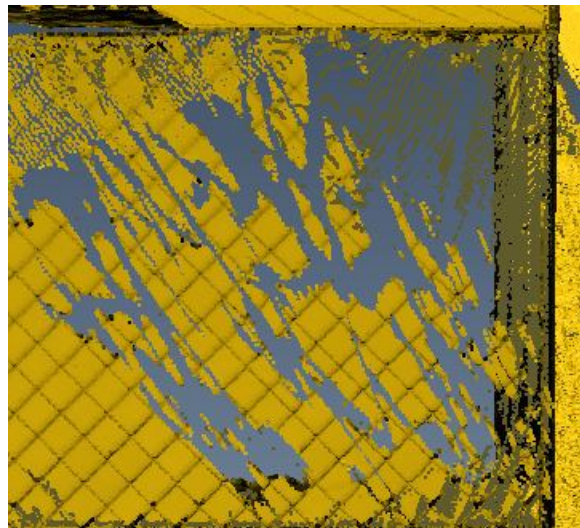


Figure 3.35. Faro scan position 6 with problematic area.

After excluding this position from triangulation procedure, the result were correct. Fortunately, Riegl's scans covered this part of the roof. Holes within the Faro scans were probably caused by the tree suited very close to the corner of the building.

When larger values for wrapping parameters were implemented, more smooth model was obtained. Figure 3.36 shows that holes were eliminated but details were lost. Settings were set for 0,1 m for maximum edge length and 0,5 m for tolerance.

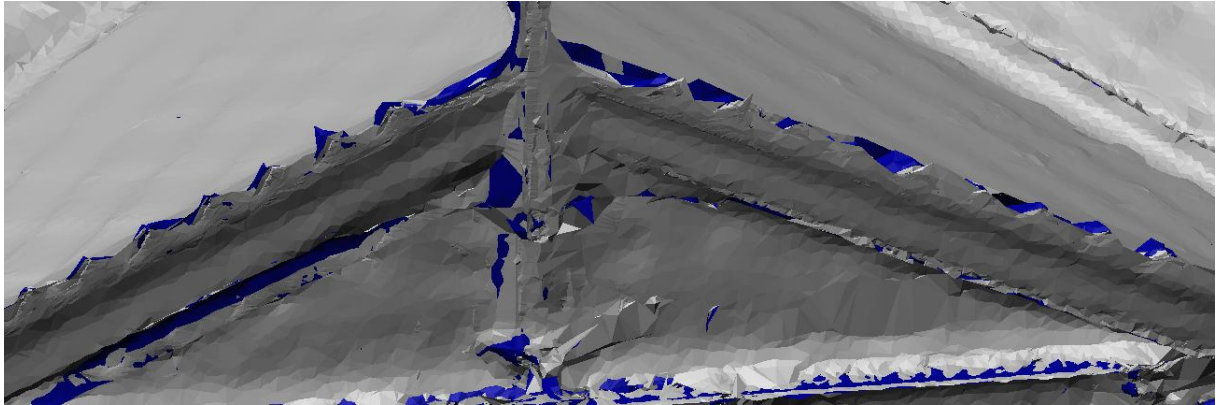


Figure 3.36. Model within IMEdit module (PolyWorks) with coarse parameters. Details are lost.

With the same parameters but with adding curvature-based sampling (50 percentage) option the result was slightly different, in the figure 3.37. the entrance to the house is visible.

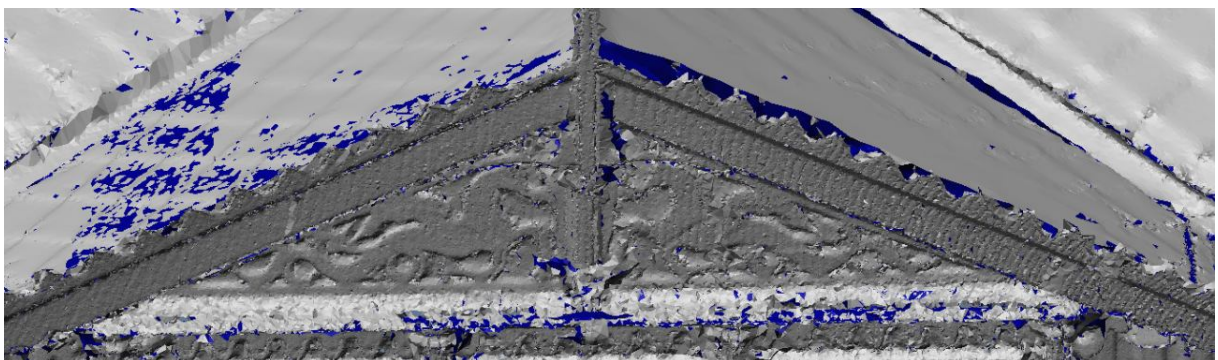


Figure 3.37. Model within PolyWorks with parameters for max edge length 0,1m and tolerance 0,02 m with additional curvature-based subsampling at 50 percentage.

In order to preserve important details model with parameters of maximum edge length 0,1 m and tolerance 0,01 m was used. It consists of many holes and still few areas of reversed triangles. Example of holes is shown in figure 3.38 together with the result after closing them. Reversed triangles can be handle by function either Propagate Triangle Orientation (when the

'right' orientated triangles are selected) or Invert Triangle Orientation (if the 'wrong' orientated triangles are selected). However, the work with repairing this problem is very time-consuming.

3.7.2.2.2 Closing holes

Next important action is closing/filling holes. It was not possible to find triangulation parameters to close perfectly whole model, also the model was missing some data. In few areas there were no points collected by the scanner. Figure 3.38 shows the example of automatic holes filling within the PolyWorks. As can be noticed, it works perfectly.

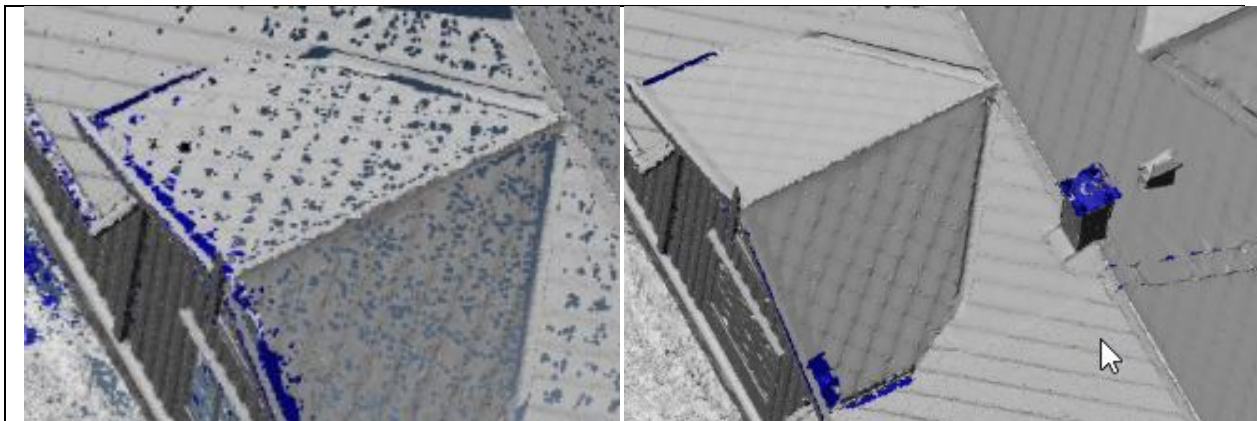


Figure 3.38. Automatic hole filling algorithm within PolyWorks

Parameters for automatic holes filling are shown in figure 3.39. In order to close other holes, besides the automatic algorithm, there was a need to use Interactive Hole Filling as well.

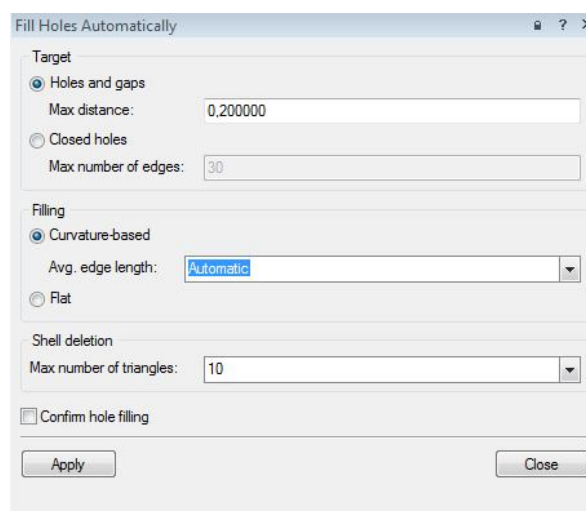


Figure 3.39. Parameter for automatic holes filling within PolyWorks.

Interactive Holes Filling algorithm includes six different ways for closing holes.

Single Boundary Hole, where operation of filling, cleaning and both cleaning and filling can be done with two options for closing the gaps, flat where all vertices are connected without adding any new vertices, and curvature-based where vertices are smoothly interpolated in order to preserve curvature as good as possible.

Multiple Boundary Holes implements the same options as single boundary holes but in one time can be applied to many holes.

Partial Hole Filling where also all three operations are available and the options of flat or curvature-based filling can be applied.

Gap Filling allows for interactive closing gaps between two surfaces. Can be applied in flat option or curvature-based.

Cylindrical Gap Filling, whenever in the surface there is a bend, the mode can be used but only in curvature-based option.

Fillet and Surroundings Filling, the mode that closes fillets and also area on both sides of the fillet. Available only in curvature-based option.

Example of closing holes is shown in figure 3.40., where the hole was closed nicely with the Single Boundary Hole mode with curvature-based option.

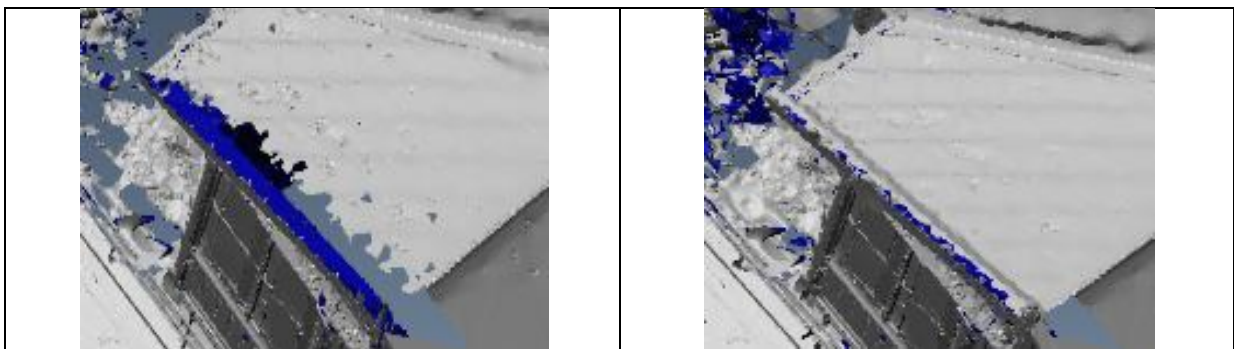


Figure 3.40. Single Boundary Hole mode, closing hole in the roof-PolyWorks

Unfortunately some of the holes were impossible to close correctly. First of the example might be the area behind bushes in front of the building. Since the beginning bushes were a trouble issue that could be handle in different ways. One way includes cutting them off

within the point cloud and then proceeding with triangulation. Figure 3.41. presents point cloud within PolyWorks without bushes in front.



Figure 3.41. Point cloud without bushes in front of the house-PolyWorks.

Unluckily, then the algorithm for closing and repair those very complicated holes did not meet the expectations, or there could be also another way of filling these kind of holes which was not discovered during working on the thesis. By the point when the license for the PolyWorks ends , holes were closed as can be seen in figure 3.42. To improve model other software package was used which will be described in further chapters.

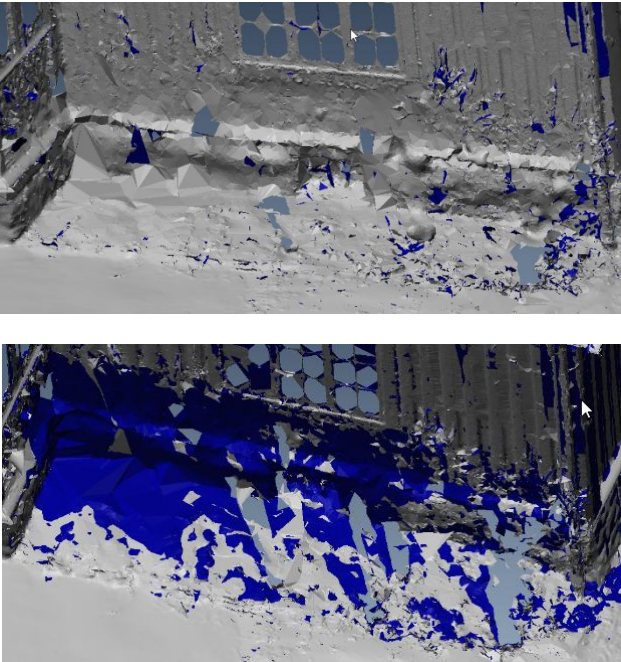


Figure 3.42. Filling holes behind the bushes in front of the house-PolyWorks.

In order to achieve better results, way more time should be devoted for closing and repairing these kind of holes.

Figure 3.43 presents how holes within windows were handle. First, all point clouds were cleaned from the noise around the boundaries and after triangulating data, windows were closed with flat mesh. Also adding extra surface was examined , however the previous idea seemed to work better. Especially when regard to time necessary for creating additional surfaces.

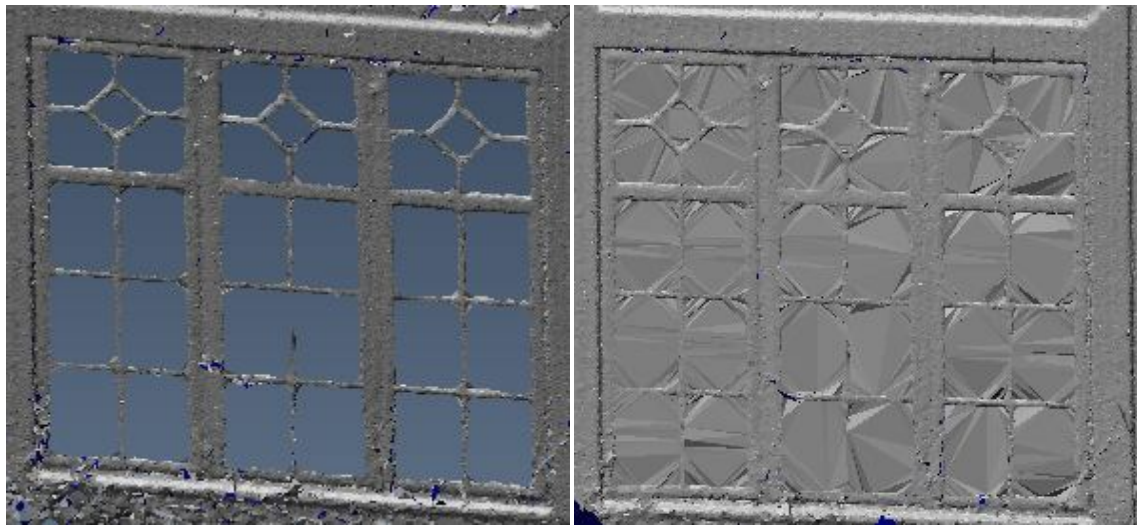


Figure 3.43. Window before and after closing in PolyWorks.

3.7.2.2.3 Smoothing and reducing triangles

For better display and handle with a heavy model, smoothing and reducing triangles should be implemented. Figure 3.44. shows basic dialog for setting up parameters for smoothing together with results in the statistic part.

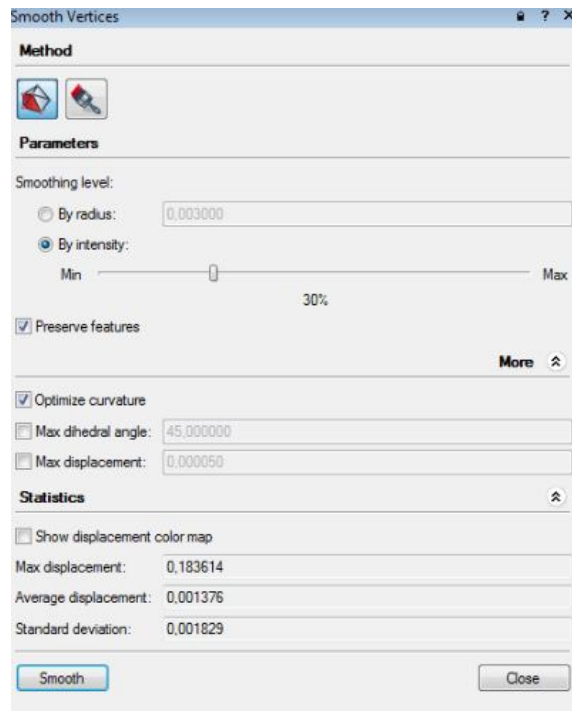


Figure 3.44. Parameters within smoothing process in PolyWorks.

Influence on actual data is shown in figure 3.45. where the same is presented before and after smoothing. .

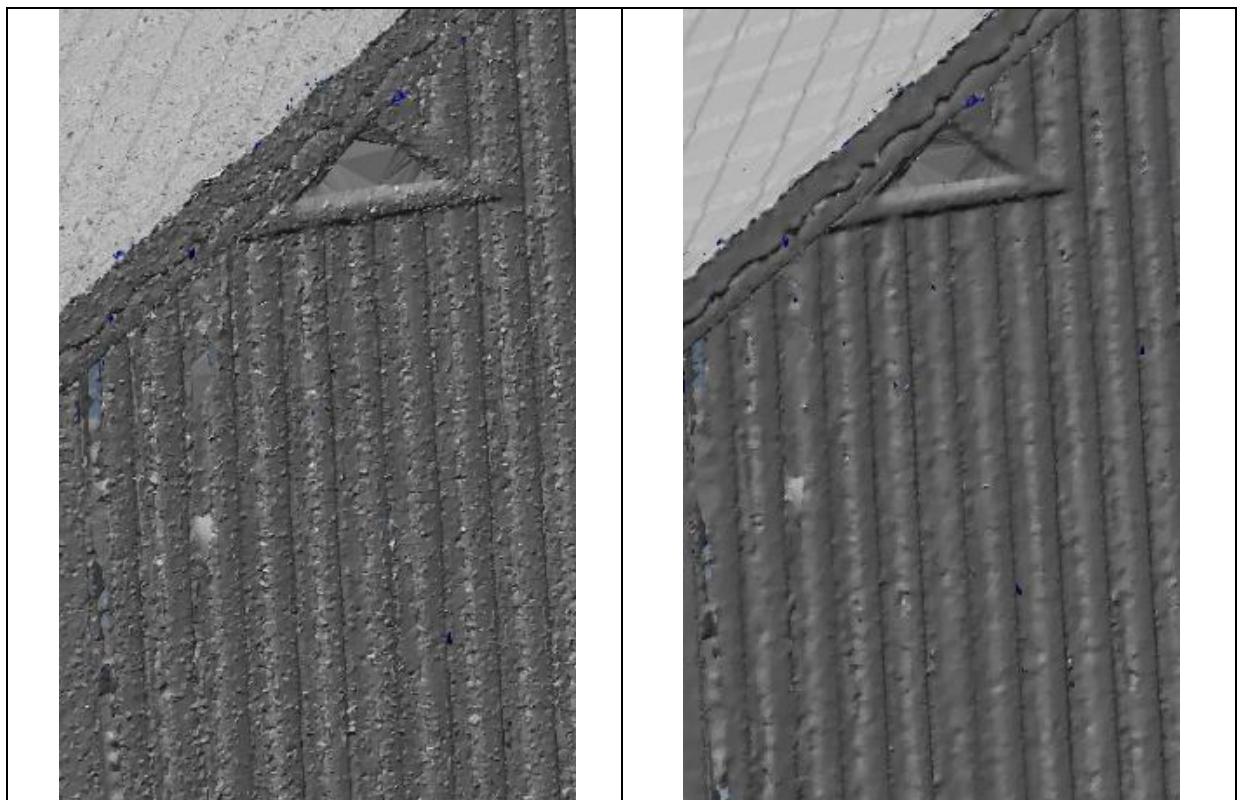


Figure 3.45. Part of surface before (left) and after (right) smoothing- PolyWorks.

After proceeding with reducing numbers of triangles, the final model which has been exported to work further in other software, consists of 6 788 348 triangles. Reducing triangles can be carried out based on fixed number of remaining triangles or fixed tolerance value. In case of the thesis the first option was used with 60 percentage of remaining points.

3.7.2.2.4 Comment

Triangulation done within the PolyWorks can be evaluated as a good algorithm. However, not all functions and operations were examined due to short available time. It can be assumed that result would be improved if more advanced functions were in use.

3.7.2.3 Nidaros Cathedral

Data from Nidaros Cathedral in Trondheim was the subject of Specialization Project [17]. The purpose to use also this dataset was to improve the result of model building and compare different datasets while using the same tools. Hence, data was already registered, cleaned, filtered and colored in RiSCAN PRO. All procedures are not described here. If necessary, refer to Specialization Project [17]. Only matter of triangulation and closing the model is included in the report.

3.7.2.3.1 Data import

Data was imported directly into IMEdit module since there was no need to register data before. From RiSCAN PRO data was exported into ASCII format, together with RGB values. Whole point cloud has been filtered in RiSCAN PRO by Octree filter and resulted in one point cloud consists of all scan stations with 8 830 996 points. Although, the RGB values were included and imported as shown in the figure 3.46. , the point cloud inside IMEdit was displayed as in the figure 3.47.

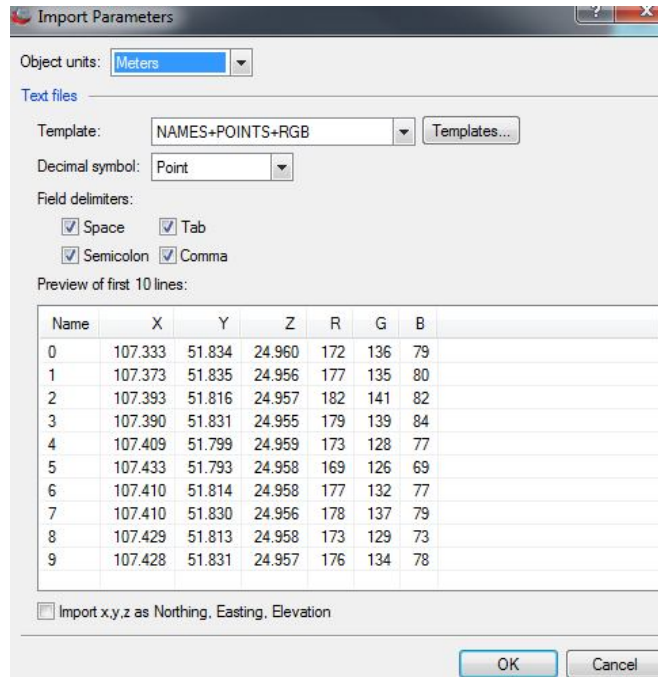


Figure 3.46. Parameters for importing data into IMEdit module, PolyWorks.

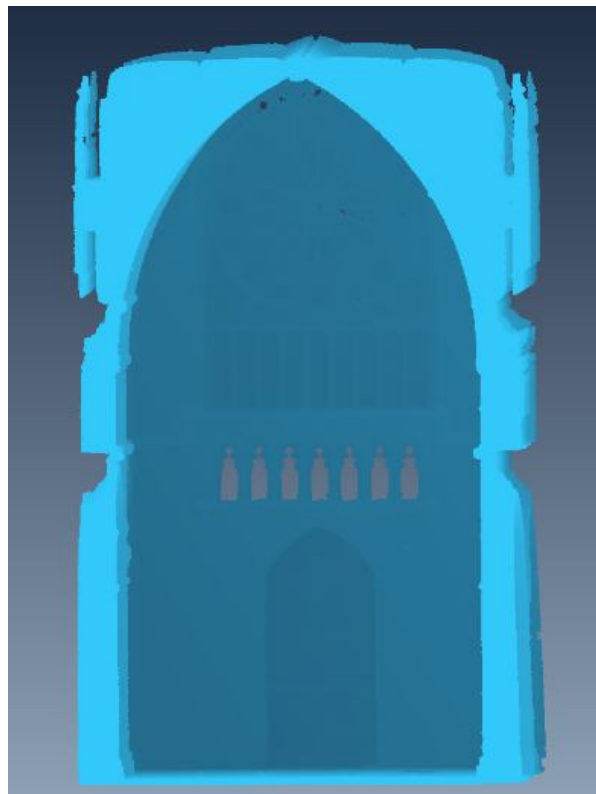


Figure 3.47. Point cloud of Nidaros Cathedral inside IMEdit module, PolyWorks.

Further work was proceeded with above point cloud. As the data was still slightly too heavy, subsampling operation was used. Uniform type with step equal 0,02 m was used, what resulted with 6 521 743 points.

3.7.2.3.2 Wrap Mesh around Point Cloud

After testing few sets of parameters for wrapping mesh it was decided that 0,02m for Tolerance parameter will be used, 50 % of curvature -based subsampling and max.edge length of 0,05 m will be used. Unfortunately, print screen from the software was taken with a wrong parameter that is the reason not showing it within the report.

However, there were two issues concerning results. First, there were lot of areas with reversed triangles, what made very difficult to close possible holes in the model. Lot of repairing -Inverting and Propagating Orientation, was necessary to carried out. Figure 3.48. shows the problem of reversed triangles.

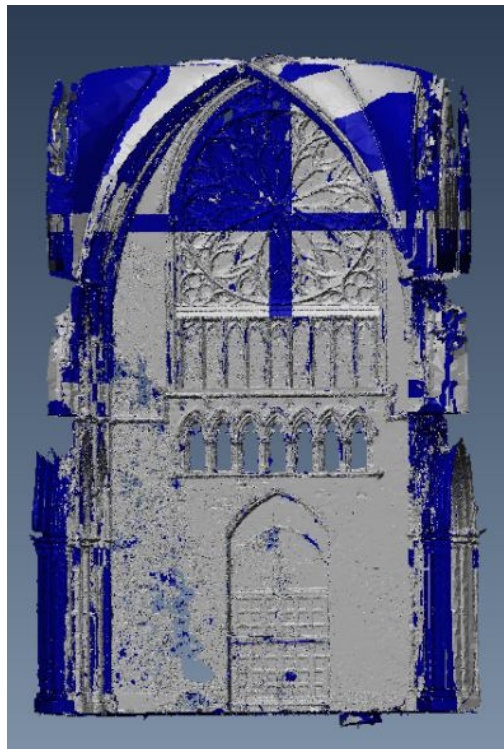


Figure 3.48. Reversed triangles within Nidaros Cathedral model, PolyWorks

Another problem occurred in the bottom-left part of the main wall, shown in figure 3.49. It looks as the data was very noisy in this part and proceeding with triangulation was difficult for this part.

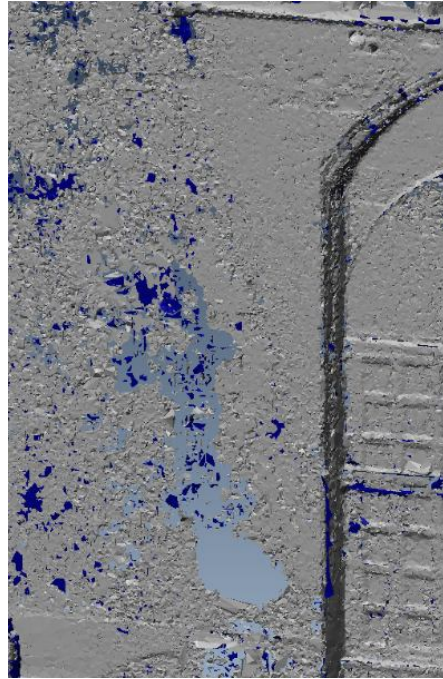


Figure 3.49. Problems with the mesh in the bottom part of Nidaros Cathedral, PolyWorks

3.7.2.3.3 Closing holes and smoothing

After choosing possibly the best parameters for triangulation, there was a need to improve mesh. Besides reversing triangles in the beginning, closing holes and smoothing was carried out. Figure 3.50. presents the procedure of closing holes, part of holes where filled by automatic holes filling algorithm but there were still lot of holes to close manually.

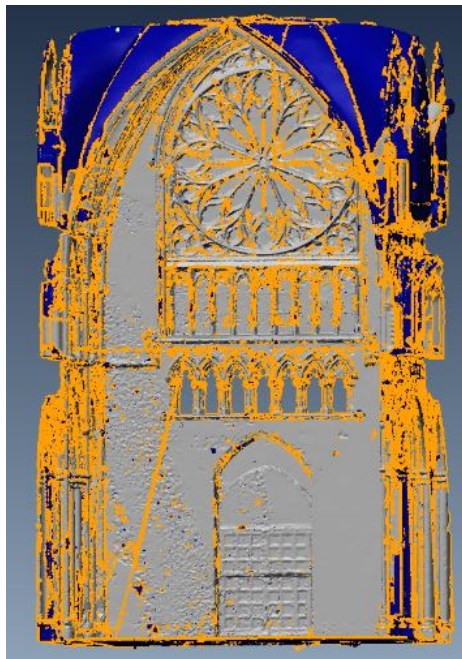


Figure 3.50. Closing holes algorithm in Nidaros Cathedral model within PolyWorks

The result of filling procedure is shown in figure 3.51, where also smoothing by intensity was applied on the smoothing level of 30 %. Problem of the bottom-left part of the wall was improved but in the end, there is still noise visible in the mesh surface.

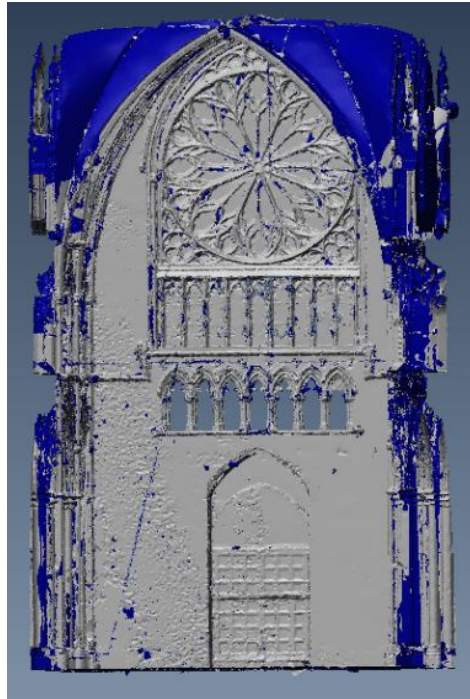


Figure 3.51. Nidaros Cathedral model after filling holes and smoothing, PolyWorks.

3.7.2.3.4 Comment

Results of triangulation procedure for Nidaros Cathedral is many times better than result derived within the Specialization Project [17]. Surface is complete in 90 % and all details are preserved. Few more repairing operations might have been used but the time did not allow for that. Texturing was not done within the PolyWorks. Result model is consider to be a fully functional 3D representation of the area. Only textures should be applied. This, however can be done in alternative software.

3.7.3 Geomagic Studio

As the final results were still not satisfactory, Geomagic Studio was decided to be used. Geomagic Studio is one of multiple available tools provided by 3D Systems Company. Solutions, they provide, improve and develop work on 3D datasets. There are distinguished few branches of Geomagic tools, 3D Scanning System, 3D Design Software, Scanning

Software and Inspection Products. Geomagic Studio is included in Scanning Software branch. More about the software can be found in the first chapter, under tools characterization.

3.7.3.1 Import data

Two ways of importing data were implemented. First included importing already existing models, in order to improve them and another way was to import colored point cloud and create model with textures from this point cloud. For Østre Gløshaugen house the first way was used and the polygon model from PolyWorks software was imported. Nidaros Cathedral object was imported as a point cloud data with applied colors and also as an already prepared model in PolyWorks. Models was generated in PolyWorks software and as .stl format exported.

3.7.3.2 Østre Gløshaugen house

3.7.3.2.1 Mesh Doctor

While importing the file, Geomagic asks if to open directly Mesh Doctor function. It automatically detects and improves errors in the polygonal model. Figure 3.52. shows the house after importing and accepting the Mesh Doctor tool. It is in analysis mode.

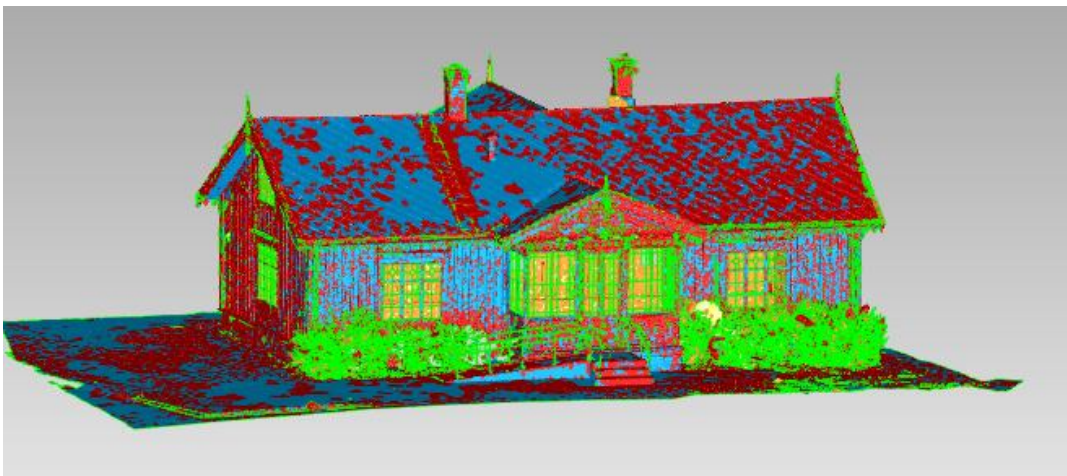


Figure 3.52. Østre Gløshaugen house imported to Geomagic Studio, Mesh Doctor function on.

Figure 3.53. presents Mesh Doctor dialog with all the options and with results after initial analyzing the model.

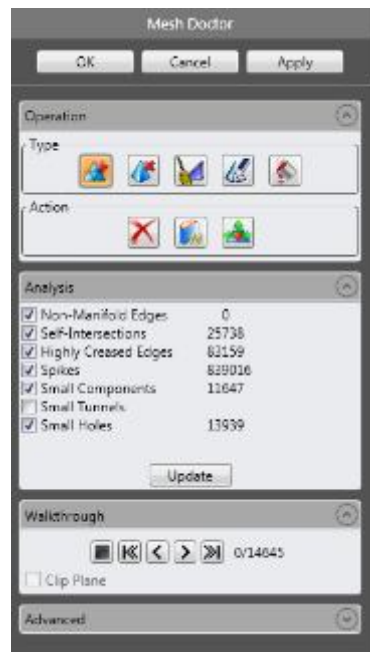


Figure 3.53. Mesh doctor dialog within Geomagic Studio

After applying several different settings and operation within Mesh Doctor the model in figure 3.54. was obtained. Bushes in front of the house were deleted, small holes were closed, the model looked way better.

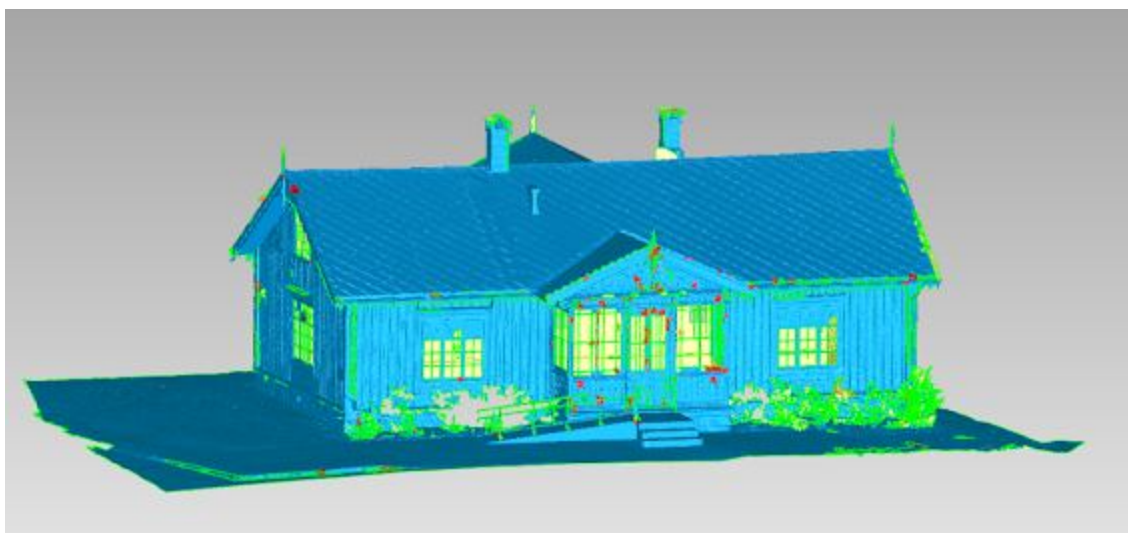


Figure 3.54. Model of Østre Gløshaugen house after applying Mesh Doctor function.

Within Mesh Doctor tool there are several function to proceed with, figure 3.55. shows the zoomed dialog for all the operations.

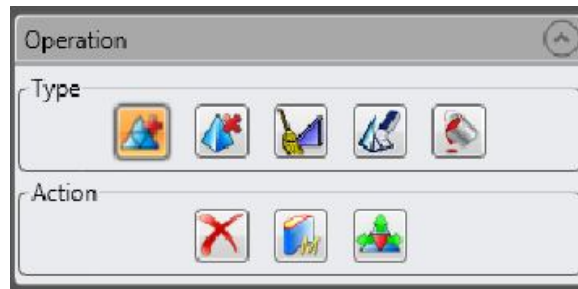


Figure 3.55. Mesh Doctor operation types-Geomagic Studio

All operations include Auto-repair function, spikes removing, holes filling, decimating, intersection checking. Entire operation took a long time to carry out but the result was more than rewarding.

3.7.3.2.2 Hole filling

After using the tool, interactive holes filling algorithm was examined. Figure 3.56. presents basic types of holes closing functions within Geomagic Studio.



Figure 3.56. Interactive holes filling dialog-Geomagic Studio.

There are three types of ways to close holes and three types of algorithms used with all possible ways. First of all, there is a possibility to close one after another entire hole, then to close hole partially and the last option is to create a bridge between data. Within all three options, three different algorithms can be used. First, the hole can be closed with a flat surface, it is the most coarse holes filling algorithm, the second way is to close hole with a tangent option, it tries to match curvature of the surrounding mesh with more tapering than the curvature technique. The last option is to fill hole with curvature option, this algorithm modifies the surrounding of the hole and gives the most precise filling. Depends on the area and data all option were used during working on the models. Figure 3.57 presents the house before and after filling holes behind the bushes in front of the house.

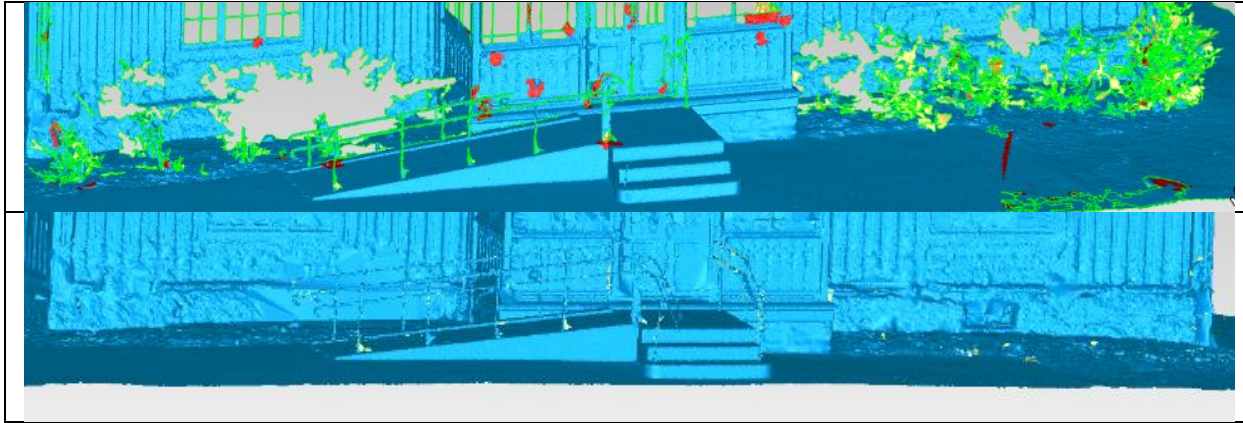


Figure 3.57. Østre Gløshaugen house before (top) and after (down) closing holes behind bushes in front of the house- Geomagic Studio.

3.7.3.2.3 Remeshing tools

To improve the model some of other functions were also used. Remeshing tools include few operations that enable fast and accurate retriangulation of entire or part of polygon models for cleaner and more usable 3D models. Figure 3.58. shows the dialog of ReWrapping function. ReWrap tool is included in all enhancing object mesh functions and is useful to recreating part of the polygon models. It is very convenient for a mesh that is damaged in a specific area. Model will not lose other improvements by wrapping original data again.

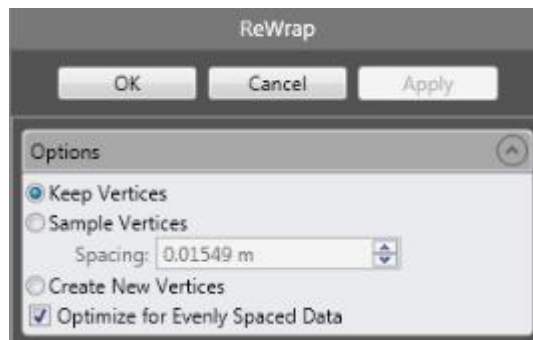


Figure 3.58. ReWrap function within Geomagic Studio.

3.7.3.2.4 Decimate

Decimate function reduces number of triangles with keeping surface detail or colors. It is very useful when the model contains an excessive number of points.

Figure 3.59 shows the parameters possible to fix before running the algorithm. Reduction mode can be set up in two ways. First, as Triangle Count where the percentage of remain triangles is fixed and second, Tolerance, where the greatest distance allowed between any original vertex and new position in a polygonal mesh is specified. When the first mode is selected, the object's shape is the highest goal, when the tolerance is chosen the surface is possible to shift by a specified maximum.

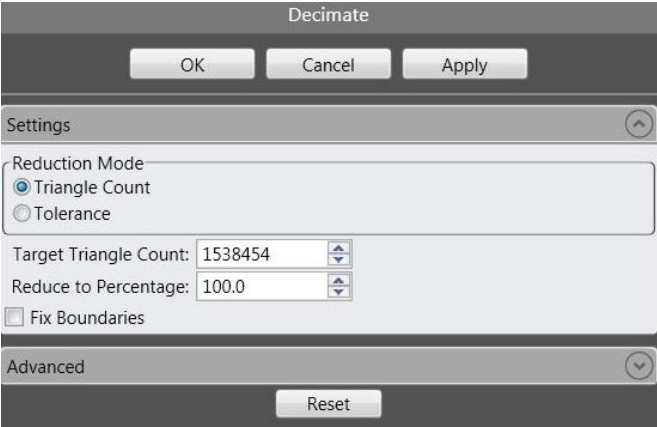


Figure 3.59. Decimation algorithm within Geomagic Studio.

Figure 3.60 shows how the algorithm works. It removes triangles in the planar regions and keep network denser in the more curved areas.

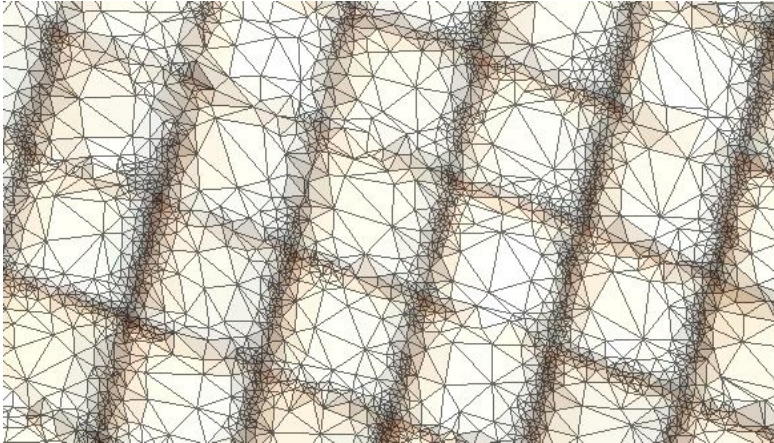


Figure 3.60. Polygonal model after decimation. Part of the roof- Geomagic Studio.

3.7.3.2.5 Smoothing

In order to smooth the object Relax function can be used. This command smoothes a model by minimizing crease angles between triangles, hence improving the quality. The function can be used effectively to reduce noise and sharp spikes in the object. Figure 3.61.

includes the parameters and results after Relax Polygons operation. In most cases parameters were fixed as in the figure.

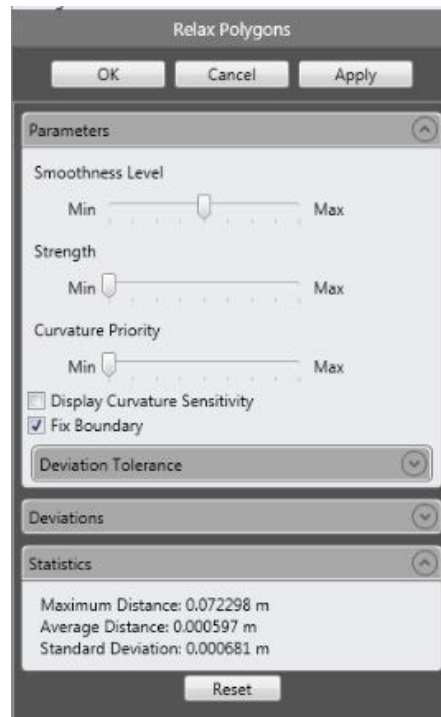


Figure 3.61. Relax polygons function within Geomagic Studio.

3.7.3.2.6 Result and export

Final result of the 3D model of the house obtained in Geomagic Studio can be seen in figure 3.62. The final model consist of 6 371 329 triangles. In order to get textures at the model, RiScan Pro software was used. The final model from Geomagic was exported as a .obj file and imported in RiScan Pro, where all images were already registered to the Project Coordinate System and could be assigned to the object.

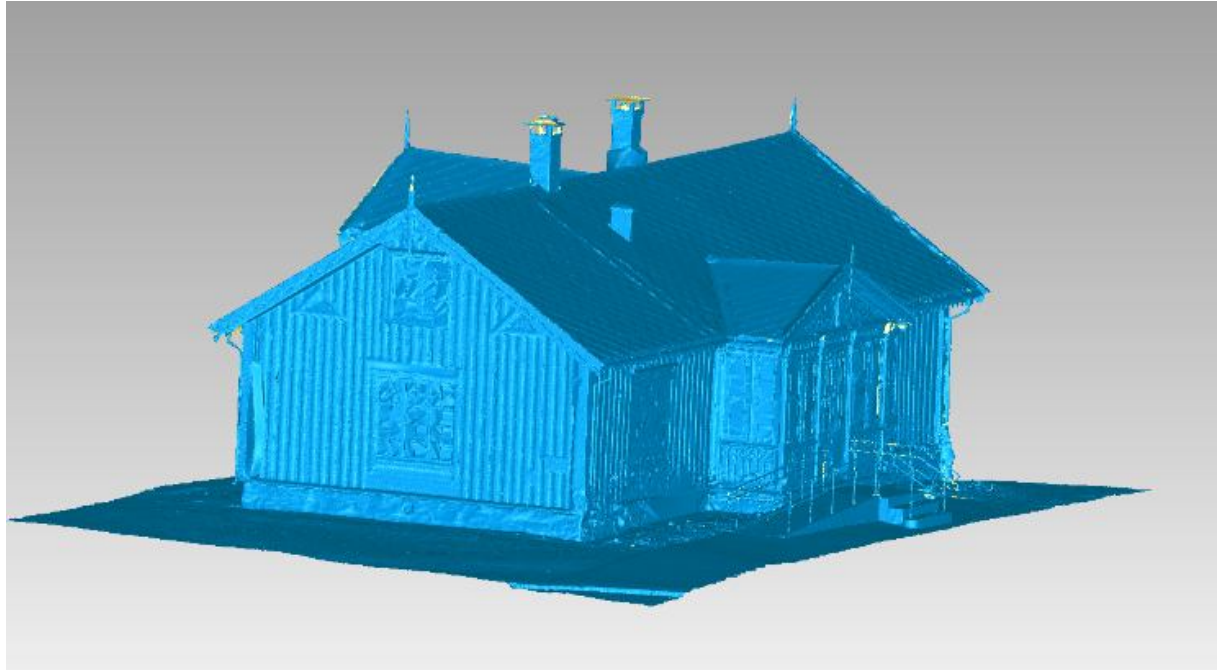


Figure 3.62. 3D model of Østre Gløshaugen house without textures- Geomagic Studio.

3.7.3.3 Nidaros Cathedral

Nidaros Cathedral data was imported in two ways, first as a colored point cloud obtained in RiScan Pro while working on the Specialization Project last semester [17]. Second as a polygonal model created in PolyWorks as .stl file.

Figure 3.63. shows the model imported from PolyWorks software and the point cloud imported directly from RiScan Pro, saved in ASCII format.



Figure 3.63. Left :model created in PolyWorks, right: point cloud from RiScan PRO.

3.7.3.3.1 Mesh doctor

The model imported from PolyWorks was treated with Mesh Doctor in the same way as the object described before. Multiple holes and spikes were removed.

Figure 3.64. presents the Cathedral while working with Mesh Doctor function. As can be seen, the left bottom part of the wall has some problems with orientation of triangles and with the noisy surface. The conflict area is the same as in model created in PolyWorks.

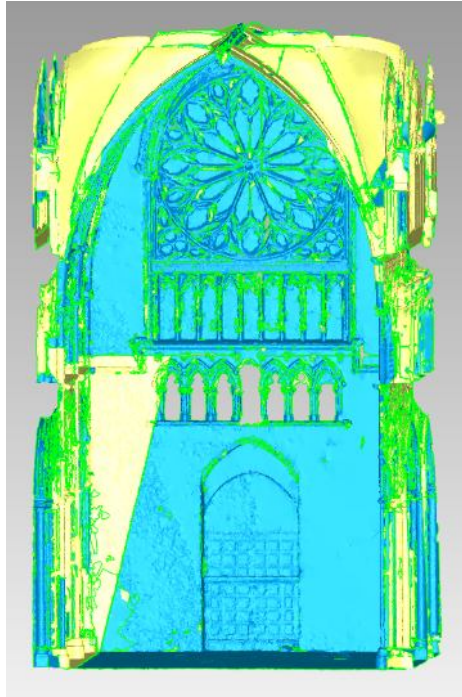


Figure 3.64. Nidaros Cathedral while mesh repairing-Geomagic Studio.

Hole filling, decimation and smoothing functions were applied for the model obtained in PolyWorks. It highly helped to improve the object. The model of Cathedral consists of more detailed areas, for example the boundaries of each nava or the main stained glass with all the details on it. However the smoothing function with the priority of smoothness and curvature preservation worked for the data with satisfactory results. The final model , previously created in PolyWorks was improved in Geomagic and is shown in figure 3.65. It consists of 8 886 322 triangles. Because the data was not colored, the model is in its default color.

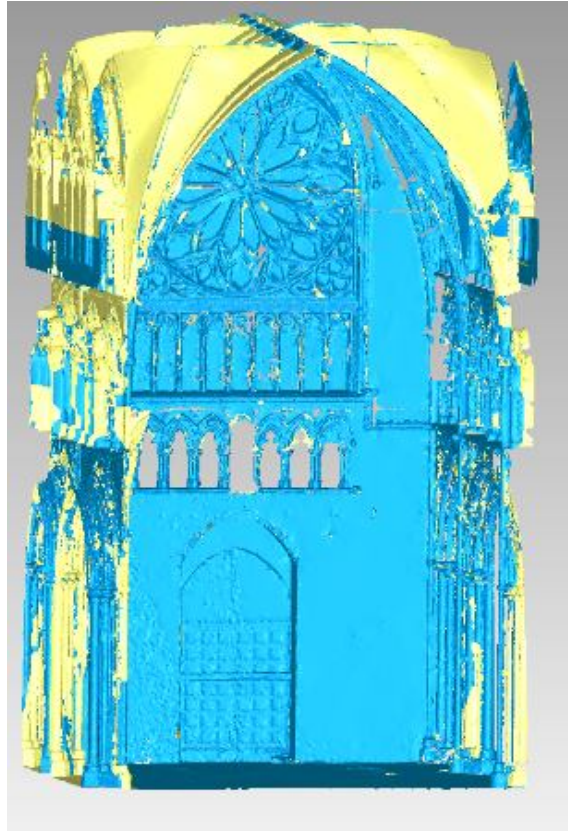


Figure3.65. Nidaros Cathedral model improved in Geomagic Studio.

3.7.3.3.2 Triangulation from colored point cloud

Noise reduction

One of the function available for point clouds within Geomagic Studio is Noise Reduction. Figure 3.66. presents all possible parameters together with statistic results. The command improves errors by moving points to statically correct position.

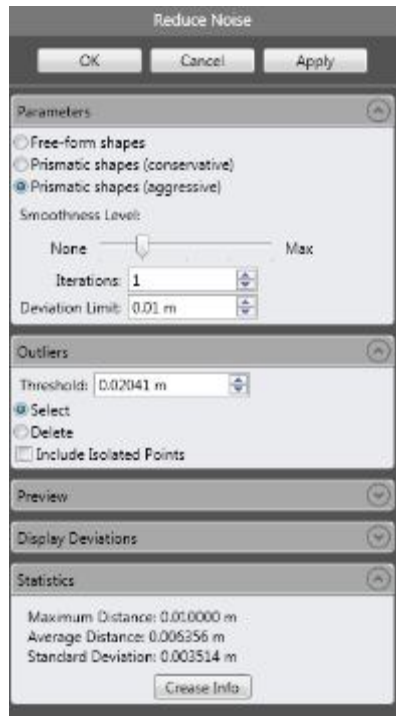


Figure 3.66. Noise reduction carried out on point cloud data from Nidaros Cathedral- Geomagic Studio.

After proceeding with the noise reduction point cloud of 13 223 498 points turned into point cloud of 10 556 598 points.

After cleaning operation, the point cloud was ready for wrapping function. Wrap function creates a mesh from point cloud with specific parameters. Dialog with the Wrap function is shown in figure 3.67.

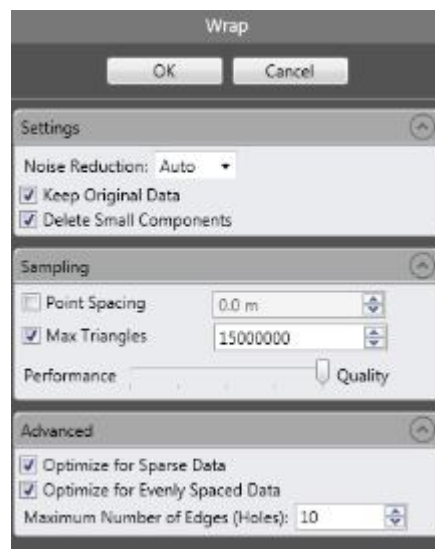


Figure 3.67. Wrap function in Geomagic Studio.

The result of meshing function is a model consist of 16 422 371 triangles. Obviously, model required some improvements, hence mesh doctor both with relax and decimation function were used. The function are described in a case of Østre Gløshaugen house and here only the results will be presented.

To generate textures from colored point cloud the tool called Generate Texture Maps was used. Figure 3.68. presents the dialog with parameters for this function.

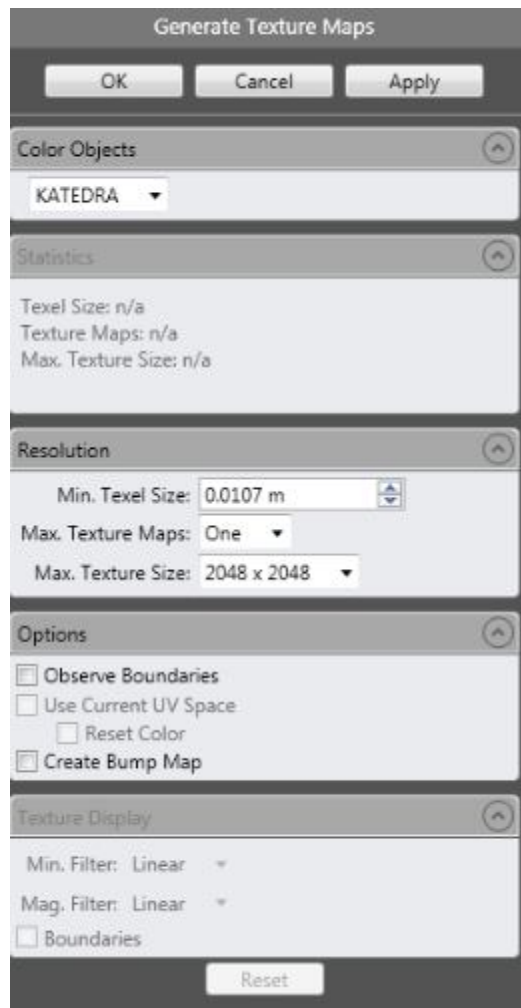


Figure 3.68. Generate Texture Maps function within Geomagic Studio.

As can be seen in figure 3.69 by implementing the function both model without textures and with textures can be obtained. Figure 3.69 presents the final versions of Nidaros Cathedral model.

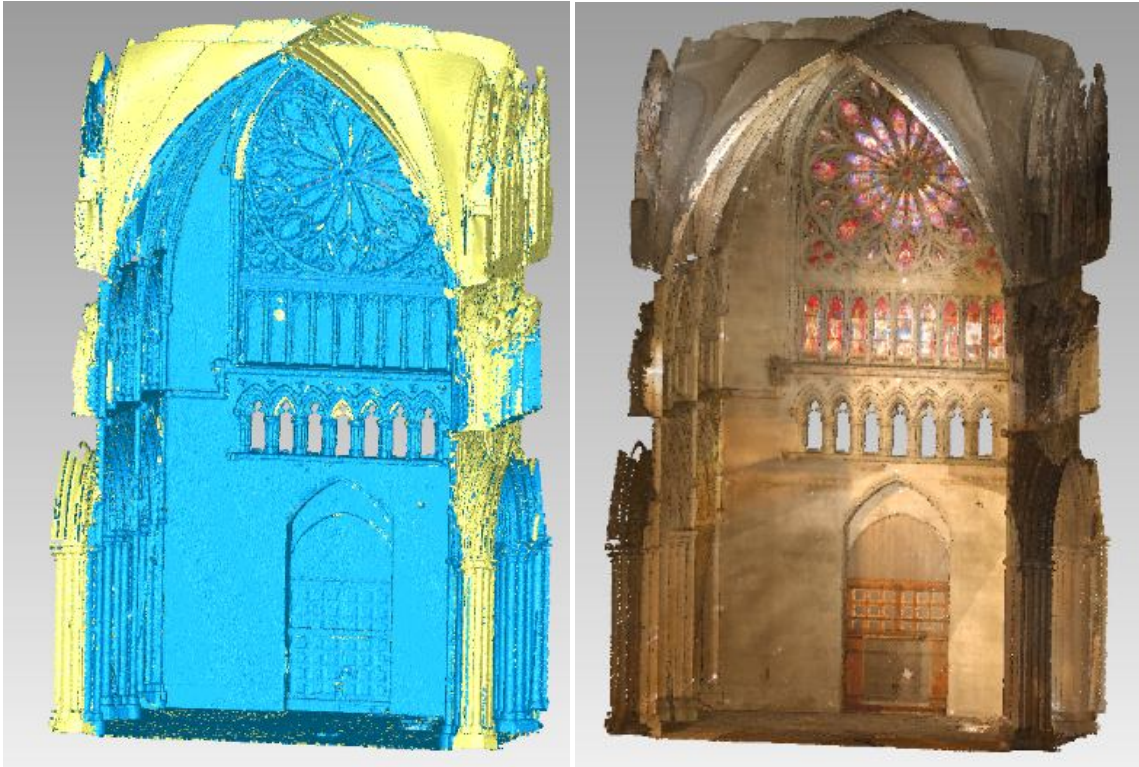


Figure 3.69. Final versions of Nidaros Cathedral model without textures (left) and with textures (right)- Geomagic Studio.

3.7.3.3.3 Result and export

Final model is shown as a 3D PDF in external appendix 1. The 3D PDF was created in another software- SimLAB and for exporting .obj format was used. Before creating the 3D PDF, numbers of triangles were decreased highly in order to make the appendix possible to open by others. The quality and the details level were not as good as it is originally but for a proper display it was sufficient.

Figure 3.70. shows a part of Cathedral opened in SimLab software. It can be seen that all details around stained glass are kept. The colors differs slightly because of different lighting conditions within the software.



Figure 3.70. Nidaros Cathedral opened in SimLab software.

3.7.4 GOM Inspect

GOM Inspect was decided to be used for Østre Gløshaugen object. The input data was saved in ASCII format. One file for each scan position of Riegl and Faro measurements. Figure 3.71. shows the entire point cloud within the software

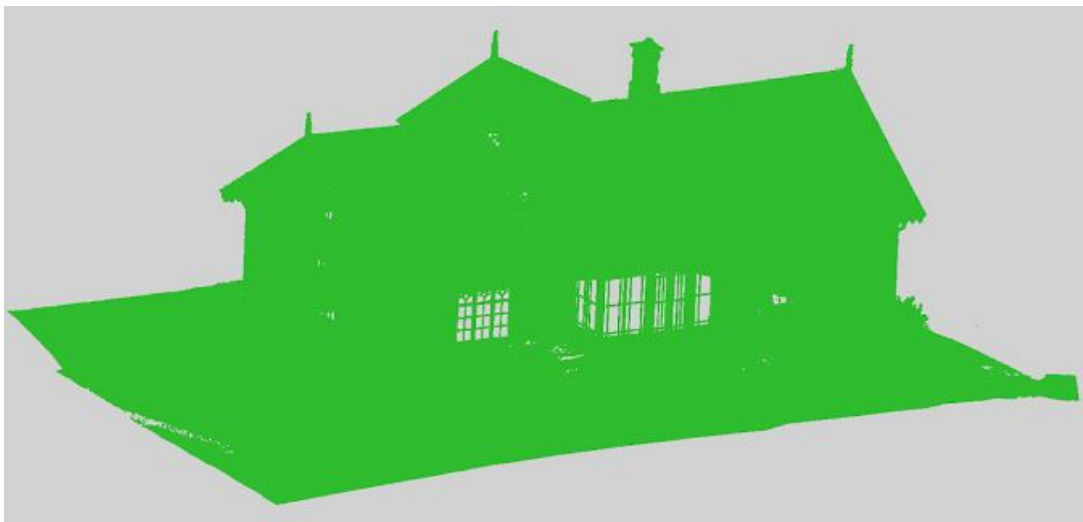


Figure 3.71. Point cloud displayed in GOM Inspect.

GOM Inspect offers one algorithm for creating an editable polygon mesh. It is called Polygonize Point Cloud and the basic window with all settings is shown in figure 3.72.

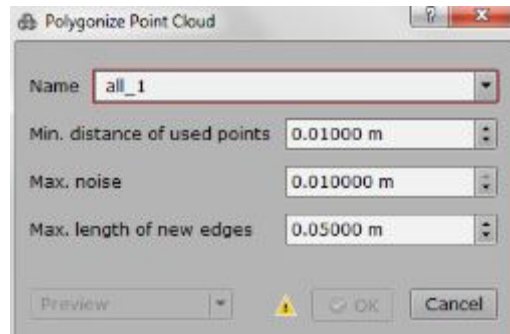


Figure 3.72. Polygonize Point Cloud operation within GOM Inspect.

As can be seen in the figure 3.72 there are three options to establish. First, Min. distance of used points, the value defines minimum distance between the point that will be processed. If the value is larger, the result mesh will be rougher. Next, Max. noise should be chosen, the value should be adjusted between the value of the existing noise and the distance between two opposite surfaces. Finally, Max. length of new edges needs to be set up. The value represents the length of the polygonized triangles. This value cannot be smaller than the existing distance between the selected points. Otherwise, holes might result in the mesh.

Unfortunately, even after testing several possible settings for the parameters holes appeared in the mesh. Figure 3.73. shows holes that can be found within the roof of the house.

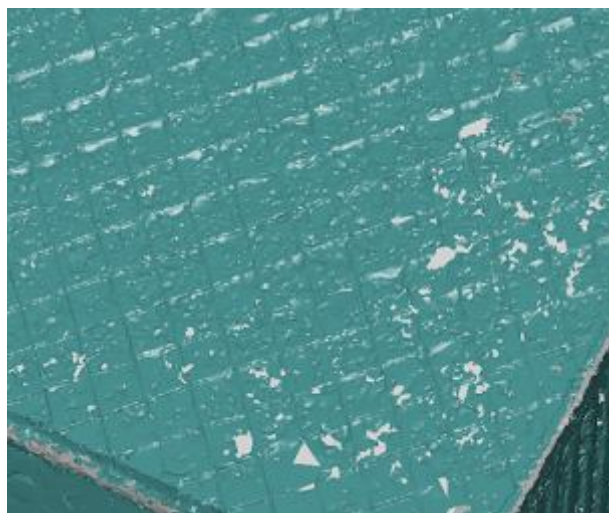


Figure 3.73. Holes within the roof of the house. GOM Inspect.

Next step of working inside the GOM Inspect was to repair the mesh from all holes that arose while meshing. Also the issue of reversed triangles appeared. To repair the issue, command Invert Selected Normals needs to be used. Entire area that was inverted needed to be selected first. It was a very time-consuming process.

3.7.4.1 Closing Holes

GOM Inspect offers two types of closing holes algorithms. One is automatic operation and is shown in figure 3.74. Another one is interactive and is shown in figure 3.76.

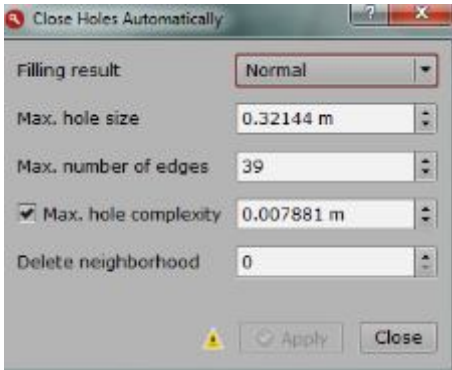


Figure 3.74. Closing holes automatically. GOM Inspect.

This function is well adapted to fill in several hole simultaneously. As can be seen in the figure 3.74. there are few parameters to adjust. First of all, there are five types of filling result. It defines how the surface after filling will look like. The choice can be made between, Normal option , when new surface is adapted to the neighborhood. Next, there is Rough option, where points of the mesh are directly connected to each other without creating any new points and it does not take into account the surface contour. Third option is a Plane-based algorithm, where a new surface is based on a plane and can be used for example while filling holes in windows. Last two options are called Smooth and Very smooth, as the names indicate new surface is being adapted to the neighborhood with additional smoothing operation.

Max. hole size and max. number of edges implicate directly to the dimension of the hole. If the value of size or number of edges is bigger than the established one , the hole will not be closed. One of the last parameters is the value of max. hole complexity and is optional to use.

Figure 3.75. presents area of the house before closing holes automatically and after. Working of the algorithm is proved.

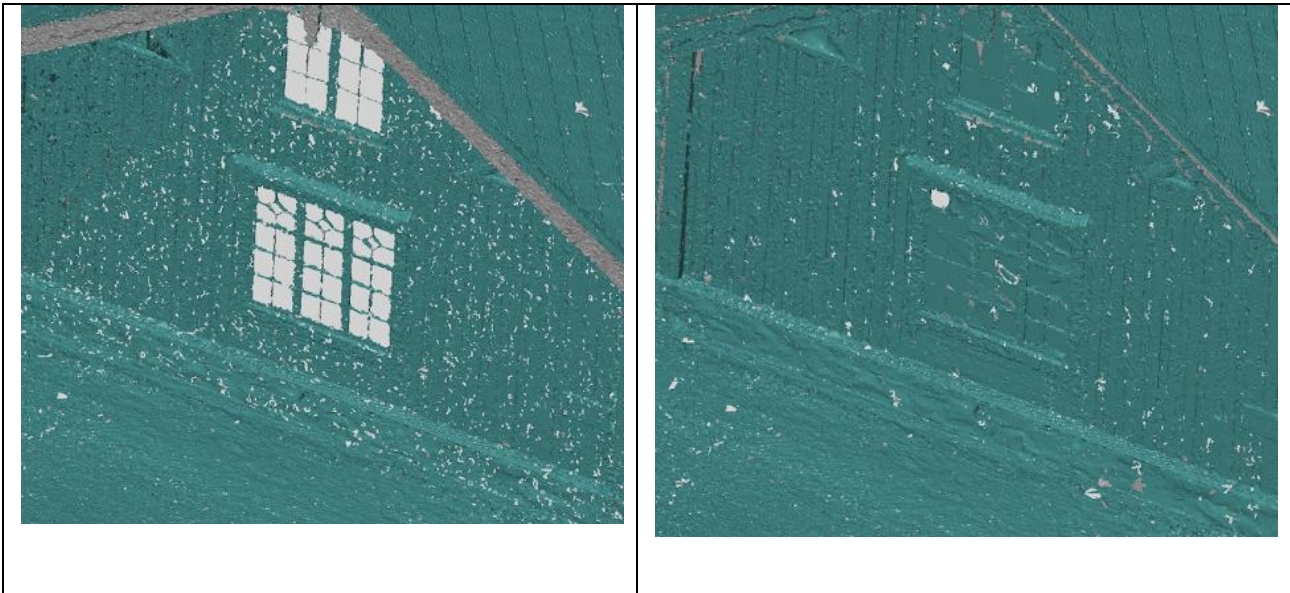


Figure 3.75. West side of the building before (left) and after (right) automatic closing holes. GOM Inspect.

Unfortunately, not all holes could have been closed automatically. In order to complete the model, Closing Holes Interactively option was used. Figure 3.76. presents the window with parameters to adjust.

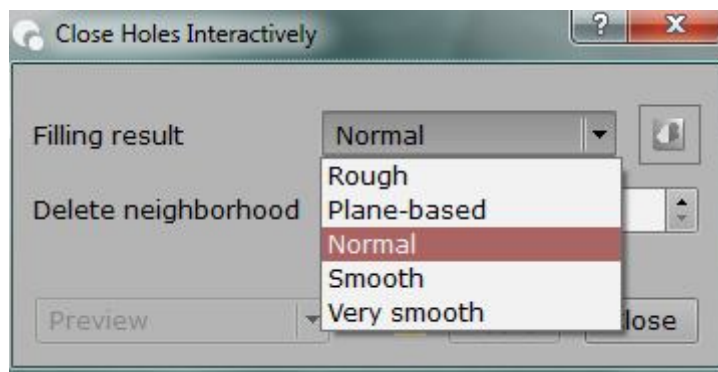


Figure 3.76. Closing holes interactively. GOM Inspect

As can be noticed, the same filling result as in automatic option, occurs also here. Additionally, what is not shown in the figure 3.76. , there is an option for closing holes partially. This alternative gives a possibility to close holes with higher accuracy.

As there were several places with very complicated holes lot of interactive operations were needed. Figure 3.77. presents for example reconstruction of the part of the chimney and closing holes in surrounding.

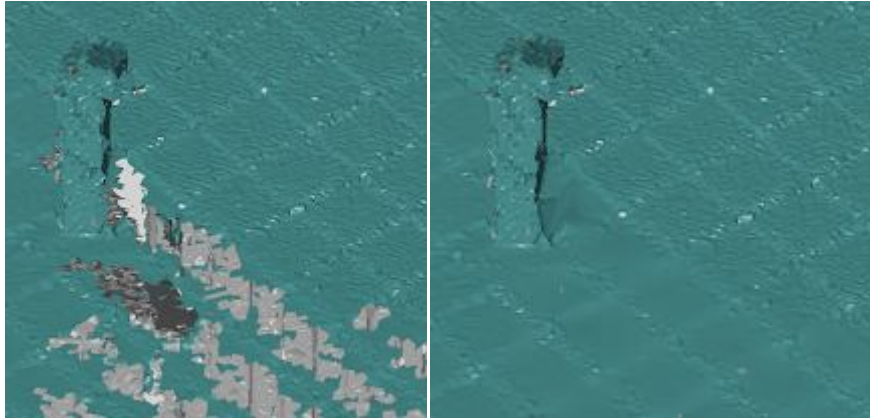


Figure 3.77. Chimney reconstruction and closing the surrounding. GOM Inspect

Also the issue with the part of the building that was covered by bushes appeared in the model. Figure 3.78. shows this part before and after filling in. The surface is reconstructed but is not quite similar to the original shape of the wall.

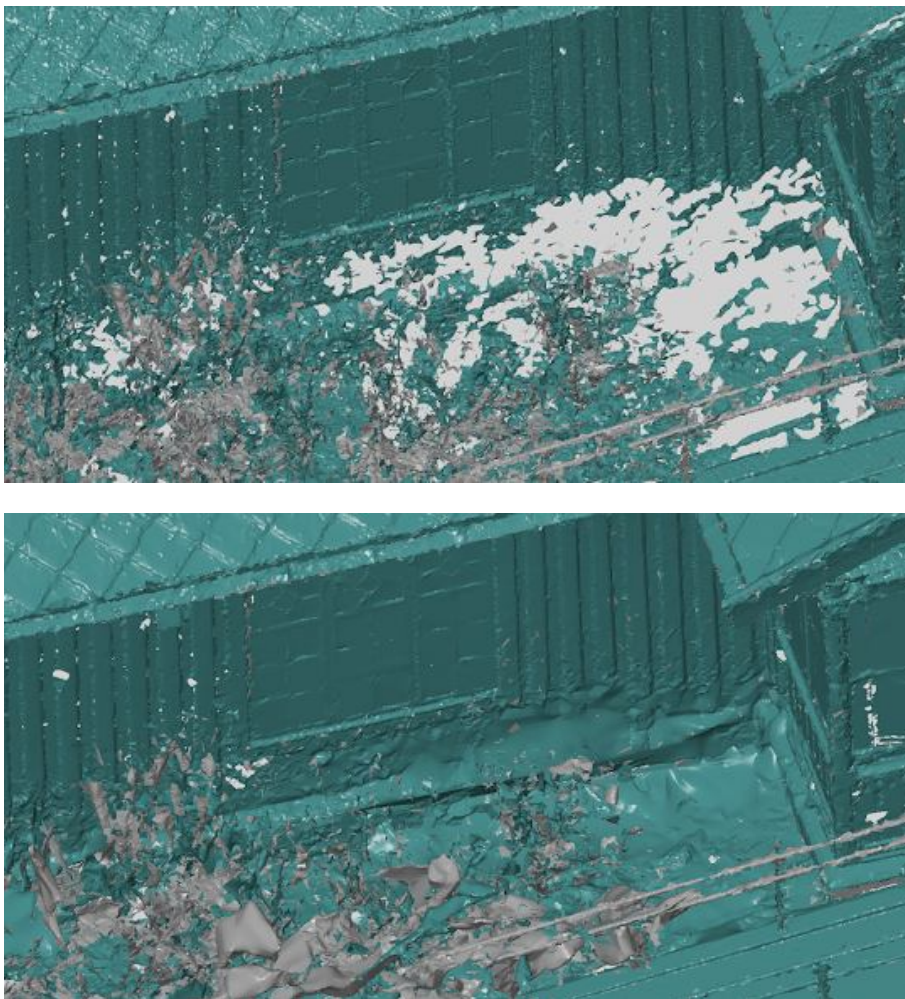


Figure 3.78. Filling holes behind bushes in front of the Østre Gløshaugen building.

Windows as in previous examples were supposed to be closed with the plane-based option with interactive holes closing operation. Figure 3.79. shows window before and after filling in.

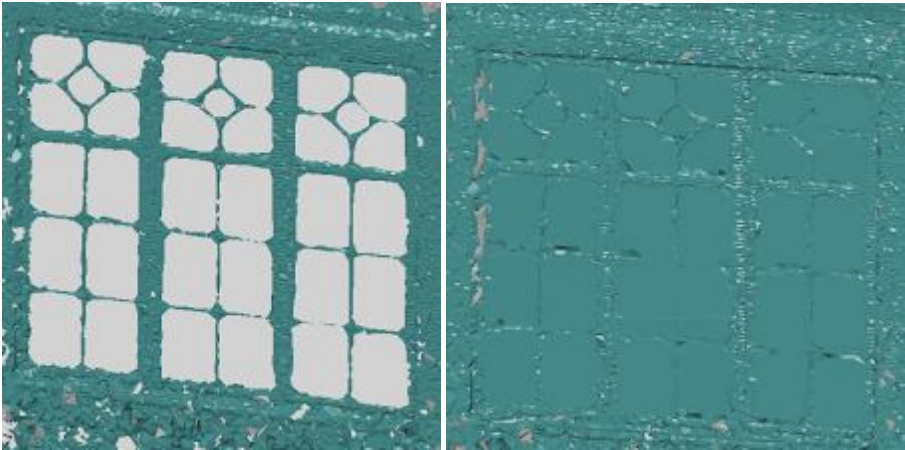


Figure 3.79. Window before (left) and after filling with the plane surfaces. GOM Inspect

After analyzing all possible ways of filling the windows, GOM Inspect seems to accomplish this task in the best way.

3.7.4.2 Smoothing

While meshing the point cloud smoothing operation is already applied and existing noise is eliminated. However, in some cases additional smoothing is required. Figure 3.80. presents the basic options for smoothing within GOM Inspect.

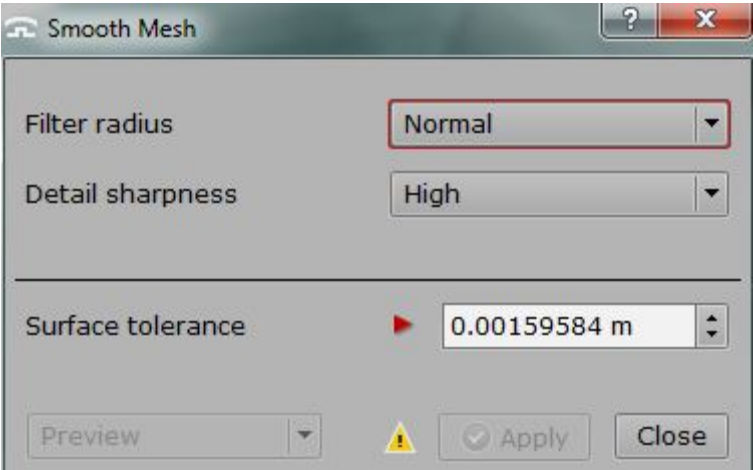


Figure 3.80. Smoothing parameters. GOM Inspect

Within the filter radius fours options are available. Small, Normal, Large and Very large. The larger the radius is the smoother the mesh is. Detail sharpness can be divided also

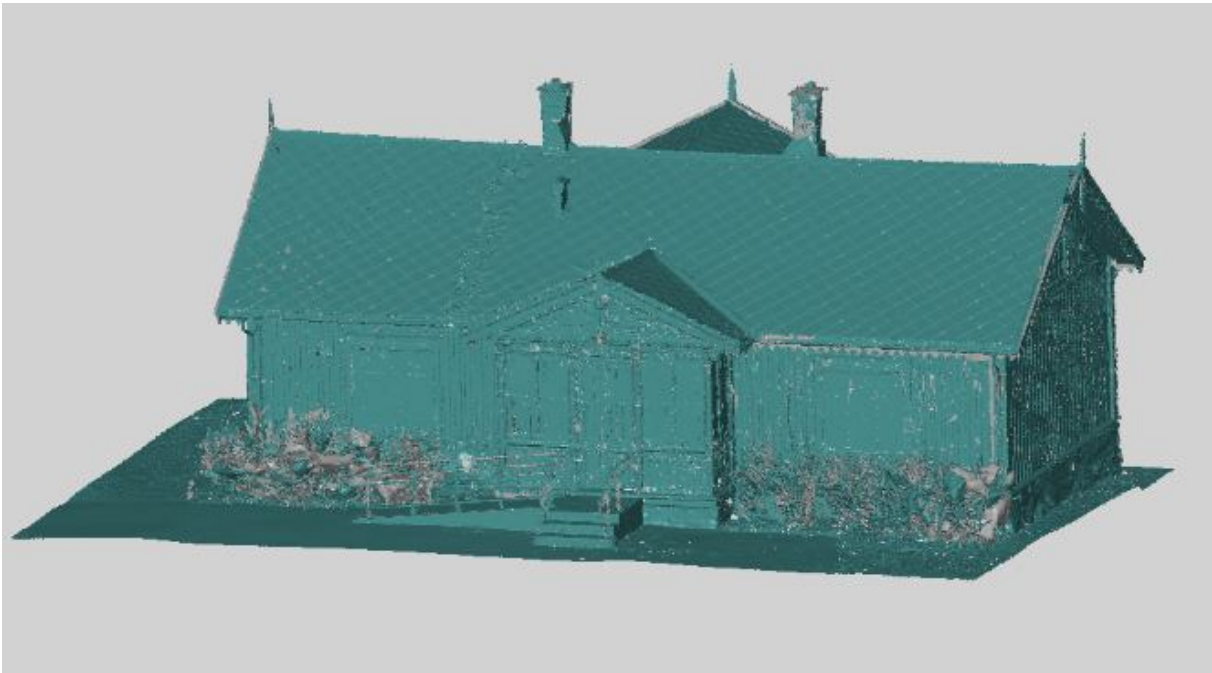
in four options. High, Normal, Low, Very low. This parameter defines how detailed parts of the object should be maintained. Surface tolerance stands for the maximum roughness which should be smoothed.

The results of smoothing can be seen in figure 3.81. The algorithm works pretty nice.



Figure 3.81. Part of the house before (up) smoothing and after (down) the operation. GOM Inspect.

The final model generated by GOM Inspect is shown, from several angles, in figure 3.82 .



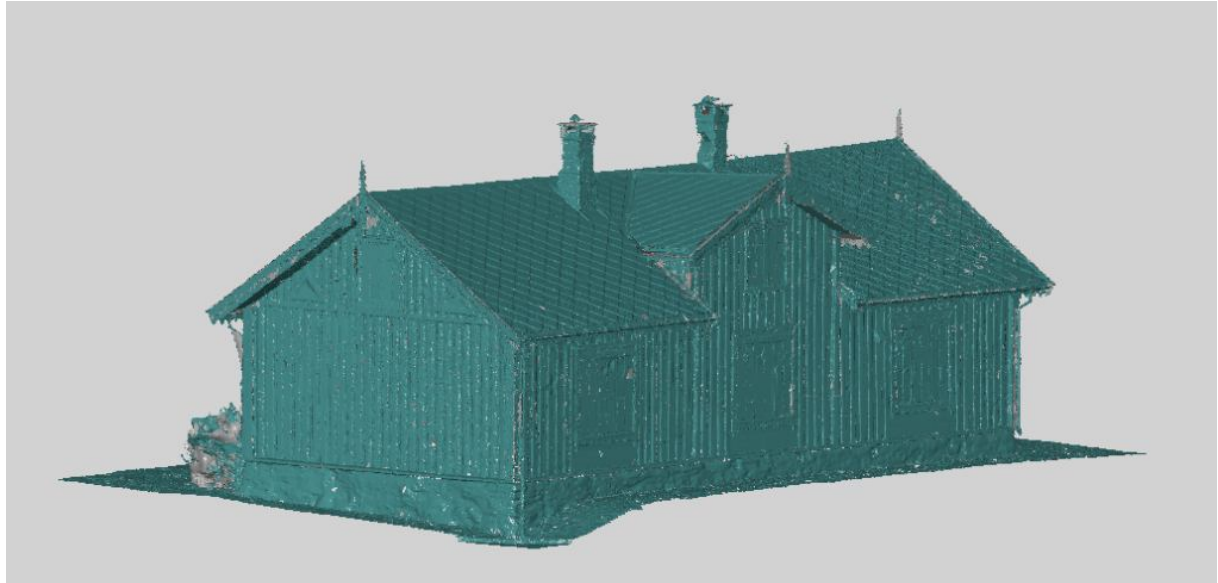


Figure 3.82. Model of the house generated in GOM Inspect software.

3.8 Texturing

3.8.1 RiSCAN PRO

Process of image registration was described in previous part of the chapter. Additional texturing refers only to 3D model of the Østre Gløshaugen house because the Nidaros Cathedral model was textured from colored point cloud what gave very good results. Description of coloring the point cloud of the Nidaros Cathedral was included in Specialization Project [17].

Model of the house was imported as .obj file under the branch Polydata objects. Project Coordinate system was automatically assigned.

In order to proceed with texturing within RiScan Pro all images need to be undistorted. The process is done automatically in the software and all images are stored in the folder *undistorted images*. Also during the process new camera calibration is created, it is the copy of the original camera calibration except the distortion values. Texturing was carried out for all images together, with the maximum texture size of 2046 pixel. The whole process was very long and highly memory consuming.

The result in RiSCAN PRO is presented in the figure 3.83. Also as can be seen in figure 3.84., several errors in data while texturing or importing to the RiSCAN software were created.



Figure 3.83. Textured house in RiSCAN PRO software.



Figure 3.84. Error after importing and texturing 3D model of the house in RiSCAN PRO.

In order to obtain the model without the error it has been exported again to .obj file and imported for the last improvements into Geomagic Studio software. After proceeding shortly with Mesh Doctor and few other functions the final model of the Østre Gløshaugen house was built. The same as in the case of final model of Nidaros Cathedral, the textured, final model of the house is presented in 3D PDF in external appendix 2.

Figure 3.85. presents the house textured in RiSCAN PRO but imported into Geomagic Studio to improve the last errors created during texturing. As can be seen, there are few areas with slightly wrong colors, shown in the figure 3.86. However, the majority of the object is textured correctly.



Figure 3.85. Textured house displayed in Geomagic Studio.



Figure 3.86. Errors in texturing the roof of the house, displayed in Geomagic.

One of the last problems concerning texturing was the area behind the bushes. As it was decided previously that the bushes are cut off from the model the images still includes the bushes. Unfortunately, the only solution for the moment was to project colors as they are. Figure 3.87. presents front of the textured house. In the future, the images could be processed in several ways to excluded bushes from the photos.



Figure 3.87. Textured front of the house with bushes projected onto walls, displayed in Geomagic.

3.8.2. MeshLab

MeshLab software was examined regarding possible texturing. Within the software several functions for texturing can be found. For the data, specially one was decided to try. Figure 3.88. shows the dialog with all possible solutions with marking on the chosen one.

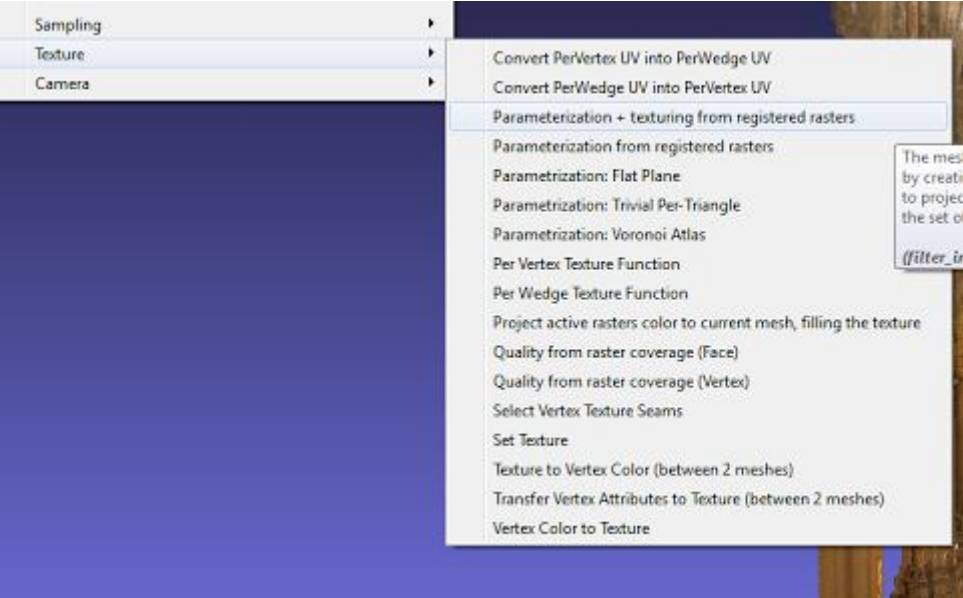


Figure 3.88. Texturing options within MeshLab software.

The one that was chosen to carry out is called *Parameterization and texturing from registered rasters*. The algorithm creates some patches that correspond to projection of parts

of the surface onto the registered rasters. Figure 3.89 presents how rasters are being registered to the mesh.



Figure 3.89. Raster registration within the MeshLab software.

Images are partially transparent and by mouse operation and zooming they should cover the entire model in the most accurate way. Unfortunately, after several attempts registration was not sufficient to proceed with texturing. The main problem was to adjust all images to the projection of the mesh. When in the foreground images covered surface perfectly, the background was totally shifted. MeshLab offers also generating textures from colored point cloud but the data was apparently too heavy for proceeding with the algorithm. Because of the lack of enough time further attempts were canceled.

Although, in future work it would be very interesting to examine the algorithm and results.

3.8.3 Comment

As the summing up, textured models of both objects were obtained in different ways and in different software. It has been shown that there are several possibilities to do it. High resolution images can be used as well as colored point clouds. The final versions of both textured models are shown in external appendices as 3D PDF. Anyone can rotate them, zoom and move within the PDF files. Both models were exported as .obj files and then imported to SimLab software which was used to create this interactive PDF files.

3.9 Data flow

Basic data flow for each object is presented in following figures 3.90 and 3.91. Also formats during each procedure are shown.

Østre Gløshaugen house

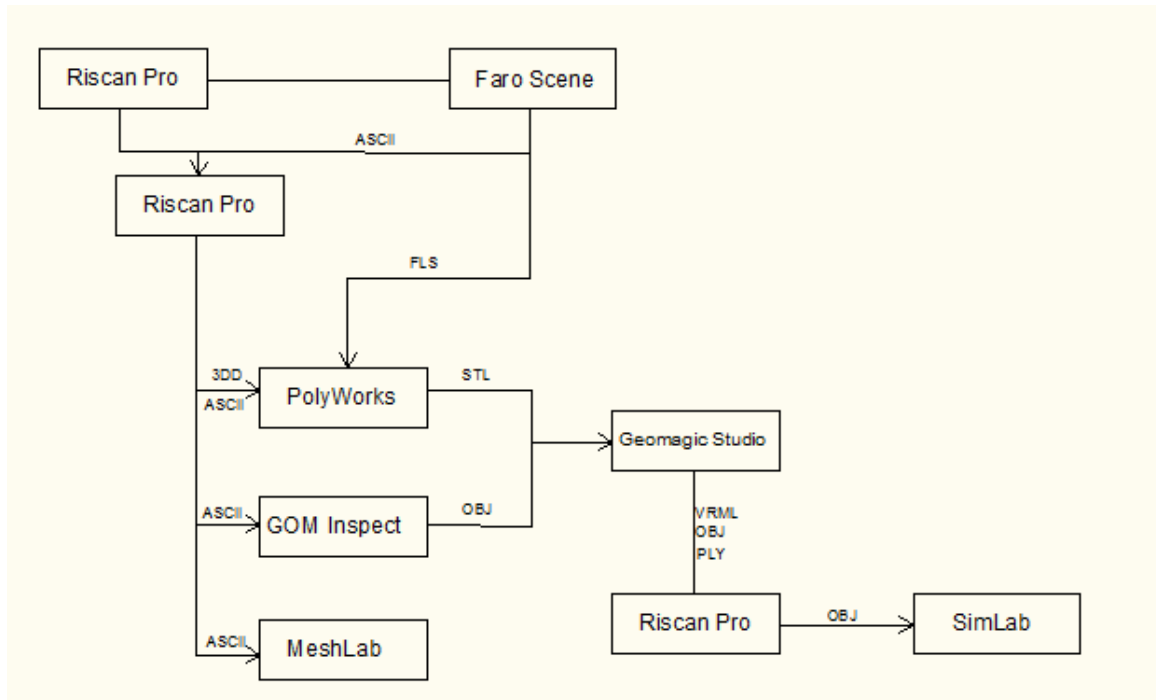


Figure 3.90. Work flow for Østre Gløshaugen house

Nidaros Cathedral

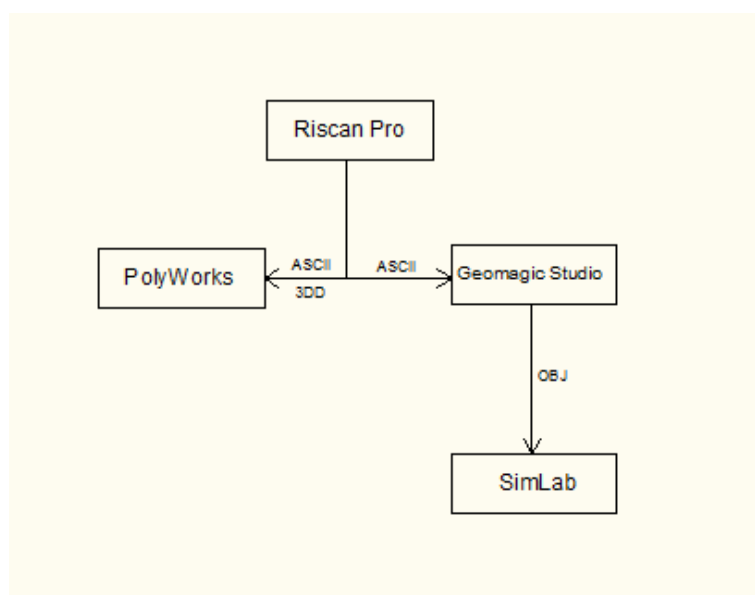


Figure 3.91. Work flow for Nidaros Cathedral.

Chapter 4

4.1 Overview

Following chapter will sum up all work that has been done for the purpose of the thesis together with the results and comments. The paragraph will try to explain the workflow of the project and final results. As the main purpose of the thesis was to evaluate and test different tools for post-processing and modeling of 3D surfaces. Wide range of software packages were investigated. Evaluation was done under few different circumstances, costs, efficiency, accuracy and final results. As also can be noticed nowadays working within one software in order to accomplish the 3D model is impossible. The most efficient way is to combine several tools and obtain the final product with cooperation between them. This statement is also proved here.

First part of the chapter will include description and list of products obtained during the project. The work was based on two different objects, inside of the Cathedral and outside of the old NTNU building. Both results will be presented. Further there will be a discussion part with basic principles and interpretation of the results. Possible future work and relationships with other projects encompassed. The final part of the chapter should consist of final discussion and conclusion marks.

4.2 Results

The focus of the paper was to investigate different ways to process 3D laser scanning data and to obtain a visually nice model in 3D. As mentioned before besides of different tools used there were two separate objects to work on. The issue of different types of objects and necessity of using different settings and algorithms was also important. Additionally, data sets for the second object, which is the Østre Gløshaugen house, was acquired by two alternative 3D sensors. The final desire was to merge the data and used both for producing the final model. After producing the models the problem of texturing arose. For both object different ways of texturing were applied for the models.

Not each software was able to create fully efficient model. As discovered during the work some of the tools, like RiSCAN PRO and FARO SCENE, were dealing very good with

the first steps of processing data and others were more adjusted to produce the final outcome, like PolyWorks, Geomagic Studio or GOM Inspect.

Despite of producing several models, only one for each object was decided to be present as a final and the best one. It was created with combination of several software packages and the workflow consists of many exporting and importing work within the different tools.

Final results are shown in external appendices as 3D PDF files where each model can be rotated, zoomed, moved. Files are also attached on the CD that is included in the report. Final project files that can be opened in the each software are stored within the workstation IBATGMM6700, specification of the workstation is attached in appendix 8 . For the purposes of display each model needed to be reduced. The original size of the files are respectively equal 3,5 GB for Østre Gløshaugen and 1,4 GB for Nidaros Cathedral. After reduction the sizes were equal 250 MB for Østre Gløshaugen and 192 MB for Nidaros Cathedral. Only at this point of reduction model could have been opened in 3D PDF.

4.2.1 Østre Gløshaugen building

Figure 4.1. present the model of the building from different angles. The model is already textured.



Figure 4.1. Østre Gløshaugen building from the south side.



Figure 4.2. Østre Gløshaugen building from the north-east side.



Figure4.3. Østre Gløshaugen building from the north-west side.

Above model was created with a cooperation of few tools. The huge influence had PolyWorks software, however final repairing and improving was done in Geomagic Studio.

As pointed out before, there were few problems concerning texturing and repairing. As can be seen in figure 4.1. where the building is presented from the front side (south side) the bushes which normally are in front of the wall were cut off the model. Decision to proceed in this way was taken because of focusing on closing whole model together. If bushes were left

as they are, the model would not been complete. Besides the bushes, there was a huge lack of data points that could be used to build up the surface. Because of that, the surface, that is now in that place , does not reflect the reality in 100 percentages. Nevertheless, the idea of removing bushes and creating a mesh from the data that left seems to be a better idea. From this point, we can notice however that the texturing on the front wall still includes the bushes. Images were as it looks at that time and there was no option to remove the bushes. As the main problem for the thesis was not investigating the best solution for texturing the final colors included also bushes. If more time and tools were available, this issue could be deal in few ways (possible solutions are described in chapter 5-discussion).

Problem with texturing did not finish only on the part where the bushes are. After several attempts to generating textures, only RiSCAN PRO managed to apply colors from images taken in the beginning. Unluckily, the algorithm had some problems with assigning correct colors for all parts of the building. Examples are presented in chapter 3-paragraph 3.8.

Although some deficiencies in the model can be noticed the final presentation which is the 3D PDF files shows that the model is complete, textured and in majority reflects reality.

4.2.2 Nidaros Cathedral

In case of Nidaros Cathedral few attempts of creating a mesh was done within the last Specialization Project in fall 2013. Unfortunately, that time only RiSCAN PRO software was available which was not able to deal with the data in the way to present them as the final output. Within the thesis, pleasing and correct model was created. All initial processing steps, like registering and merging was not done again. The input for creating the model was filtered, colored and registered point cloud presented the area of interest.

Majority of work was carried out within the Geomagic Studio. However also PolyWorks was used for generating the model. The only issue in PolyWorks model is that the final product in uncolored and the textures were not applicable. Figure 4.4 presents the final model for the Nidaros Cathedral , next figure 4.5. presents zoomed part of the Cathedral with the main stained glasses. Model is also attached in the 3D PDF file and can be seen with multiple and various angles.



Figure 4.4. Final, textured model of Nidaros Cathedral



Figure 4.5. Final, textured model of Nidaros Cathedral, zoomed part.

The hard part within this object was to deal with all small details that were supposed to be captured. Also all columns were really difficult to triangulate. Finally, both PolyWorks

package and Geomagic Studio managed to deal with the object. However, model built within PolyWorks tool was not fully complete (several holes that were impossible to fill in) and textures were not applied.

4.3.3 Conclusions

Within the thesis several processes and methods were discussed for producing high-quality 3D models for cultural heritage purposes. The main investigation concerns evaluation of alternative tools for processing 3D data, however other issues were also examined. All the work and study proved that in order to gain a highly accurate 3D model not only one method and solution can be applied. First of all, combination of laser scanning and high-resolution images is very significant. Secondly, proceeding with all 3D processes from the very beginning as cleaning, merging and registering point clouds until filtering, meshing and texturing need to be carried out with cooperation of multiple tools. Each situation needs different approach and cannot be treated with the same methodology. Above thesis does not give the general solution and techniques for the similar examples. It is an investigation of available tools based on just two cultural heritage objects. Any other site and project might not find an application with above workflow.

As was explained before, in order to proceed with the initial parts of processing mainly two software packages were used. RiSCAN PRO and FARO SCENE which are connected to 3D sensors that acquired data on the scenes. These tools allowed to carried out essential operations on raw data. Automatic registration and merging were done with high accuracy. Also other software -PolyWorks was tested in respect of scans alignment. The all steps are described in the chapter 3, under the registration part. Results of this alignment were highly precise and were used in further steps of working within the software. The methodology applied in PolyWorks tool was very efficient and convenient. However, for the person who has never used the software before beginning of the work might seem to be tough.

Besides registering and initial point cloud cleaning processes RiSCAN PRO was used to apply textures for the Østre Gløshaugen building. Registration of images that were collected afterwards was carried out also in the software. Although, there were still few parts of the building with incorrect colors the results were considered to be the best. Texturing was also tested in MeshLab software and Geomagic Studio tools but the final outputs were under satisfactory level.

As for the main goal of the project, producing a 3D surface from the point cloud, mainly three tools managed to proceed with the operation. PolyWorks software, Geomagic Studio and open free GOM Inspect tool. Results were different and not all were decided to be the final one. The best combination for triangulation was creating a surface within the PolyWorks tool and then exporting the model into Geomagic Studio. Geomagic Studio offers numbers of effective features for repairing and improving 3D mesh. GOM Inspect , as only one free tool that were able to deal with the data and create a surface is considered to be very good solution also. The quality of the model is not high enough and in comparison to the model obtained by PolyWorks and Geomagic cannot be displayed as the final product. However, if there was more time for cleaning and repairing data, the model could have been highly accurate.

Considering working separately in each software in respect of intuitiveness, accessibility and hardware limitations there are few conclusions. The most convenient and easy to investigate proved to be Geomagic Studio. Although, the trial version was available only for 14 days, majority of functions were known and the final product could be delivered. Multiple tutorials and information that can be found in the Internet helped with the work. Additionally, the software was installed on the workstation IBATGMM6700 (specification included in appendix 8) that is less powerful than the second one that was also used within the thesis- workstation IBATGMT7610 with specifications included in appendix 8. It could handle several projects at one time. MeshLab together with GOM Inspect can be found on the same level of difficulty. They are quite easy to work with and all the functions can be operate and examine without spending too much time on it. Numerous of tutorials can help with the software packages. Both of the tools were running on the less powerful workstation and managed to operate on the data. PolyWorks as the most powerful tool while working on the thesis after 30 days of availability can be considered to be the hardest one to learn. The software is certainly the best if it is about quality and accuracy and has application in countless areas. However, personally I believe that one month for creating a model from the bottom to the top is very difficult within the software for the completely new user. Additionally, the workstation IBATGMT7610, the most powerful at the Norwegian University of Science and Technology, in the Geomatic department could not handle the project properly. The time for every opening and saving files was enormously long. The professional support from InnovMetric Software Inc. was very helpful and if the time would be slightly longer the results and the work would go better.

The last part of conclusions and commenting the results is comparison both 3D laser sensors and data obtained by them. Point clouds acquired by Riegl and by Faro 3D differ. Faro's datasets seem to be in better order, without redundant noise. Shapes of details were kept with higher accuracy by Faro 3D scanner than with Riegl. The images are shown in chapter 3-paragraph 3.4. What is more, the work and handling the equipment is way more easy in the case of Faro company. The scanner is few times lighter and smaller and can be carried on the scene by maximum two people. There is no need to use computer or any other additional devices. In the case of scanning by Riegl device, except of the scanner there was a necessity to use a computer with an access to the power. On the other hand, Faro 3D scanner does not allow to attach the high-resolution camera and capture images for texturing purposes. It gathers RGB values but the quality is at the low level. Also, Faro scanner does not have an option of using GPS device for measuring the Global Coordinate System. Newest version of the equipment however has already inbuilt GPS devices. The time that was dedicated for the field work, for both measurements, varies a lot. Riegl's measurements took about 7 hours in total with carrying the equipment and measuring only 4 scanner's stations while Faro's measurements lasted around 4 hours in total with gathering data from 7 different scanner's stations.

Chapter 5

5.1 Discussion and further work

Several issues arose while working on the following master thesis. Acquiring data and processing it in order to obtain a fully functional 3D model is very complex task. It includes wide range of planning, learning new technologies, following the newest trends in the field and finally producing the model. At each step of the workflow there can be found some troubles. The main advantage of using scanning is the very fast and direct collection of enormous number of surface points. On the other hand, its accuracy cannot reach the level of accuracy of geodetic measurements what makes it similar to image matching in photogrammetry. [3]. Consequently, when complex objects have to be captured and the accuracy can be moderated, laser scanning techniques are nowadays the best solution for cultural heritage documentation. However, how mentioned before it requires lot of experience and good planning skills. Because the main object of the thesis is Østre Gløshaugen building and Nidaros Cathedral was the subject of previous Specialization Project [17], in this chapter primarily problems and concerns about the building will be discussed.

5.1.1 Lack of data

The building basically is easy accessible place and almost perfect to scan from each angle and direction. However, in front of the south wall, the bushes are covering down part of this wall. Scan stations were placed all over this wall since it is also the most complex wall of all. Nevertheless, scanners were not able to gather all information from behind the bushes. Because of the short time and lot of work ahead it was decided to work on the data that has been acquired. As can be seen in the report some tools were able to deal with these large holes. The result may not be as perfect as it could be but the model is fully complete. Of course if the time allows there could be twice or even triple as many stations as it was and data from behind the bushes might have been captured.

Besides areas with bushes, there were few places around the roof where points were not collected. One slightly large area was suited near to the eastern chimney and was not able to capture from any angle. Software packages, Geomagic Studio, PolyWorks and GOM Inspect managed to reconstruct the area.

Also area under the protruding part of the roof was not captured. The basic assumption for the thesis was to collect accurate data of the building without redundant details. The assumption was made to compensate between the time and the accuracy.

5.1.2 Texturing issues

As the data was obtained from two 3D sensors and only Riegl scanner is able to acquire high-resolution images while scanning it was impossible to use them for texturing entire data. Another set of free images was taken and register as a free stations images. After testing few possible solution for using images only RiSCAN PRO seemed to deal with texturing. Although, in the beginning there were lot of problems with importing the final model into the software. After multiple attempts finally, the OBJ format worked for the data and textures could be applied. As mentioned before, in the result section, there were few parts that were colored incorrectly. The reason for that can be a huge memory consumption during the texturing process which was carried out on the less powerful workstation.

5.1.3 Hardware limitations

Hardware limitations within the project are directly connected to software limitations and requirements. As the main goal was to evaluate alternative tools for processing 3D data the hardware and software issues had to arise. There were two workstation available to work on. Both specifications are included in appendix 8.

One of the challenges faced during the scope of this master thesis was to overcome the lack of highly powerful hardware. Available work station unfortunately limited the amount of processes that could be carried out simultaneously. It also caused that complex operations were very time-consuming. There should be noticed, on the other hand, that more powerful workstations could result in highly detailed model what would still caused some hardware limits. The best idea is to find a balance between details and hardware possibilities.

Very alike issue concerns software limitations. As has been proved, there are numerous of tools available to process 3D data, however not all software packages are able to work on particular amount of data. Of course, if the workstation is more powerful, the software will work more efficient. However, limits of the software cannot be overcome in some situations.

The most important problem with hardware limits, within the project, could be noticed with PolyWorks package. The software uses enormous memory while working what resulted in multiple breaking down the whole project. Importing and every opening the project took very long time. Also all processes were running during the night due to long waiting time. Not only PolyWorks caused troubles with memory usage and time-consuming process. Also RiSCAN PRO while texturing needed very long time and crashed down several times. The same happened with GOM Inspect while closing holes within the model. The solution for all that issues was to reduce the models and to limit range of the problem. They were tried to be kept as detailed as possible with reducing the amount of the data.

5.2 Additional Comments

Few additional comments concern PolyWorks software should be included in the report. As there are multiple different possible solutions for proceeding with the following subject of the thesis and not all of them could have been investigated because of the time and small experience with handling the software, Support Zone of InnovMetric Software Inc. suggested few better ways afterwards. This could help reduce significantly memory usage and improve speed of processes. Workstation that was in use during the thesis was not good enough for proceeding with the data. If higher quality of computer were available the process speed would improve. Working with other solution, which is involving IMAlign in the work flow, would help to reduce the memory-consumption. Also, textures and colors could have been applied with some more advanced functions. After Wrap Mesh function, Vertex Color should be used in order to generate textures. Remarks that have been suggested by InnovMetric Software Inc. would definitely help with working on the project and would significantly improve the final result. All the solution would have been examined with more available time.

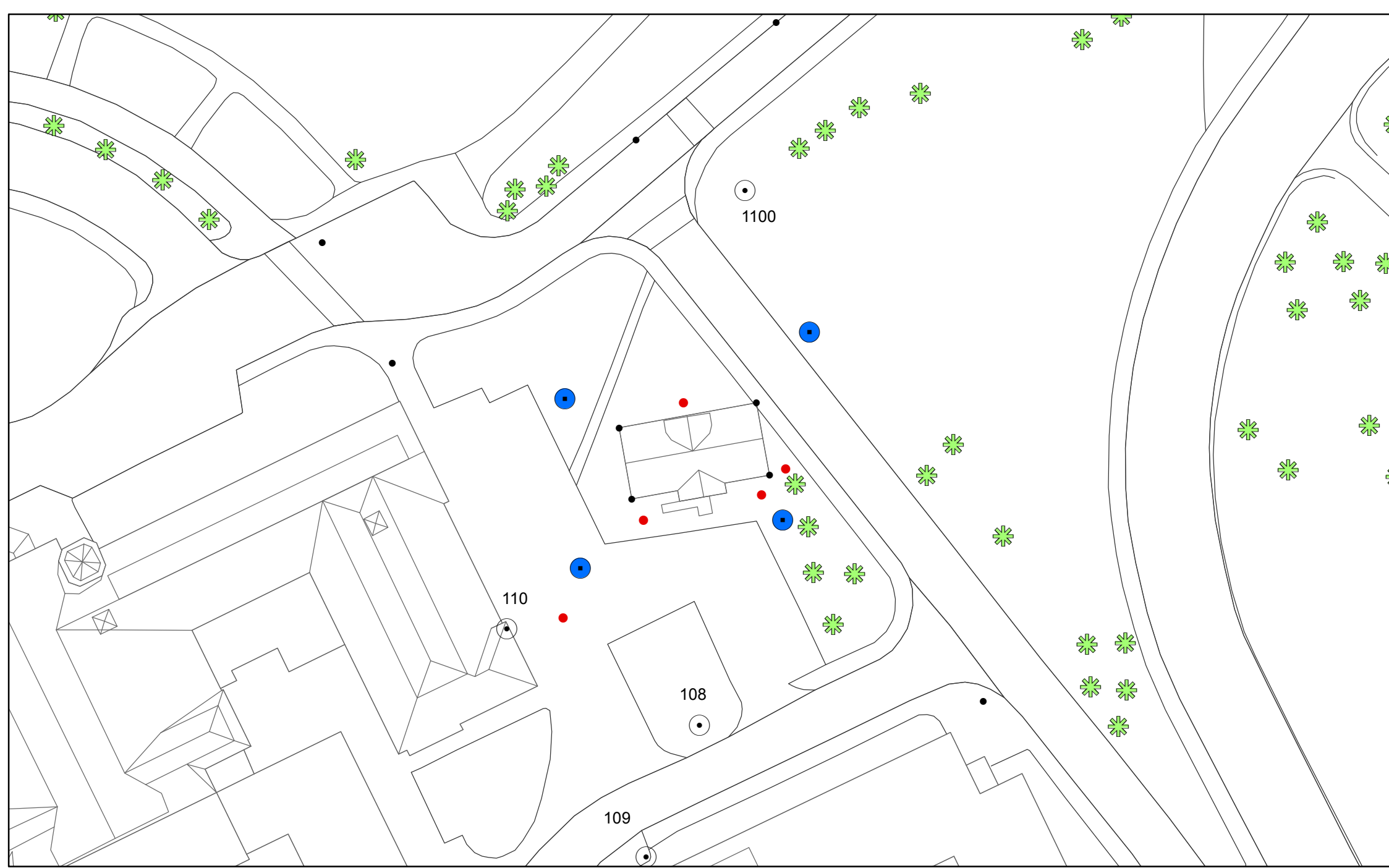
References:

- [1] Al-kheder S., Al-shawabkeh Y., Haala N., *Developing a documentation system for desert palaces in Jordan using 3D laser scanning and digital photogrammetry*, Journal of Archeological Science 2008, 1-10
- [2] Barber D. , J. Mills, D. Andrews, *3D laser scanning for cultural heritage (second edition): advice and guidance to users on laser scanning in archeology and architecture*, Technical report, English Heritage, Swindon, 2011.
- [3] Boehler W., Heinz G., Marbs A., *The potential of non-contact close range laser scanners for cultural heritage recording*, CIPA Working Group VI, 2001
- [4] FARO, www.faro.com, Last visit: 14/06/2014
- [5] FARO manual
- [6] Herraез J., Navarro P., Denia J., Martin M., Rodrigues J., *Modeling the thickness of vaults in the church of Santa Maria de Magdalena (Valencia, Spain) with laser scanning techniques*, Journal of Cultural Heritage 2013
- [7] InnovMetric Software Inc., Training materials, *IMSurvey Reference Guide*
- [8] Kadobayashi R., Koch N., Otani H., Furukawa R., *Comparison and evaluation of laser scanning and photogrammetry and their combined use for digital recording of cultural heritage*, *ISPRS Annals of the Photogrammetry*, Remote Sensing and Spatial Information Sciences 2004
- [9] Nidaros Cathedral in Trondheim, Norway , <http://www.nidarosdomen.no/> , Last visit: 15/05/2014
- [10] Pesci A., Bonali E., Galli C., Boschi E., *Laser scanning and digital imaging for the investigation of an ancient building: Palazzo d'Accursio study case (Bologna, Italy)*, Journal of Cultural Heritage 13 (2012) 215-220
- [11] Pieraccini M., Guidi G., Atzeni C., *3D digitizing of cultural heritage*, Journal of Cultural Heritage 2 (2001) 63-70
- [12] Remondino F., *From point cloud to surface: The modeling and visualization problem*. International Archives of Photogrammetry, Remote Sensing and Spatial Information Sciences, Vol. XXXIV-5/W10, 2003.
- [13] RIEGL, *Training Material for RIEGL VZ-XX, Module 3, Data Registration, RIEGL Laser Measurement System, Austria, 2009*
- [14] Riegl Company, www.riegl.com, Last visit: 14/06/2014
- [15] RiSCAN PRO manual

- [16] Sansoni G., Trebeschi M., Doccio F., *State-of-The-Art and Applications of 3D Imaging Sensors in Industry, Cultural Heritage, Medicine, and Criminal Investigation*, Sensors 2009, 9(1), 568-601
- [17] Setkowicz J., *3D Modeling of a part of Nidaros Cathedral in Trondheim by laser scanning* Specialization Project, NTNU, Fall 2013
- [18] Theiler P.W., Schindler K., *Automatic registration of terrestrial laser scanner point clouds using natural planar surfaces*, ISPRS Annals of the Photogrammetry, Remote Sensing and Spatial Information Sciences, Volume I-3, 2012
- [19] Trigui A., *Post-processing of Laser Scanning Point Clouds for the As-built Modeling of Petrochemical Installations*, FIG Working Week, 2011, International Federation of Surveyors, Pages:1-9, Date: 18-22 May 2011
- [20] Vosselman G., Maas H-G., *Airborne and Terrestrial Laser Scanning*, Dunbeath, Whittles Publ., 2010
- [21] Wikipedia, <http://en.wikipedia.org/wiki/ASCII> , Last visit: 19-06-14
- [22] Wikipedia, http://en.wikipedia.org/wiki/Wavefront_.obj_file , Last visit: 19-06-14
- [23] Yastikli N., *Documentation of cultural heritage using digital photogrammetry and laser scanning*, Journal of Cultural Heritage 8 (2007) 423-427
- [24] Yilmaz H.M., Yakar M., Gulec S.A., Dulgerler O.N., *Importance of digital close-range photogrammetry in documentation of cultural heritage*, Journal of Cultural Heritage 8 (2007) 428-433
- [25] Zlot R., Bosse M., Greenop K., Jarzab Z, Juckes E., *Efficiently capturing large cultural heritage sites with a handheld mobile 3D laser mapping system*, Journal of Cultural Heritage 2013
- [26] <http://www.ennex.com/~fabbers/StL.asp> Last visit:19-06-14






Appendices

Appendix 1

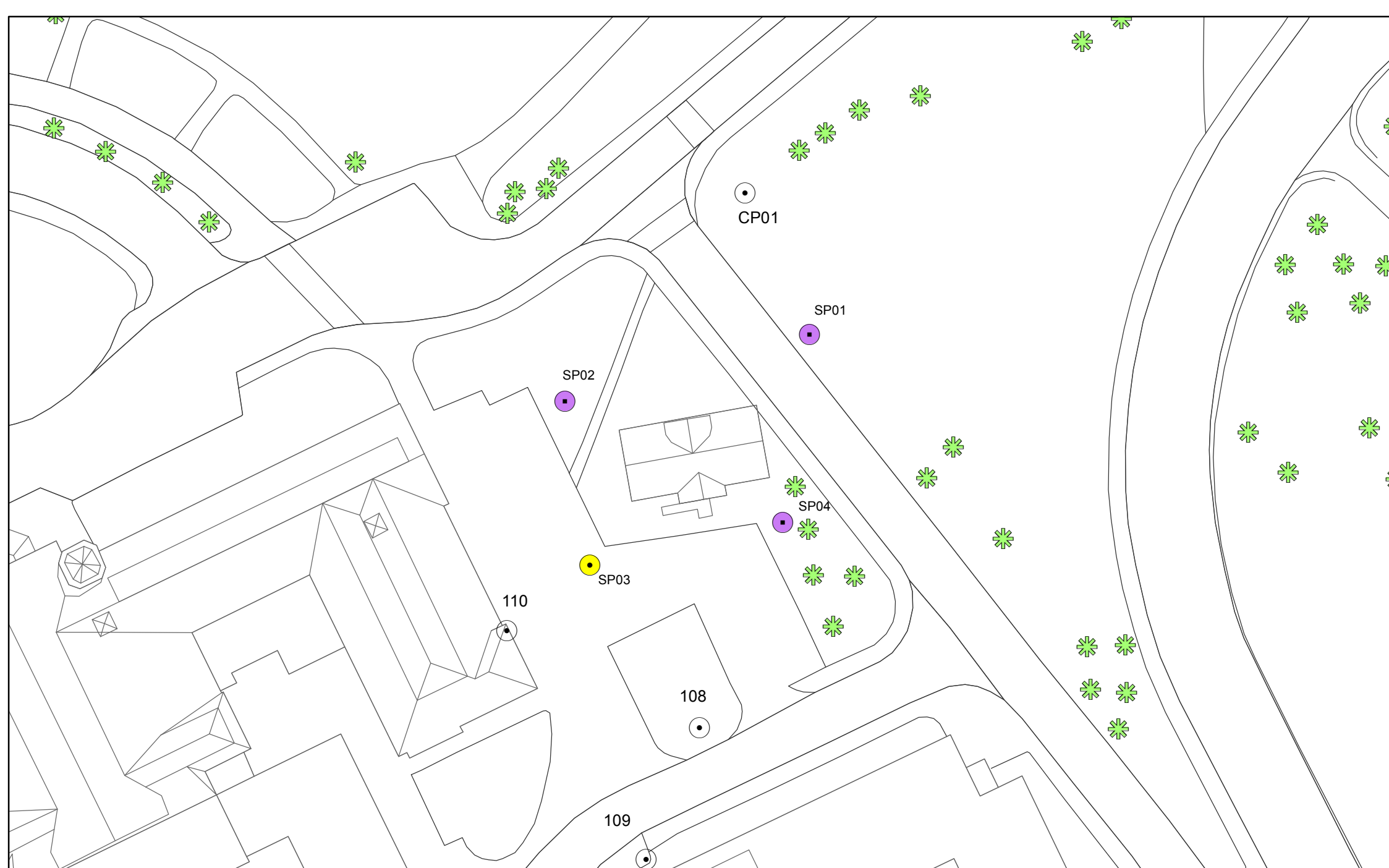


1:550

Legend





-  CONTROL_points
-  possible stations_FARO
-  Trees
-  reflectors
-  stations_riegl

Appendix 2

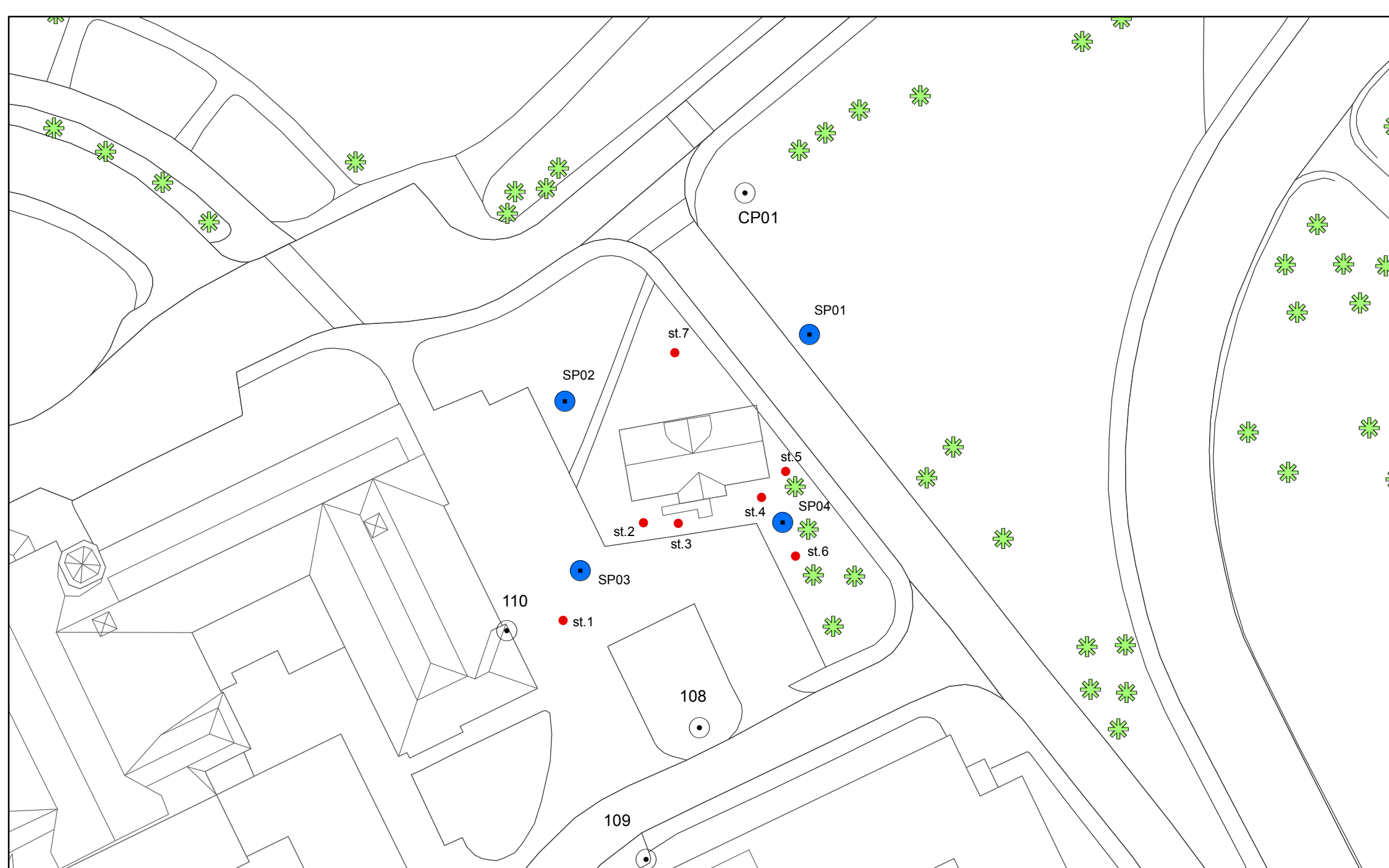


1:550

Legend





-  Riegl scan stations without GPS
-  Riegl scan stations with GPS
-  Control points
-  Trees

Appendix 3



1:550

Legend

-  Control points
-  FARO scan stations
-  Riegl scan stations
-  Trees

Appendix 4

Technical Data 3D Scanner Hardware *RIEGL* LMS-Z420i

Laser Product Classification

Class 1 Laser Product according to IEC60825-1:2007

The following classes apply for instruments delivered into the United States:
Complies with 21 CFR 1042.10 and 1042.11, except for deviations pursuant
to Laser Notice No. 50, dated June 24, 2007.



Rangefinder Performance¹⁾

Max. Measurement Range²⁾

for natural targets, $\rho \geq 80\%$

for natural targets, $\rho \geq 10\%$

Minimum Range

Accuracy³⁾⁴⁾

Repeatability⁴⁾⁵⁾

Measurement Rate

Laser Wavelength

Beam Divergence⁶⁾

up to 1000 m

up to 350 m

2 m

10 mm

8 mm (single shot), 4 mm (averaged)

up to 11000 pts/sec @ low scanning rate (oscillating mirror)

up to 8000 pts/sec @ high scanning rate (rotating mirror)

near infrared

0.25 mrad

1) Rot. Last. or Alternating Target Mode selectable
from scan line to scan line.

2) Typical values under average conditions. Maximum range is
specified for flat targets with size in excess of the laser beam
diameter and near perpendicular angle of incidence of
the laser beam, atmospheric visibility in excess of 23 km.,
in bright sunlight the operational range is considerably shorter
than under an overcast sky.

3) Accuracy is the degree of conformity of a measured quantity to its actual
(true) value.

4) Precision, also called reproducibility or repeatability, is the degree to which
further measurements show the same result.

5) One sigma @ 50 m range under RIEGL test conditions.

6) 0.25 mrad correspond to 25 mm increase of beamwidth per 100 m
of range.

Scanner Performance

Vertical (Line) Scan

Scan Angle Range

Scanning Mechanism

Scan Speed

Angular Stepwidth $\Delta \theta$ ⁷⁾

between consecutive laser shots

Angle Measurement Resolution

0° to 80°

rotating / oscillating mirror

1 scan/sec to 20 scans/sec @ 80° scanning range

$0.004^\circ \leq \Delta \theta \leq 0.2^\circ$

0.002°

Horizontal (Frame) Scan

Scan Angle Range

Scanning Mechanism

Scan Speed⁸⁾

Angular Stepwidth $\Delta \varphi$ ⁷⁾

between consecutive scan lines

Angle Measurement Resolution

0° to 360°

rotating optical head

0.01°/sec to 15°/sec

$0.004^\circ \leq \Delta \varphi \leq 0.75^\circ$

0.0025°

Inclination Sensors

optional, for vertical scanner setup position
(specifications to be found in separate data sheet)

Internal Sync Timer

option for real-time synchronized time stamping of scan data
(specifications to be found in separate data sheet)

7) Selectable via Ethernet Interface or RS232.

8) Horizontal scan can be disabled, providing 2D-scanner operation.

General Technical Data

Interfaces: for configuration & data output
for configuration
for data output

Power Supply Input Voltage

Power Consumption

Current Consumption @ 12 V DC

@ 24 V DC

Main Dimensions

Weight

Temperature Range

Protection Class

TCP/IP Ethernet, 10/100 Mbit/sec

RS 232, 19.2 kbd

ECP standard (enhanced capability port) parallel

12 - 28 V DC

typ. 78 W max. 94 W

typ. 6.5 A max. 7.8 A

typ. 3.25 A max. 3.9 A

463 mm x 210 mm (length x diameter)

16 kg

0°C to +40°C (operation), -10°C to +50°C (storage)

IP64, dust and splash-proof



RIEGL[®]
LASER MEASUREMENT SYSTEMS

RIEGL Laser Measurement Systems GmbH, 3560 Han, Austria
Tel.: +43-2982-4211, Fax: +43-2982-4210, E-mail: office@riegl.co.at

RIEGL USA Inc., Colorado, Frisco 32819, USA
Tel.: +1-407-246-9927, Fax: +1-407-246-2636, E-mail: info@rieglusa.com

RIEGL Japan Ltd., Tokyo 104013, Japan

Tel.: +81-3-3382-7340, Fax: +81-3-3382-5843, E-mail: info@riegl-japan.co.jp

www.riegl.com

Information contained herein is believed to be accurate and reliable. However, no responsibility
is assumed by RIEGL for its use. Technical data are subject to change without notice.

Data sheet LMS-Z420, 03/05/2010

Appendix 5

FARO Focus^{3D}
www.faro.com/focus

FARO

Performance Specifications



Ranging Unit

Unambiguity interval: 153.49m (503.58ft)

Range Focus^{3D} 120: 0.6m - 120m indoor or outdoor with low ambient light and normal incidence to a 90% reflective surface

Range Focus^{3D} 20: 0.6m - 20m at normal incidence on >10% matte reflective surface*

Measurement speed: 122,000 / 244,000 / 488,000 / 976,000 points/sec

Ranging error: ±2mm

Ranging noise ¹⁾	@10m	@10m - noise compressed ⁴⁾	@25m	@25m - noise compressed ⁴⁾
@ 90% refl.	0.6mm	0.3mm	0.95mm	0.5mm
@ 10% refl.	1.2mm	0.6mm	2.20mm	1.1mm

Color Unit

Resolution: Up to 70 megapixel color

Dynamic color feature: Automatic adaption of brightness

Deflection unit

Vertical field of view (vertical/horizontal): 305° / 360°

Step size (vertical/horizontal): 0.009° (40,960 3D pixels on 360°) / 0.009° (40,960 3D pixels on 360°)

Max. vertical scan speed: 5,820rpm or 97Hz

Laser (Optical transmitter)

Laser power (cw Ø): 20mW (Laser class 3R)

Wavelength: 905nm

Beam divergence: Typical 0.19mrad (0.011°)

Beam diameter at exit: 3.0mm, circular

Data handling and control

Data storage: 3D, SDHC™, SDXC™; 32GB card included

Scanner control: Via touch-screen display

New WiFi(WLAN) access: Remote control, Scan Visualization and download are possible on mobile devices with Flash®

Multi-Sensor

Dual axis compensator: Levels each scan with an accuracy of 0.015° and a range of ±5°

Height sensor: Detects the height relative to a fixed point via an electronic barometer and adds it to the scan

Compass: Electronic compass gives the scan an orientation. A calibration feature is included.

1) Depends on ambient light, which can act as a source of noise. Bright ambient light (e.g. sunlight) may shorten the actual range of the scanner to lower distances. In low ambient light, the range can be more than 100m for normal incidence on high-reflective surfaces. 2) Ranging error is defined as the systematic measurement error or constant 1σ and 2σs, one sigma. 3) Ranging noise is defined as a standard deviation of values about the zero-ft plane for measurement speed of 122,000 points/sec. 4) A noise-compression algorithm may be activated to average points in sets of 4 or 16, thereby compressing raw data noise by a factor of 2 or 4. Subject to change without prior notice.

Patented: US 7,430,068 B2; 7,733,544; 7,847,922 B2

*Focus^{3D} 20 not available for distributor use



Hardware Specifications

Power supply voltage: 19V (external supply), 14.4V (internal battery)
Power consumption: 40W and 80W respectively (while battery charges)
Battery life: Up to 5 hours
Ambient temperature: 5° - 40°C
Humidity: Non-condensing

Cable connector: Located in scanner mount
Weight: 5.0kg
Size: 240x200x100mm³
Maintenance calibration: Annual
Parallax-free: Yes



For more information call 800.736.0234
or visit www.faro.com/focus

Appendix 6




GPS Controller CS15

Technical Specifications

CS15 and CS10 Hardware Specifications		CS10	CS15
Ergonomic and cable-free GNSS Handheld			
Operating System	Windows CE 6.0	•	•
Display	8.9 cm (3.5 in) 640 x 480 pixel (VGA) colour TFT, touch screen, sunlight-readable, LED backlight	portrait	landscape
Camera	Integrated 2MP fixed focus camera	•	•
I/O	SD slot (SDIO), CF Type I / II slot, 5-pin custom connector (USB) RS232 module: RS232, USB A Host, USB MiniAB OTG, 7-pin connector, Power Lemo module: Lemo (USB and serial), USB A Host, 7-pin connector, Power	• • •	• • •
Interface	Touch screen, Ergonomic cable-free Handheld with keyboard, virtual keyboard	Numeric: 26 keys	QWERTY: 65 keys
Processor	Freescall iMX31 533 MHz ARM Core	•	•
Memory	512 MB DDR SDRAM	•	•
Storage	1 GB (non-volatile NAND Flash)	•	•
Audio	Integrated sealed speaker and microphone Bluetooth® audio headset support	• •	• •
LEDs	Battery and Bluetooth® status LED	•	•
Wireless connectivity	Bluetooth® 2.0 Class 2 Wireless LAN 802.11b/g Integrated 2.4 GHz FHSS total station radio with fully integrated internal antenna Integrated GSM/GPRS 3.5G module with fully integrated internal antenna	• • • •	• • • •
Software			
Application Software	Viva Controller runs Leica SmartWorx Viva and SmartWorx Viva LT. In addition, a number of regional solutions are available. For more information on the field software that's best for you, contact your local Leica authorized distribution partner.	•	•
Standard Software	Internet Explorer Mobile, File Explorer, Word Mobile, Microsoft Windows Media™ Player, Camera Software, Online Help	•	•
Power Management			
Removable Battery	CEB212 (7.4V / 2600mAh Li-Ion rechargeable)	•	•
Battery Charging Time	2 hours	•	•
Power	Nominal 12 V DC Range 10.5 – 28 V DC	•	•
Operating Time	10 hours (depending on use of embedded devices)	•	•
Dimensions and Weight			
Size	CS10: 200 mm / 102 mm / 45 mm (7.87 in / 4.01 in / 1.77 in) CS15: 245 mm / 125 mm / 45 mm (9.65 in / 4.92 in / 1.77 in)	•	•
Weight ¹	CS10: 0.56 kg (1.23 lbs) CS15: 0.71 kg (1.57 lbs)	•	•
Environmental Specifications			
Operating / Storage temperature range	Operation: -30 to 60° C (-22 to 140° F), Storage: -40 to 80° C (-40 to 176° F)	•	•
Dust and Water / Humidity	IP67 (IEC 60529) / 100% non-condensing (MIL-STD-810F, Method 507.4-1)	•	•
Drop / Vibration	1.2 m (4 ft) / MIL-STD-810F, Method 514.5 - Cat24	•	•
Accessories			
100 – 240V AC power supply for all regions		•	•
Stylus		•	•
2 x anti-glare display foils		•	•
Documentation CD		•	•
Docking station		•	•
12V DC vehicle charger		•	•
Additional cables		•	•
Hand strap		•	•
Pole holder set		•	•
Soft bag		•	•

Appendix 7

GPS Receiver GS15

Leica GS15 GNSS receiver 		Leica GS15 Single Frequency	Leica GS15 Performance	Leica GS15 Professional	
Supported GNSS Systems					
GPS L2		○	●	●	
GPS L5		○	○	●	
GLONASS		○	○	●	
Galileo		○	○	●	
BeiDou		○	○	○	
RTK performance					
DGPS / RTCM		○	●	●	
RTK up to 5 km		○	●	●	
RTK unlimited		○	●	●	
Network RTK		○	●	●	
Leica Libe RTK		○	○	●	
Position update & data recording					
5 Hz positioning		●	●	●	
20 Hz positioning		○	●	●	
Raw data logging		●	●	●	
SBEX logging		○	○	●	
IMBA out		○	○	●	
Additional features					
RTK Reference Station functionality		○	●	●	
		● = Standard	○ = Optional		
GNSS Performance					
	GNSS technology	Leica patented SmartTrack technology: <ul style="list-style-type: none"> Advanced measurement engine Jamming resistant measurements High precision pulse aperture multipath correlator for pseudorange measurements Excellent low elevation tracking Very low noise GNSS carrier phase measurements with <math>\pm 0.5</math> mm precision Minimum acquisition time 			
	No. of channels	120 channels			
	Max. simultaneous tracked satellites	Up to 60 Satellites simultaneously on two frequencies			
	Satellite signals tracking	<ul style="list-style-type: none"> GPS: L1, L2, L2C, L5 GLONASS: L1, L2 Galileo (Test): GIOVE-A, GIOVE-B Galileo: E1, E5a, E5b, Alt-BOC BeiDou: B1, B2 SBAS: WAAS, EGNOS, GAGAN, MSAS, QZSS 			
	GNSS measurements	Fully independent code and phase measurements of all frequencies <ul style="list-style-type: none"> GPS: carrier phase full wave length, Code (C/A, P, C Code) GLONASS: carrier phase full wave length, Code (C/A, P narrow Code) Galileo: carrier phase full wave length, Code BeiDou: carrier phase full wave length, Code 			
Reacquisition time	≤ 1 sec				
Measurement Performance & Accuracy					
	Accuracy (rms) Code differential with DGPS / RTCM ¹	Typically 25 cm (rms)			
	DGPS / RTCM				
	Accuracy (rms) with Real-Time-Kinematic (RTK) ¹				
	Standard of compliance	Compliance with ISO17123-8			
	Single Baseline (≤ 30 km)	Horizontal: 8 mm + 1 ppm (rms) Vertical: 15 mm + 1 ppm (rms)			
	Network RTK	Horizontal: 8 mm + 0.5 ppm (rms) Vertical: 15 mm + 0.5 ppm (rms)			
	Accuracy (rms) with Post Processing ¹				
	Static (phase) with long observations	Horizontal: 3 mm + 0.1 ppm (rms) Vertical: 3.5 mm + 0.4 ppm (rms)			
	Static and rapid static (phase)	Horizontal: 3 mm + 0.5 ppm (rms) Vertical: 5 mm + 0.5 ppm (rms)			
	Kinematic (phase)	Horizontal: 8 mm + 1 ppm (rms) Vertical: 15 mm + 1 ppm (rms)			
	On the Fly (OTF) Initialization				
	RTK technology	Leica SmartCheck technology			
	Reliability of OTF Initialization	Better than 99,999%			
	Time for Initialization	Typically 4 sec ²			
	OTF range	up to 70 km ²			
Network RTK					
Supported RTK network solutions	VRS, FKP, IMAX				
Supported RTK network standards	MAC (Master Auxiliary Concept) approved by RTCM SC 104				

Appendix 8

Hardware specifications

Two workstations were used during working on following master thesis.

1. Workstation IBATGMT7610

Name	IBATGMT7610
Operation system	Windows 7 Professional
Processor	Intel(R) Xeon(R) CPU E5-2670 v2@2.50 GHz (2 processors)
Memory	32,0 GB
System type	64-bit Operating System

2. Workstation IBATGMM6700

Name	IBATGMM6700
Operation system	Windows 7 Professional
Processor	Intel(R) Core(TM) i7-3720QM CPU @ 2.60 GHz
Memory	16,0 GB
System type	64-bit Operating System